Aus dem Institut BIH Center for Regenerative Therapies
der Medizinischen Fakultät Charité – Universitätsmedizin Berlin

DISSERTATION

# Strategien zur Nutzung des Potenzials menschlicher Herzvorläuferzellen für die Herzzelltherapie

*Strategies to harness the potential of human cardiac progenitor cells for heart cell therapy*

Zur Erlangung des akademischen Grades
Doctor of Philosophy (PhD)

vorgelegt der Medizinischen Fakultät
Charité - Universitätsmedizin Berlin

von

Ana Garcia Duran

aus Lloret de Mar, Spanien

Datum der Promotion: 03.12.2021

*‘‘Almost everything offered today for the treatment of heart disease is at the level of [halfway] technology, with the transplanted and artificial hearts as ultimate examples. When enough has been learned to know what really goes wrong in heart disease, one ought to be in a position to figure out ways to prevent or reverse the process.’’*

Lewis Thomas, ‘‘The Lives of a Cell’’ (1974)

# TABLE OF CONTENTS

# LIST OF ABBREVIATIONS

**APC**: allophycocyanin

**CDC**: cardiosphere-derived cells

**CM**: cardiomyocyte

**cTNI**: cardiac troponin I

**cTNT**: cardiac troponin T

**CVD**: cardiovascular disease

**c-kit**: tyrosine kinase receptor

**DOX**: doxycycline

**d2eGFP**: destabilized 2 hour enhanced green fluorescent protein

**EC**: endothelial cell

**EGF**: epidermal growth factor

**EU**: European Union

**FGF-2**: fibroblast growth factor 2

**FT**: flowthrough; unbound Sca-1 negative fraction

**GFP**: green fluorescent protein

**GOI**: gene of interest

**GSK3β**: glycogen synthase kinase 3β

**Isl-1**: Islet 1

**hCF**: human cardiac fibroblast

**hCPC**: human cardiac progenitor cell

**hCMPC**: human cardiomyocyte progenitor cell population

**hESC**: human embryonic stem cell

**hiPSC**: human induced pluripotent stem cell

**hiPSC-CM**: human induced pluripotent stem cell-derived cardiomyocyte

**hiPSC-rtTA**: human induced pluripotent stem cell constitutively expressing rtTA in the ROSA26 locus

**hPSC**: human pluripotent stem cells

**iCPC$^{Sca-1}$:** hiPSC-derived human cardiomyocyte progenitor cell population based on Sca-1 expression

**Lrp5/6**: low density lipoprotein receptor-related proteins 5/6

**LV**: left ventricle

**LVEF**: left ventricular ejection fraction

**MACS**: magnetic activated cell sorting

**MESP1**: mesoderm posterior 1

**MI**: myocardial infarction

**miRNA**: microRNA

**PDT**: population doubling time

**pre-miRNA**: precursor miRNA

**pri-miRNA**: primary transcript

**RNAi**: RNA interference

**rtTA**: reverse tetracycline-controlled transactivator

**rtTA3:** reverse tetracycline-controlled transactivator third generation

**rtTA3G:** reverse tetracycline-controlled transactivator third generation, high affinity

**Sca-1**: stem cell antigen 1

**SFRP**: secreted frizzled related proteins

**shRNA**: short hairpin RNA

**siRNA**: silencing RNA

**SSEA-1**: stage specific embryonic antigen 1

**SMC**: smooth muscle cell

**SP**: side population

**TCF/LEF**: lymphoid enhancer-binding factor

**Tet systems**: tetracycline regulated gene expression system

**TRE**: tetracycline response element

**TSA**: trichostatin A

**WT**: wildtype

**ZFN**: zinc finger nuclease

# LIST OF FIGURES

# LIST OF TABLES

# ABSTRACT

Ischaemic heart disease is the most common cause of death worldwide. Yet, standard procedures to treat myocardial damage still heavily depend on the availability of heart transplants. Cardiac cell therapy has arisen as a prospective strategy to halt the progression and potentially revert heart failure. Cardiac progenitor-like cells, such as stem cell antigen-1 (Sca-1) positive cells, are an attractive cell population as they proliferate and represent a source of cardiac cells. These Sca-1 positive progenitors, also known as human cardiomyocyte progenitor cells (hCMPCs), have been isolated from fetal and adult human hearts. However, despite promising preclinical data, clinical application of hCMPCs relies on heart tissue availability or is bound to carry patient associated co-morbidities, which can ultimately influence the cells' therapeutic potential. In addition, as a result of hCMPCs multipotent nature, another challenge is to predict cell fate upon transplantation into the myocardium. This thesis aims to address these issues.

Genetically reprogrammed embryonic-like stem cells namely human induced pluripotent stem cells (hiPSCs) could represent a readily available unlimited source of hCMPCs. In this study, Sca-1 positive cells isolated from hiPSCs undergoing cardiomyocyte differentiation (iCPC$^{Sca-1}$) were highly proliferative and resembled fetal hCMPCs as assessed by expression of CD105, and absence of CD34 and CD45 expression. Also, 84% of iCPCs$^{Sca-1}$ were cardiac troponin I positive and 15% expressed NKX 2-5, both markers associated to the cardiac lineage. Morphological changes and increased α-actinin expression when cultured in differentiation medium suggested that iCPCs$^{Sca-1}$ might hold cardiomyogenic potential. Next, a conditional gene expression system was combined with state-of-the-art RNA interference (RNAi) technology to modulate the Wnt signaling pathway, which governs differentiation of cardiac progenitors into cardiomyocytes. Founding experiments in a HeLa reporter cell line suggested that homogeneous and robust induction of RNAi expression can be achieved by inserting gene regulatory elements in different genomic loci. In this configuration, silencing β-catenin, a Wnt key mediator, led to 85% β-catenin knockdown in hiPSCs harboring a single copy of RNAi. Moreover, silencing β-catenin in hiPSC-derived mesoderm cells for 4 days led to nearly 3-fold cardiac troponin T positive cells at day 11 of differentiation as compared with untreated cells. Although the lower differentiation efficiency of cells harboring the RNAi targeting β-catenin remains to be investigated, conditional β-catenin silencing may be a promising strategy to increase the conversion rate of mesoderm cells into cardiomyocytes.

# ZUSAMMENFASSUNG

Ischämische Herzkrankheiten sind weltweit die häufigste Todesursache und Standardverfahren zur Behandlung von Myokardschäden hängen stark von der Verfügbarkeit von Herztransplantaten ab. Die Herzzelltherapie hat sich als eine vielversprechende Strategie erwiesen, um das Fortschreiten von Herzschäden zu stoppen und möglicherweise die Herzinsuffizienz umzukehren. Herzvorläufer-ähnliche Zellen, wie Stammzell-Antigen-1 (Sca-1)-positive Zellen, stellen hierfür eine attraktive Zellpopulation dar, da sie sich vermehren und in Herzzellen differenzieren. Diese Sca-1-positiven Zellen, auch als humane Kardiomyozyten-Vorläuferzellen (hCMPCs) bekannt, können aus fötalen und erwachsenen menschlichen Herzen isoliert werden. Trotz vielversprechender präklinischer Daten hängt die klinische Anwendung von hCMPCs von der Verfügbarkeit von Herzgewebe ab und ist mit patientenassoziierten Komorbiditäten verbunden, die letztendlich das therapeutische Potenzial der Zellen beeinflussen können. Aufgrund der multipotenten Natur von hCMPCs besteht eine weitere Herausforderung darin, das Schicksal dieser Zellen vorherzusagen, wenn sie in das Myokard transplantiert werden. Das Ziel der vorliegenden Arbeit bestand daher darin, diese Sca-1-positiven Zellen näher zu untersuchen.

In dieser Arbeit wurden Sca-1-positive Zellen aus induzierten pluripotenten Stammzellen (hiPSCs) isoliert und einer Kardiomyozyten-Differenzierung unterzogen. Sie waren hochproliferativ, exprimierten CD105 und ähnelten fötalen hCMPCs. Eine Expression von CD34 und CD45, zwei Marker für endotheliale Vorläuferzellen, wurde nicht nachgewiesen. Im Gegensatz dazu waren 84% der isolierten iCPC$^{Sca-1}$s positiv für kardiales Troponin I und 15% der Zellen exprimierten NKX 2-5, zwei Marker, die mit der kardialen Linie assoziiert sind. Morphologische Veränderungen und eine erhöhte α-Aktinin-Expression während der Kultivierung in Differenzierungsmedium deuteten zudem darauf hin, dass iCPC$^{Sca-1}$s möglicherweise ein kardiomyogenes Potenzial besitzen. Um den Wnt-Signalweg zu modulieren, welcher die Differenzierung von Herzvorläuferzellen in Kardiomyozyten steuert, wurde ein konditionelles Genexpressionssystem mit der RNA-Interferenz (RNAi)-Technologie kombiniert. Experimente in einer HeLa-Reporterzelllinie zeigten, dass eine homogene und robuste Induktion der RNAi-Expression durch die Insertion von Genregulationselementen in verschiedene Genomloci erreicht wird. In dieser Konfiguration resultierte die Stummschaltung von β-Catenin, einem wichtigen Wnt-Mediator, in einem 85%igen β-Catenin-Knockdown in hiPSCs. Zudem führte die Stummschaltung von β-Catenin in von hiPSC-abgeleiteten Mesodermzellen für 4 Tage

zu einer annähernden Verdreifachung der Anzahl von kardialen Troponin T-positiven Zellen am Tag 11 der Differenzierung im Vergleich zu unbehandelten Zellen. Daher kann die Stummschaltung von β-Catenin eine vielversprechende Strategie zur Erhöhung der Umwandlungsrate von Mesodermzellen in Kardiomyozyten sein.

# 1 Introduction

## 1.1 Cardiovascular diseases: a socio-economic burden

Cardiovascular diseases (CVDs) are the leading cause of death globally (1). In Europe, it is estimated that CVDs account for 45% of all deaths and cost the European Union (EU) economy €210 billion a year, of which 53% are healthcare costs (2).

The main risk factors in the development of CVD include genetic predisposition, hypertension, diabetes, obesity, and smoking (3). By addressing lifestyle choices such as unhealthy diet, physical inactivity, and tobacco use, 80% of premature deaths caused by CVD could be avoided (4). However, despite preventive measures such as nutrition education, the prevalence of obesity has increased in the EU (2), suggesting that CVD will continue to be a key health issue in the coming decades.

Ischaemic heart disease, which can lead to myocardial infarction (MI), is the most common type of death related to CVD affecting over 800,000 patients every year in the EU (2). The gold standard treatments are heart transplants, limited by donor-availability, and left ventricle assist devices. The latter only offers mechanical support until a heart transplant is available but has no curative effect as seen by recurrent cardiovascular events and short lifespan after treatment. Current treatments are not only suboptimal for patients, but also represent a socio-economic burden that costs the EU economy €39 billion each year in healthcare- and non-healthcare-related costs (2). As a result, curative treatments offering long-term solutions by for instance limiting ischemic injury shortly after infarction or regenerating and replacing damaged tissue have been a major focus in cardiovascular research.

Atherosclerosis, or narrowing of the arteries due to plaque accumulation, often precedes MI. During MI, this blockage leads to vessel occlusion and thus ischemia, which causes massive cell death in the affected area. The damage can be greater when the occluded vessel is opened, known as reperfusion injury. Unlike lower vertebrates, which can grow large areas of functional myocardium after amputation via cardiomyocyte (CM) proliferation (5), humans clearly lack the ability to overcome ischemic injury damage. In the human heart, dead tissue is replaced by non-contractile scar tissue in an attempt to preserve heart integrity and, if untreated, can lead to progressive heart failure.

Cardiac cell therapy aims to provide the infarcted myocardium with cells that will engraft, proliferate and differentiate, thereby substituting the scar for a new healthy tissue (direct

approach). In turn, the transplanted cells may also activate beneficial mechanisms, including pro-angiogenic, anti-fibrotic and anti-inflammatory processes –known as cardioprotective mechanisms (indirect approach). These mechanisms will potentiate the overall healing response and can be provided by cells or cell-derivatives such as extracellular vesicles (6). Cardiac cell therapy has thus the potential to stabilize or even revert heart failure and could be a game changer in the treatment of MI. However, although conceptually attractive, the promise of cell therapy-mediated regeneration for the heart is so far unfulfilled.

Clinical studies of heart-targeted cell therapies began two decades ago with autologous skeletal myoblasts and showed efficacy at the expense of increased arrhythmogenesis (7). Later, bone marrow cells were claimed to be able to generate *de novo* myocardium in mice (8). Despite this discovery was immediately discredited (9), numerous clinical trials using bone marrow cells or purified populations such as mesenchymal stromal cells have followed.

The benefits of adult progenitor cell therapy still remain uncertain due to controversial and insufficiently designed studies (10–12). Notably, the reported therapeutic benefits is inversely correlated to the study quality (12). Nevertheless, heart therapy with autologous and allogeneic adult progenitors is considered safe based on the results of clinical trials such as the POSEIDON (NCT01087996), ATHENA (NCT01556022) and MyStromalCell (NCT01449032) among other (13–15). In addition, despite some trials show short term benefits, studies like the 3-year follow up from the MyStromalCell trial do not report lasting benefits (16).

In a nutshell, current cell therapies are safe but do not provide long-term benefits for patients suffering from ischemic cardiomyopathy as they do not show regenerative potential. In other words, indirect mechanisms described mainly for stromal cells might not be sufficient to induce sustained and long-term beneficial effects in cardiac function (17). As a consequence, promoting myogenesis by the addition of cells with cardiomyogenic potential has been contemplated as a promising alternative to overcome the limitations of current cardiac cell therapy strategies.

## 1.2 Heart regeneration

Adult lower vertebrates like the zebrafish are able to fully regenerate their heart after ventricular injury or amputation, mainly by de-differentiation and proliferation of the remaining CMs (5). Although adult mammals fail to regenerate the heart, the existence of a developmental program leading to heart regeneration in the early stages of mammals' life has motivated years of research in heart homeostasis and regeneration. If the human heart had some endogenous regenerative abilities, these could be therapeutically supported to promote heart regeneration after ischemia.

The mammalian heart consists of a mosaic of cell types, including atrial and ventricular CMs, cardiac fibroblasts, endothelial cells, smooth muscle cells, and cells forming the conduction system such as pacemaker cells and those forming Purkinje fibers. In the quest to find cells with cardiomyogenic potential, answers to questions like: "How is this variety of cells generated and maintained? Is there a common cell ancestor that gives rise to these diverse cell types? Do any of these cells persist after birth, and if so could they be used in either *in vivo* or *ex vivo* regeneration of specific heart components?" lie at the core of modern regenerative medicine (18).

Although initially considered a post-mitotic organ (19), compelling evidence has accumulated in the last decades suggesting that the adult human heart might be responding to external triggers (**Figure 1**). For instance, an increase in muscle fibers has been reported upon cardiac overload (20), as well as mitotic figures and signs of DNA synthesis upon cardiac stress, injury, and homeostasis (21,22). These observations raised the question of whether the heart could undergo some kind of regenerative process after injury.

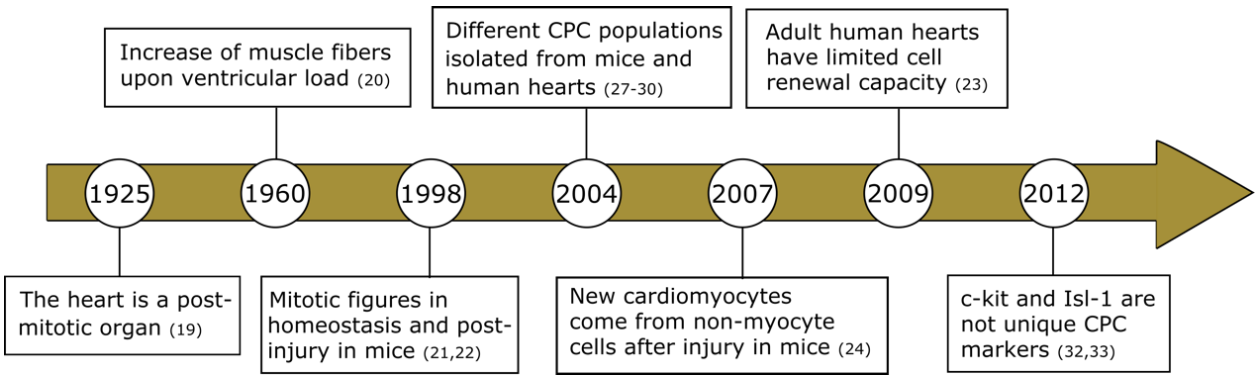


***Figure 1. Main discoveries in heart regeneration***

To date, the most definitive evidence that human CM are renewed during the adult life was provided by Bergmann and colleagues (23). By using DNA radiocarbon dating, the authors calculated that CM renewal ranges for 0.5-1% per year. This translates into about half of an individual's CMs being replaced over an average lifespan at a rate that decreases with age. Although these studies provided sound evidence of CM renewal, they did not provide insights about the origin of these new CMs; *i.e.,* if they originate from resident progenitor cells, CMs proliferation or through transdifferentiation of other cells in the heart. To tackle this question, Hsieh *et al*. used green fluorescent protein (GFP)-labeled CMs in a mouse model, and observed that the percentage of GFP-labeled CMs decreased after MI. The authors concluded that the new CMs had originated from a GFP-negative progenitor (24). Along with this observation, the discovery of different myocardium resident cells based on markers such as tyrosine kinase receptor (c-kit) (25,26), stem cell antigen-1 (Sca-1) (27,28), side population (SP) (29) or Islet-1 (Isl-1) (30) raised the question of whether these resident cells were contributing to the observed CM renewal. In fact, c-kit, Sca-1, or SP cell populations re-enter the cell cycle when growth of the heart is attenuated, proliferate in culture, and form cells expressing cardiac markers (31). The last suggests that some of these progenitor-like cells might be contributing to CM renewal after heart injury. Unfortunately, the validity of the markers used to identify true CPCs have been called into question and still remain controversial. For instance, lineage-tracing studies in mice showed that Isl-1 and c-kit co-localize with other cell type markers such as sinoatrial node cells, and endothelial cells, respectively (32,33). In turn, expression of Sca-1 in the hematopoietic lineage raised the question of whether the Sca-1 positive cells found in the adult mice heart might have extracardiac origin (34).

Regardless of cell origin, the emerging consensus is that c-kit and Sca-1 positive cells reside in the adult heart and have cardiomyogenic potential, yet none are capable of regenerating the damaged heart to a physiologically meaningful extent (35,36). Therefore, the *ex vivo* expansion or manufacturing of these populations arise as promising strategies to enhance the intrinsic regenerative potential of the heart.

## 1.3 Human cardiac progenitor cells for regenerative medicine

Cardiac progenitors have self-renewal properties and can thus technically be isolated from the heart and expanded *in vitro* before transplantation. To date, different myocardium-resident CPCs have been identified in human hearts either using mouse CPC markers, including c-kit (37), Sca-1 (28) and Isl-1 (38,39), or based on their ability to form cardiospheres – known as cardiosphere-derived cells (CDCs) (40) (**Table 1**).

***Table 1. Simplified list of different cardiac progenitor cells populations isolated from human adult, fetal and post-natal hearts.*** *Associated markers and functionality in vitro and in vivo are also listed. CM: cardiomyocyte; EC: endothelial cell; SMC: smooth muscle cell; LVEF: Left ventricular ejection fraction; LV: left ventricle; n.d. not determined.*

| Population | Phenotype | Differentiation in vitro | in vivo | Ref. |
|---|---|---|---|---|
| c-kit+ | CD34-, CD45-, Sca-1+, Abcg2+, CD105+, CD166+. GATA4+, NKX2-5+/-, MEF2C+ | CM, EC, SMC | Attenuation of chamber dilation, improvement of ventricular function | (37,41) |
| Sca-1+ | CD105+, CD34-, CD45-, c-KIT+/-, GATA4+, NKX2-5+/-, MEF2C+ | CM, EC, SMC | New cardiac tissue, improved LVEF, and reduced LV remodeling | (28,41,42) |
| CDC | CD31+, CD34+, c-KIT (low), Sca-1+, CD45+, CD105+, ABCG2+ | CM, EC, SMC | Improved LVEF and wall thickness, reduced infarct size | (40,41) |
| Isl-1+ | CD31-, Sca-1-, c-KIT+/-, GATA4+, NKX2.5+ | Right ventricle, atria, outflow cells, and cardiac neural crest | n.d. | (30,41) |

Preclinical studies have confirmed that adult CPC therapy is beneficial for the myocardium as it improves left ventricular function and reduces adverse remodeling

(**Table 1**). The mechanisms of action involve direct and indirect pathways leading to induced angiogenesis, increased viable heart muscle mass, enhanced cell survival by preventing ageing, and reduced inflammation and scar size (**Figure 2**) (6). Novel research venues focus on the indirect mechanisms, usually extracellular vesicle-mediated, and have shown that they modulate extremely specific gene regulatory pathways (43).

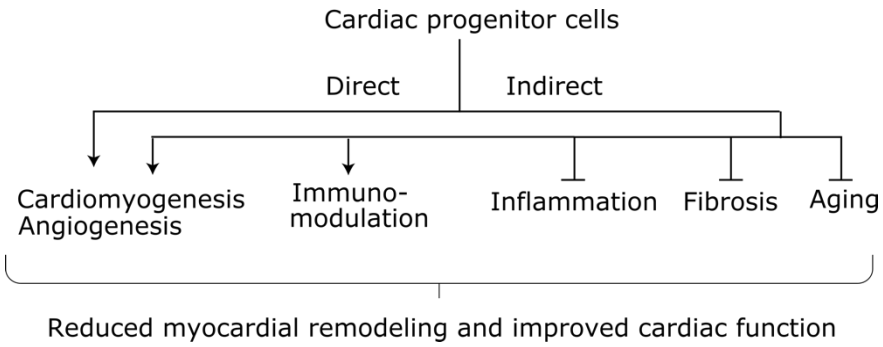


***Figure 2. Direct and indirect mechanisms of action of cardiac progenitor cells.*** *Adapted from* (6)*. Processes that can be stimulated by these mechanisms are indicated with arrows, and processes that can be inhibited, by lines.*

However, similar to other adult progenitors, clinical studies with CPCs have so far demonstrated safety and only shown a modest effect on cardiac function (44,45). The latter suggests that the injected CPC might have similar shortcomings as other adult progenitors. For instance, pre-clinical studies have shown that fetal and adult CPC have different developmental potential suggesting that age and possibly donor morbidity affects the quality of the cells (46). To avoid the ethical dilemma of using fetal cells to obtain high quality cells for cell therapy, the possibility of generating *de novo* heart tissue from ethically uncharged sources like human induced pluripotent stem cells has been intensively investigated.

## 1.4 Human pluripotent stem cells as a source of *de novo* cardiac progenitors

Human pluripotent stem cells (hPSCs), including embryonic stem cells (hESCs) and induced pluripotent stem cells (hiPSCs), which can recapitulate heart development *in vitro*, were initially regarded as the ultimate source of *de novo* CM. Pre-clinical studies in large animals have shown that hiPSC-derived cardiomyocytes (hiPSC-CM) electrically couple with host CMs (47,48). Yet that is at the cost of an increased incidence of

ventricular tachycardia, thereby increasing the risk of arrhythmias (48). The most accepted explanation is that current differentiation protocols fail to recreate the developmental spatial-temporal cues needed to promote full maturation of hiPSC-CM, which eventually have a fetal-like phenotype (49).

hPSCs have also been instrumental in identifying and characterizing progenitor cell populations in the early stages of human cardiac development and could therefore be a potential source of *de novo* CPC-like cells.

Current strategies to obtain *de novo* CPCs from hPSCs rely on differentiation towards mesoderm and cardiac lineages followed by isolation of CPCs based on surface markers (*e.g.,* SSEA-1, KDR, PDGFR-α) or reporter gene expression in genetically engineered hiPSC. Also, direct CPC differentiation protocols using chemically defined media have recently been published (**Table 2**) (50). Several strategies to induce CM lineage differentiation of hPSC include the formation of embryoid bodies, monolayer cultures supplemented with growth factors, serum or small molecules, matrices or inductive co-cultures (51). All these hPSC differentiation processes are thought to proceed through a similar hierarchy of CPCs as described for cardiac development in mammals (52).

Briefly, the earliest precursors originate in the mesoderm germ layer, marked by T-box transcription factor Brachyury, and transition to expressing mesoderm posterior 1 (MESP1) (53). MESP1- expressing cells encompass all cardiac progenitor cells, but have not yet committed to the cardiac fate (54). These cells expand rapidly, and ultimately segregate into two spatially and temporally distinct cardiogenic heart fields. The first heart field, marked by TBX5, NKX 2-5 and HCN4, will contribute to the left ventricle (55,56), and the second heart field, marked by NKX 2-5, ISL-1 and MEF2C will develop right ventricle, atria, and the outflow tracts (57). At this stage the heart precursor cells have irreversibly committed to the cardiac lineage and will become cardiac progenitor cells. Finally, the epicardial lineage, marked by TBX5, TBX18 and WT1, will further differentiate into CMs, smooth muscle cells, endothelial cells and fibroblasts (58).

***Table 2. Strategies to derive cardiac progenitor cells from human iPSC or ESC and current limitations****. CM: cardiomyocyte; EC: endothelial cell; SMC: smooth muscle cell; (¥) in vitro, (‡) in vivo, n.d: not determined*

| Marker | CPC-markers | Differentiation | Expansion | Limitations | Ref. |
|---|---|---|---|---|---|
| (i) | **Surface marker isolation** | | | | |
| SSEA-1 | OCT4+, SSEA-1+, MESP1+, GATA4+, MEF2C+, NKX 2-5+, ISL1+, | CM, EC, SMC (¥)<br>CM (‡) | Clonal expansion | Heterogeneous CPC population: early and late CPC-markers<br>Only one ESC line tested<br>No long-term expansion | (59–63) |
| KDR low/ C-KIT- cells | n.d. | CM, EC, SMC (¥)<br>EC (‡) | n.d. | Low yield due to multiple sorting steps<br>No engraftment reported in diseased hearts | (64,65) |
| KDR/ PDGFR-α | n.d. | CM (¥) | n.d. | iPSC line variability<br>Presence of this population does not correlate to CM differentiation | (66) |
| (ii) | **Reporter-based isolation** | | | | |
| ISL-1 | NKX 2-5+, KDR+, MESP1+, TXB20+, GATA4+ | CM, EC, SMC (¥) (‡) | n.d. | No expansion reported<br>Effect in cardiac function not assessed | (67) |
| ISL-1+ CD24 - | ISL1+, MESP1+, GATA4+, MEF2C+, T-BRACHURY+ | CM, EC, SMC (¥ )(‡) | Clonal (30 passages) | Differentiation potential *in vivo* is affected by expansion<br>Mainly EC differentiation at high passage<br>Effect in cardiac function not assessed | (68,69) |

| | | | | | |
|---|---|---|---|---|---|
| NKX 2-5 | n.d. | CM, EC, SMC (¥)<br>CM, EC, SMC (‡) | >40 population doublings | C-MYC mediated expansion<br>Limited expandability<br>No cardiac function improvement | (70–72) |
| (iii) **Chemically-defined media** | | | | | |
| BMP4, CHIR99021, AA, ROCK inhibitor | SSEA-1+ MESP1/2+ ISL1+ GATA4+ MEF2C+ | CM, EC, SMC (¥) | $10^7$ expansion | Only one iPSC line tested<br>Heterogeneous CPC population: early and late CPC-related markers co-expressed<br>Subculturing leads to a decrease in the proliferation rate<br>Differentiation in vivo not fully assessed | (73,74) |
| CHIR99021 | MESP1+ NKX2.5+ ISL1+ MEF2C+ PDGFRa + | CM, EC, SMC(¥)<br>SMC (‡) | Similar to (73) | Only SMC differentiation in vivo<br>CM differentiation *in vivo* not proved | (75,76) |

Consensually*, de novo* CPC's identity is confirmed by the expression of CPC-related markers, the ability to self-renew for at least 30-40 passages and to differentiate into CM, endothelial and smooth muscle cells *in vitro* and *in vivo*. Unfortunately, current strategies fail to generate *de novo* CPCs that fulfill all these criteria (**Table 2**). Generally, cells that phenotypically resemble CPCs do not hold proliferative capacity or proliferate at the expense of multipotency loss. To increase proliferation capacity, immortalization strategies by forced expression of oncogenes such as C-MYC have been employed (70). However, this hinders clinical translation as it increases the risk of tumorigenesis upon transplantation. Likewise, in the case of surface marker-based isolation such as stage specific embryonic antigen 1 (SSEA-1), the resulting cells are too early in development and express pluripotent factors such as OCT4, which raises the concern of tumor development from remaining hPSCs (60). Similar concerns apply to CPC-like cells generated using chemically induced protocols without additional enriching steps, which

essentially leads to a mixture of cells at different stages of development (73). In addition, these protocols are bound to vary from batch-to-batch and may have unpredictable therapeutic effects. In this context, the use of widely studied CPC-associated surface markers such as Sca-1 may be advantageous to select proliferative CPCs.

Sca-1 is a member of the Ly-6 family that was first reported as a hematopoietic stem cell surface marker in mouse (77). Although Sca-1 has not been described in humans (78), Sca-1 positive cells can be reproducibly isolated from fetal and adult human hearts with the anti-Sca-1 mouse antibody (28,79). These so-called human cardiomyocyte progenitor cells (hCMPCs) resemble clonally isolated cells from the heart, and express Isl-1, c-kit, CD31, GATA-4 and NKX 2-5 (46,80). hCMPCs can be expanded and differentiated into electrically mature CMs *in vitro* (28,81) and generate new cardiac tissue of human origin when injected in the infarcted myocardium of mice (42). In addition, hCMPCs show long-term benefits in cardiac function as assessed by higher ejection fraction and reduced left ventricular remodeling in mice (42). Also, it has recently been shown that Sca-1 cells contribute to CM mass during mice embryonic development (82), suggesting that hCMPCs could also be obtained from human embryos. In this thesis, the possibility to isolate Sca-1 positive cells from hiPSCs undergoing CM differentiation will be investigated as a potential strategy to obtain fully competent *de novo* CPCs from an ethical source of cells.

In addition to tumorigenesis due to residual oncogene expression, arbitrary differentiation upon transplantation is also a challenge when using multipotent stem cells. In fact, although CM differentiation *in vivo* has been reported with some *de novo* CPCs (**Table 2**) most of them differentiate mainly into endothelial and smooth muscle cells (64,69,75). As a result, strategies to modulate cell fate toward CM upon transplantation would not only be beneficial to reduce the risk of aberrant replication *in vivo,* but also to ensure that new heart muscle is regenerated.

## 1.5 Conditional modulation of cardiac progenitor cell fate

With the growing understanding of cell phenotype and cell differentiation, it has become increasingly possible to manipulate cells to produce effective customized cell products for regenerative medicine. In this context, synthetic gene systems such as Tetracycline controlled transcriptional activation systems (Tet systems) could be used to temporarily

modulate key signaling pathways involved in cell differentiation to ensure that myocyte biomass is formed after the cells have been implanted.

Tet systems can be divided into Tet-OFF and Tet-ON types based on whether gene expression is allowed in the absence or presence of small doses of tetracycline antibiotics. Concretely, the Tet-ON system, which supports gene expression in the presence of doxycycline (DOX), a tetracycline derivative, consists of two elements: (i) a constitutively expressed transcriptional activator protein responsive to DOX, called reverse tetracycline-controlled transactivator (rtTA), and (ii) the inducible Tet promoter formed by the tetracycline response element (TRE) fused to a minimal promoter that is regulated by the rtTA and conditionally drives expression of the transgene of interest (83). Originally, the Tet-ON system relied on introducing both elements in two subsequent rounds of genetic engineering until Tet-ON-all-in-one single vectors were developed to deliver all the elements within a single gene construct (**Figure 3**).

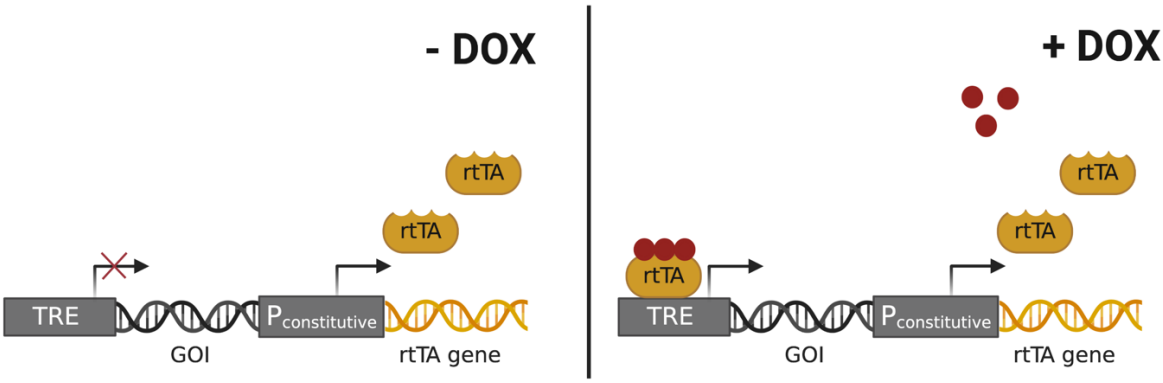


***Figure 3. Tet-ON controlled gene expression in a Tet-ON-all-in-one vector.*** *TRE: tetracycline response element; GOI: gene of interest; $P_{constitutive}$: constitutive promoter; rtTA: reverse tetracycline-controlled transactivator; DOX: doxycycline. Created with BioRender.com*

During development, cells up- and down-regulate gene expression of key regulatory molecules according to decision-making checkpoints *e.g.*, pluripotent stem cells to mesoderm cells. Thus, by inducing or repressing signaling pathways that may modulate competing gene expression, cell fate commitment can be exogenously steered during *in vitro* differentiation. For instance, Wnt/β-catenin signaling is an attractive strategy.

The Wnt/β-catenin signaling pathway has vital functions during embryonic development, adult homeostasis, and tissue and organ regeneration (84). Concisely, the activation of

this pathway relies on the availability of Wnt ligands such as *Wnt11*, the expression of Frizzled receptors, and the co-receptor low-density lipoprotein receptor related proteins 5/6 (Lrp5/6) in the target cell. In the presence of Wnt ligands, "WNT-on-state", the ligand-receptor interaction stabilizes the downstream effector molecule, β-catenin. Cytoplasmic β-catenin is translocated into the nucleus, where it transactivates target genes expression in a complex with lymphoid enhancer-binding factor (TCF/LEF) (**Figure 4**) (84). When Wnt ligands are absent or sequestered by secreted frizzled related proteins (SFRP), "WNT-off-state", β-catenin is phosphorylated by a cytoplasmic complex of proteins that includes the glycogen synthase kinase 3β (GSK3β), the scaffolding protein Axin, and the tumor suppressor adenomatous polyposis coli (APC). Phosphorylated β-catenin is ubiquitinated and targeted for degradation by the proteasome pathway (**Figure 4**) (84).

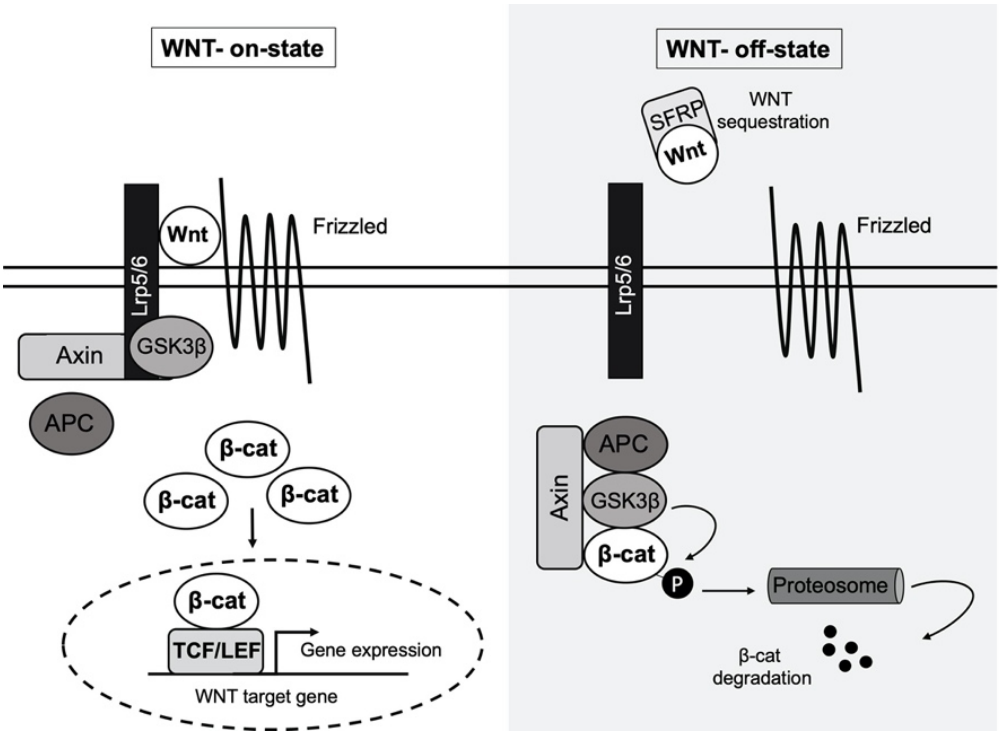


***Figure 4. Canonical Wnt signaling pathway (simplified)**. Lrp5/6, low-density lipoprotein receptor related proteins 5/6. Wnt: Wnt ligands; GSK3β: glycogen synthase kinase 3β; APC: adenomatous polyposis coli; β-cat: β-catenin; TCF/LEF: lymphoid enhancer-binding factor; SFRP: secreted frizzled related proteins.*

During *in vitro* differentiation of hiPSCs the WNT-on-state is necessary to induce mesoderm cell commitment, followed by a WNT-off-state to further modulate differentiation of cardiac mesoderm cells into CMs (85). The exogenous modulation of the Wnt/β-catenin signaling pathway could be brought about by a plethora of pathway

inhibitors (86) or by RNA interference (RNAi)-mediated knockdown of Wnt mediators such as β-catenin (85).

RNAi is an evolutionarily conserved mechanism of post-transcriptional gene regulation that uses small RNAs produced by multi-complex machineries to control the suppression of complementary transcripts. The most extensively characterized endogenous RNAi triggers are microRNAs (miRNAs). miRNAs are expressed as hairpin-like structures in primary transcripts (pri-miRNAs), which are translocated to the cytoplasm as precursor miRNAs (pre-miRNAs), where they are further processed into mature small RNA duplexes ("stem") (87–89). A myriad of synthetic RNAi triggers has been developed mimicking miRNAs at different stages of their maturation pathway. While small interfering RNAs (siRNAs) – equivalent to RNA duplexes – provide an efficient approach for transient gene knockdown, short hairpin RNAs (shRNAs) – equivalent to pre-miRNAs – can be expressed from DNA vectors that enable stable and regulated expression (**Figure 5**). However, shRNA enforced expression can saturate endogenous miRNA pathways and result in severe cell toxicity (90). Alternatively, synthetic shRNA stems can be embedded into the context of endogenous miRNAs that can be integrated into the cell genome. The resulting structures named shRNAmir serve as natural substrates in miRNA biogenesis pathways and can trigger potent knockdown (91). shRNAmir systems such as the miRE developed by Fellmann *et al*. (91) offer several advantages when compared with shRNA or siRNA: (i) miRE can be expressed from tissue-specific polymerase-II promoters and enables tissue-specific expression as well as remote control of expression when combined with Tet systems; (ii) miRE is less prone to cause toxicity by interfering with endogenous miRNA pathways (92); and finally, (iii) miRE leads to 10- to 30-fold higher mature small RNA levels, even when expressed under low- or single-copy conditions (91).

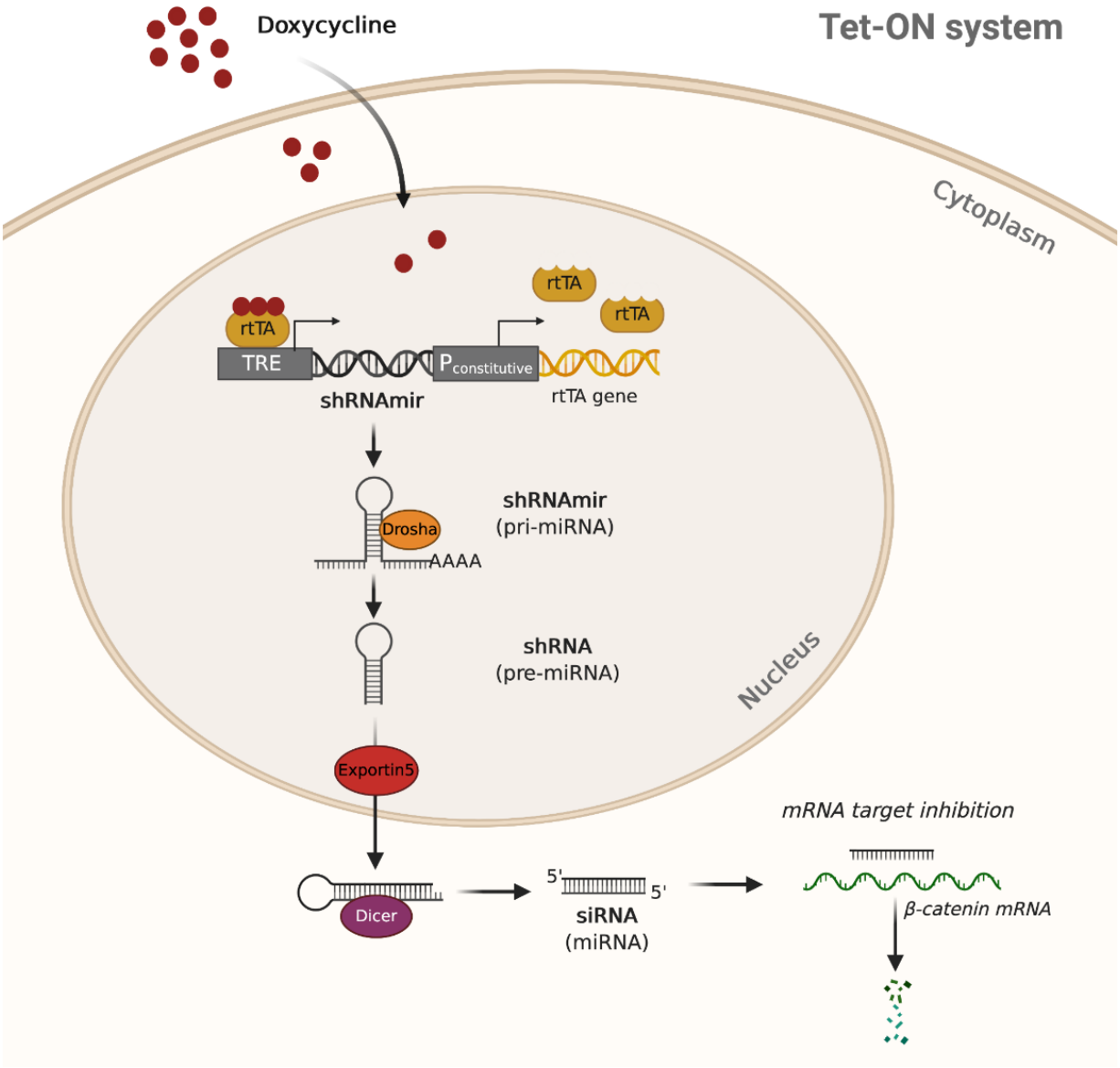


***Figure 5. Tetracycline controlled shRNAmir expression and miRNA biogenesis.*** *For simplicity, not all the factors involved in miRNA biogenesis are shown. Synthetic silencing RNA names are shown in bold and the equivalent biologic miRNA is indicated in brackets. Created with BioRender.com.*

For stable chromosomal integration into the genome of the therapeutic cells, the genes of interest can be delivered to the target cells using lentiviral particles, non-viral vectors such as transposons (*e.g.*, *Sleeping Beauty* or *Piggybac* transposon systems), or by site-specific recombination technology such as Zinc-finger nucleases (ZFN) or CRISPR-Cas9 technology. In this thesis, different gene delivery strategies are investigated to deliver Tet promoter-driven expression of miREs targeting β-catenin with the aim to modulate cell

fate in hiPSC-derived cardiac mesoderm cells. Unlike small molecule-mediated modulation, this strategy is cell-specific and will only modulate Wnt signaling in the modified cells that have been implanted into the heart.

## 1.6 Aims

This work aimed to explore solutions to overcome the current challenges associated with CPC-based therapies, such as the uncontrolled differentiation of CPCs after implantation or the limited availability of healthy CPCs. The aims are based on the following hypotheses:

I. Remote control of the Wnt signaling pathway is sufficient to steer differentiation of hiPSC-derived cardiac mesoderm cells into CMs.

II. Sca-1 positive CPCs can be derived from hiPSCs.

Accordingly, the results in this thesis are divided into two main chapters:

I. “Conditional expression of miREs to modulate the Wnt signaling pathway”, which includes Tet-ON system optimization experiments in a HeLa reporter cell line.
II. “Expandable Sca-1-positive CPC-like cells from hiPSCs”, which describes a differentiation protocol and includes a phenotypical characterization of hiPSC-derived CPC-like cells.

# 2 MATERIALS AND METHODS

# 2.1 Materials

## 2.1.1 Reagents

***Table 3. List of reagents***

| Product name | Cat. number | Manufacturer/supplier |
|---|---|---|
| Accutase® Cell Detachment Solution | 423201 | BioLegend, Inc. |
| Agarose broad range | T846.3 | Carl Roth GmbH + Co. KG |
| Alt-R® Cas9 Nuclease 3NLS | 1081058 | Integrated DNA Technologies, Inc. |
| Alt-R® CRISPR-Cas9 tracRNA | 1072534 | Integrated DNA Technologies, Inc. |
| Bambanker™ serum-free freezing | BB01 | Lymphotec Inc., Nippon Genetics |
| BamHI-HF® restriction enzyme | R3136S | New England Biolabs, Inc. |
| B-27 minus Insulin (50x) | A1895601 | Gibco™, Thermo Fischer Scientific Inc. |
| B-27 supplement (50x), serum-free | 17504044 | Gibco™, Thermo Fischer Scientific Inc. |
| B-27 supplement without vitamin A (50x) | 12587010 | Gibco™, Thermo Fischer Scientific Inc. |
| Bone morphogenetic protein 4 (BMP4) | 120-05ET | PeproTech, Inc |
| Bovine Serum Albumin (BSA) | 8076.2 | Carl Roth GmbH + Co. KG |
| cDNA Synthesis (Maxima First Strand cDNA Synthesis Kit for RT-qPCR) | K1632 | Thermo Fischer Scientific Inc |
| CHIR99021 | SML1046 | Sigma-Aldrich, Merck KGaA |
| DAPI (4',6-Diamidino-2-Phenylindole, dihydrochloride) | D1306 | Invitrogen, Thermo Fischer Scientific Inc. |
| DAPI staining solution | 130-111-570 | Miltenyi Biotec, GmbH |
| DH5α Competent Cells | 18265017 | Thermo Fischer Scientific Inc. |
| Distilled Water (UltraPure™ DNase/RNase-Free Distilled Water) | 10977035 | Gibco™, Thermo Fischer Scientific Inc. |
| DMEM, high glucose, GlutaMAX™ Supplement | 10566016 | Gibco™, Thermo Fischer Scientific Inc. |
| DMSO (Dimethyl sulfoxide) | A3672,0050 | AppliChem GmbH |

| | | |
|---|---|---|
| Doxycycline monohydrate, 97% | 458890250 | Acros Organics™, Thermo Fischer Scientific Inc. |
| Dulbecco's Phosphate-Buffered Saline without $MgCl_2$/ $CaCl_2$ (PBS) | 14190144 | Gibco™, Thermo Fischer Scientific Inc |
| Dulbecco's Phosphate-Buffered Saline with $MgCl_2$/$CaCl_2$ (PBS+) | 14040091 | Gibco™, Thermo Fischer Scientific Inc. |
| EcoRI-HF® restriction enzyme | R3101S | New England Biolabs, Inc. |
| Ethylenediaminetetraacetic acid (EDTA) | 8043.3 | Carl Roth GmbH + Co. KG |
| EGM-2 (EGM™ 2 Endothelial Cell Growth Medium-2 BulletKit™) | CC-3162 | Lonza Group AG |
| Ethanol | 9065.1 | Carl Roth GmbH + Co. KG |
| Ethidium Bromide solution | 15585-011 | Invitrogen, Thermo Fischer Scientific Inc. |
| Essential 8™ medium | A1517001 | Gibco™, Thermo Fischer Scientific Inc |
| Fetal Bovine Serum (FBS) | 10270106 | Gibco™, Thermo Fischer Scientific Inc. |
| Fibroblast Growth Factor-2 (FGF-2) | 100-18B | PeproTech, Inc. |
| Gel Loading Dye, Purple (6X) | B7024S | New England Biolabs, Inc. |
| Gelatin from bovine skin | G9391 | Sigma-Aldrich, Merck KGaA |
| Geltrex™ | A1413202 | Gibco™, Thermo Fischer Scientific Inc. |
| HCS CellMask™ Blue Stain | H32720 | Invitrogen, Thermo Fischer Scientific |
| HyperLadder™ 1kb | BIO-33053 | Bioline © |
| IWR-1-endo | S7086 | Selleck Chemicals LLC |
| KnockOut™ DMEM/F-12 | 12660012 | Gibco™, Thermo Fischer Scientific Inc. |
| KpnI-HF® restriction enzyme | R3142S | New England Biolabs, Inc. |
| LB agar | X965.3 | Carl Roth GmbH + Co. KG |
| LB medium | X946.1 | Carl Roth GmbH + Co. KG |
| Lipofectamine™ 2000 Transfection Reagent | 11668019 | Invitrogen, Thermo Fischer Scientific Inc. |
| Lipofectamine™ 3000 Transfection Reagent | L3000015 | Invitrogen, Thermo Fischer Scientific Inc. |

| | | |
|---|---|---|
| Lipofectamine™ RNAiMAX Transfection Reagent | 13778100 | Invitrogen, Thermo Fischer Scientific Inc. |
| Medium 199 (M199) + GlutaMAX™ | 41150020 | Gibco™, Thermo Fischer Scientific Inc. |
| MEM non-essential amino acids | 11140035 | Gibco™, Thermo Fischer Scientific Inc. |
| 2-Mercaptoethanol (50mM) | 31350010 | Gibco™, Thermo Fischer Scientific Inc. |
| MluI-HF® restriction enzyme | R3198S | New England Biolabs, Inc. |
| MS Columns | 130-042-201 | Miltenyi Biotec, GmbH |
| mTeSR™1 medium | 85850 | Stem Cell Technologies™ |
| Natriumazid >99% ($NaN_3$) | K305.1 | Carl Roth GmbH + Co. KG |
| NdeI restriction enzyme | R0111S | New England Biolabs, Inc. |
| Neomycin, G418 sulfate | BP6731 | Fisher Scientific, Thermo Fischer Scientific Inc |
| Nuclease-free duplex buffer | 11-05-01-12 | Integrated DNA Technologies, Inc. |
| Opti-MEM™ I Reduced Serum Medium, no phenol red | 11058021 | Gibco™, Thermo Fischer Scientific Inc |
| Paraformaldehyde (PFA) | 0335.3 | Carl Roth GmbH + Co. KG |
| Penicillin/Streptomycin (P/S) | 15140122 | Gibco™, Thermo Fischer Scientific Inc. |
| Puromycin | ant-pr-1 | InvivoGen © |
| Propidium Iodide solution | 130-093-233 | Miltenyi Biotec, GmbH |
| Quick Ligation kit ™ | M2200S | New England Biolabs, Inc. |
| Q5® High-Fidelity 2X Master Mix | M0492S | New England Biolabs, Inc. |
| RNaseZap® | AM9784 | Applied Biosystems, Thermo Fischer Scientific Inc. |
| ROCK inhibitor | 253-00513 | FUJIFILM Wako Pure Chemical Corporation |
| RPMI 1640 Medium, GlutaMAX™ | 61870010 | Gibco™, Thermo Fischer Scientific Inc. |
| SalI-HF® restriction enzyme | R3138S | New England Biolabs, Inc. |
| SpeI-HF® restriction enzyme | R3133S | New England Biolabs, Inc. |
| SYBRGreen | 4367659 | Gibco™, Thermo Fischer Scientific Inc. |

| | | |
|---|---|---|
| SOC medium | P/N 46-0700 | Invitrogen, Thermo Fischer Scientific Inc. |
| Taq 2X Master Mix | M0270L | New England Biolabs, Inc |
| TGF-ß1 | PHG9204 | Invitrogen, Thermo Fischer Scientific Inc. |
| 1-Thioglycerol | M6145-25ML | Sigma-Aldrich, Merck KGaA |
| Triton X100 | 3051.3 | Carl Roth GmbH + Co. KG |
| Trypan Blue solution | T8154 | Sigma-Aldrich, Merck KGaA |
| TrypLE™ Express Enzyme (with phenol red) | 12605010 | Gibco™, Thermo Fischer Scientific Inc. |
| Trypsin-EDTA (0.05%), phenol red | 25300054 | Gibco™, Thermo Fischer Scientific Inc. |
| XhoI-HF® restriction enzyme | R0146S | New England Biolabs, Inc |
| 100 bp DNA-Ladder | 15628-019 | Invitrogen, Thermo Fischer Scientific Inc. |
| 50 bp DNA-Ladder | 10416-014 | Invitrogen, Thermo Fischer Scientific Inc. |

***Table 4. List of kits***

| **Kit name** | **Cat. number** | **Manufacturer/supplier** |
|---|---|---|
| Anti-Sca-1 Microbeads (Cardiac Progenitor Cell Isolation Kit (Sca-1), mouse) | 130-098-374 | Miltenyi Biotec, GmbH |
| eBioscience™, Foxp3 / Transcription Factor Staining Buffer Set | 00-5523-00 | Invitrogen, Thermo Fischer Scientific Inc. |
| LIVE/DEAD™ Fixable Aqua Dead Cell Stain Kit, for 405 nm excitation | L34957 | Invitrogen, Thermo Fischer Scientific Inc. |
| NucleoSpin Gel and PCR Clean-up, Mini kit for gel extraction and PCR clean up | 740609.50 | Macherey-Nagel GmbH & Co. KG |
| NucleoSpin Plasmid, Mini kit for plasmid DNA | 740588.50 | Macherey-Nagel GmbH & Co. KG |
| NucleoSpin RNA, Mini kit for RNA purification | 740955.50 | Macherey-Nagel GmbH & Co. KG |

| | | |
|---|---|---|
| NucleoSpin Tissue, Mini kit for DNA from cells and tissue | 740952.50 | Macherey-Nagel GmbH & Co. KG |
| NucleoBond Xtra Midi EF, Midi kit for endotoxin-free plasmid DNA | 740420.50 | Macherey-Nagel GmbH & Co. KG |

***Table 5. List of antibodies.*** *FC: flow cytometry, IF: immunofluorescence*

| **Antibodies** | **Species** | **Concentration (technique)** | **Cat. number** | **Manufacturer/supplier** |
|---|---|---|---|---|
| **Primary and conjugated antibodies** | | | | |
| α-actinin | mouse | 1:800 (IF) | A7811 | Sigma-Aldrich, Merck KGaA |
| β-catenin | rabbit | 1:200 (FC) | ab32572 | Abcam plc. |
| CD34-PE | mouse | 1:20 (FC) | 12-0349-42 clone: 4H11 | eBioscience™, Thermo Fischer Scientific Inc. |
| CD45-FITC | human | 1:20 (FC) | 130-080-202 | Miltenyi Biotec, GmbH |
| CD105-APC | mouse | 1:20 (FC) | 17-1057-42 clone: SN6 | eBioscience™, Thermo Fischer Scientific Inc. |
| cardiac troponin T-APC | human recombinant | 1:50 (FC) | 130-106-689 | Miltenyi Biotec, GmbH |
| cardiac troponin I | goat | 1:100 (IF) | 4T21/2 | HyTest Ltd |
| mCherry- Alexa Fluor 596 | rat | 1:100 (FC) | M11240 clone: 16D7 | Invitrogen, Thermo Fischer Scientific Inc. |
| Nkx-2.5 | mouse | 1:100 (IF) | sc-376565 | Santa Cruz Biotechnology |
| Sca-1-PE | rat | 1:10 (FC) | 130-102-832 Clone D7 | Miltenyi Biotec, GmbH |
| **Secondary Antibodies** | | | | |
| Alexa Fluor 488 (donkey anti-mouse IgG (H+L)) | donkey | 1:200 (FC, IF) | A21202 | Invitrogen, Thermo Fischer Scientific Inc. |

| | | | | |
|---|---|---|---|---|
| Alexa Fluor 488 (Donkey anti-Rabbit IgG (H+L)) | donkey | 1:200 (FC) | A32790 | Invitrogen, Thermo Fischer Scientific Inc. |
| Alexa Fluor 647 (donkey anti-goat IgG (H+L)) | donkey | 1:200 (IF) | A21447 | Invitrogen, Thermo Fischer Scientific Inc. |

## 2.1.2 Primers and synthetic DNA probes

***Table 6. List of primer sequences used listed by purpose***

| Primer name | Sequence 5' to 3' |
|---|---|
| **Cloning** | |
| mCherry_SpeI fw | ACTTACTAGTATGGTGAGCAAGGGCGA |
| miRE-EcoRI-rv | TCTCGAATTCTAGCCCCTTGAAGTCCGAGGCAGTAGGC |
| mirE_KpnI rv | CCCGGGTACCCGCGTCAATTGAAAAAAGTGA |
| miRE-Xho-fw | TGAACTCGAGAAGGTATATTGCTGTTGACAGTGAGCG |
| pPB-mirE-NdeI fw | CTAATCATATGTGGCCTGGAG |
| pPB-mirE-Sal I rv | AATCGTCGACCATGAATGGATCCGCTGG |
| rtTA3-BamHI-fw | ATTCGGATCCATGAGTAGACTGGACAAGAGCAA |
| rtTA3-MIu-rv | AGCTACGCGTTACCCGGGGAGCATGTCAA |
| **Plasmid sequencing** | |
| bGH C-ter seq | GAAGACAATAGCAGGCATGC |
| bGH seq | AACAACAGATGGCTGGCAAC |
| CMV seq | AACCGTCAGATCGCCTGGA |
| mCherry-C Seq | CCATCGTGGAACAGTACGAAC |
| M12 seq rev | GACTTTGCTCTTGTCCAGTCT |
| M13 puc fwd | CCCAGTCACGACGTTGTAAAACG |
| ROSA-rtTA seq | CTGCTAACCATGTTCATGC |
| SV40pA-R-156-175 | GAAATTTGTGATGCTATTGC |
| **Genotyping** | |
| hAAVS1-genome (5') | CTGTTTCCCCTTCCCAGGCAGGTCC |
| hAAVS1-genome (3') | TGCAGGGGAACGGGGCTCAGTCTGA |
| mCherry-C-ter genotyping | CCATCGTGGAACAGTACGAACGCGC |
| pUC-AAVS1- vector BB (3') | ATGCTTCCGGCTCGTATGTT |
| Puro-N-ter rv | TCGTCGCGGGTGGCGAGGCGCACCG |

| **Real time- PCR** | |
|---|---|
| b-Actin fw | CGTCTTCCCCTCCATCGTG |
| b-Actin rv | TCGATGGGGTACTTCAGGGT |
| GAPDH fw | TGCACCACCAACTGCTTAGC |
| GAPDH rv | GGCATGGACTGTGGTCATGAG |
| GATA4 fw | CAACTGCCAGACCACCACC |
| GATA4 rv | CCCTCTTTCCGCATTGCAAG |
| ISL 1 fw | TGATGAAGCAACTCCAGCAG |
| ISL 1 rv | TTTCCAAGGTGGCTGGTAAC |
| Nkx2.5 fw | CCCGCCTTCTATCCACGTG |
| Nkx2.5 rv | GCCTCTGTCTTCTCCAGCTC |

***Table 7. Target specific crRNA sequences to synthesize sgRNA to knock the puromycin cassette out***

| **Guide #** | **Score** | **Seq (PAM)** | **Position** |
|---|---|---|---|
| PURO crRNA 1 | 99 | ACGCGCGTCGGGCTCGACAT (CGG) | 163 |
| PURO crRNA 2 | 98 | CACGCGCCACACCGTCGATC (CGG) | 96 |

***Table 8. List of shRNA 97-mer oligonucleotides***

| **Name** | **Sequence** |
|---|---|
| shRNA-Ren713 (miRE mock) | TGCTGTTGACAGTGAGCGCAGGAATTATAATGCTTATCTATAGTGAA GCCACAGATGTATAGATAAGCATTATAATTCCTATGCCTACTGCCTC GGA |
| shRNA-CTNNB1_2 (miRE β-cat) | TGCTGTTGACAGTGAGCGCCAAGAACAAGTAGCTGATATATAGTGAA GCCACAGATGTATATATCAGCTACTTGTTCTTGATGCCTACTGCCTC GGA |
| shRNA-d2eGFP (miRE d2eGFP) | TGCTGTTGACAGTGAGCGACCAACGAGAAGCGCGATCACATAGTGA AGCCACAGATGTATGTGATCGCGCTTCTCGTTGGGTGCCTACTGCC TCGGA |

## 2.1.3 Plasmids

***Table 9. List of plasmids***

| **Plasmid name** | **Origin** | **Description/ experiment** |
|---|---|---|
| LT3GEPIR_mCherry-miRE_ PGK_Puro _rtTA3_pA | Modified from Fellmann *et al.* (91) | Lentivirus donor plasmid/ HeLa Tet-all-in one |

| | | |
|---|---|---|
| pMD2.G | Addgene. #12259 | VSV-G envelope expressing plasmid/ HeLa Tet-all-in one |
| psPAX2 | Addgene. #12260 | 2nd generation lentiviral packaging plasmid/ HeLa Tet-all-in one |
| pPB transposase | Gossen's lab stock | Piggybac transposase/ HeLa Tet-all-in one |
| pPB-TRE_mCherry_miRE_PGK_Puro _rtTA3_pA | Modified from pPB-CAG Gossen's lab stock. | Piggybac donor plasmid/ HeLa Tet-all-in one |
| pUC_AAVS1_p-Responder-miRE | Modified from Pawlowski *et al.* (93) | Tet-ON miRE unit flanked with AAVS1 locus homology arms/ hiPSC conditional differentiation |
| pUC-ROSA26-CAG-rtTA3G/rtTA3 | Modified from Pawlowski *et al.* (93) | rtTA flanked with ROSA26 locus homology arms/ rtTA3G rescue |
| pZFN-AAVS1-L-ELD | Pawlowski *et al.* (93) | AAVS1 locus ZFN left/ hiPSC conditional differentiation |
| pZFN-AAVS1-R_KKR | Pawlowski *et al.* (93) | AAVS1 locus ZFN right/ hiPSC conditional differentiation |
| ROSA26-guideA_Cas9n | Pawlowski *et al.* (93) | Cas9 nuclease guide A/ rtTA3 rescue in ROSA 26 |
| ROSA26-guideB_Cas9n | Pawlowski *et al.* (93) | Cas9 nuclease guide B/ rtTA3 rescue in ROSA 26 |

## 2.1.4 Recipes

***Table 10. Cell culture media formulations***

| **Media** | **Composition** |
|---|---|
| Basal medium | RPMI 1640 plus B-27 minus insulin supplement (1x) |
| Cardiac priming medium | Basal medium plus 3-6 μM CHIR99021 |
| Cardiac induction medium | Basal medium plus 5 μM IWR-1 endo |
| CM differentiation medium (CDM) | Basal medium plus 10 ng/ml BMP4 and 4 or 5 μM IWR-1 endo |
| CM maintenance medium (CMM) | RPMI 1640 plus B-27 supplement (1x) |
| hCPC medium | 4:1 (M199 GlutaMAX™:EGM-2) medium plus 1% NEAA, 10% FBS (non-heat inactivated) and 1% P/S |
| DMEM | DMEM GlutaMAX™ plus 10% FBS (non-heat inactivated) and 1% P/S |

***Table 11. Buffer recipes.*** *FACS: fluorescent-activated cell sorting; MACS: magnetic-activated cell sorting.*

| Buffer | Composition |
|---|---|
| Blocking buffer | 1% BSA in PBS+ |
| FACS buffer | 0.5% BSA, 0.1% $NaN_3$ and 2 mM EDTA in PBS, 0.2 µm filtered |
| MACS buffer | 1% FBS, 2 mM EDTA in PBS |
| Permeabilization/ blocking buffer | 0.1% TritonX100, 1% BSA in PBS+ |

## 2.1.5 Instruments

***Table 12. List of instruments***

| Device | Model | Developer/Manufacturer |
|---|---|---|
| Centrifuges | Allegra™ X-15R Centrifuge | Beckman Coulter GmbH |
| | Allegra™ X-22 Centrifuge | |
| | Micro Star 17/17R | VWR International, LLC. |
| | Rotilabo®-mini-centrifuge | Carl Roth GmbH + Co. KG |
| High content screener | Operetta™ | PerkinElmer Inc. |
| | Opera Phenix™ | PerkinElmer Inc. |
| Incubator | HERAcell 240i $CO_2$ Incubator | Thermo Fischer Scientific Inc. |
| Flow cytometry device | MACSQuant® VYB | Miltenyi Biotec GmbH |
| Microscope | Nikon Eclipse Ti | Nikon Corporation |
| Microscope camera | DS-Qi2 | Nikon Corporation |
| Nanodrop | NANODROP 1000 Spectrophotometer | PEQLAB Biotechnologie GmbH |
| RT-PCR device | QuantStudio 6 Flex Real-Time PCR System | Applied Biosystems™, Thermo Fischer Scientific Inc. |
| Thermocycler | Mastercycler® pro S mit Bedienfeld | Eppendorf AG |

## 2.1.6 Software

***Table 13. List of software***

| Software | Developer |
|---|---|
| Columbus™ Image Data System, version 2.9.1 | PerkinElmer Inc. |
| FlowJo, version 10 | Becton, Dickinson and Company |
| GraphPad Prism, version 6.0 and 8.0 | GraphPad Software |
| Harmony® High-content Imaging and Analysis Software | PerkinElmer Inc. |
| ImageJ 1.440 | National Institutes of Health (NIH) |
| Inkscape, XQuartz 2.7.11 | Inkscape Project |
| MACSQuantify™, Version: 2.13.0 | Miltenyi Biotec |
| Mendeley Desktop, version 1.16.3 | Elsevier |
| Microsoft Office Professional 2011 | Microsoft Corporation |
| SnapGene®, version 3.3.4 | GSL Biotech LLC |

# 2.2 Methods

## 2.2.1 Cell culture

### 2.2.1.1 HeLa d2eGFP cells

HeLa d2eGFP cells were cultured in DMEM (**Table 10**). Medium was changed three times a week and cells were typically passaged once or twice a week in a ratio of 1:10.

### 2.2.1.2 hiPSCs

Unless otherwise stated, hiPSCs were cultured in Essential 8$^{TM}$ medium (E8 medium) on Geltrex-coated plates. Cultures were fed daily and the differentiating cells were removed regularly. Cells were passaged every 4-6 days with 0.5 mM EDTA. Briefly, cells were washed once and incubated with 0.5 mM EDTA solution for 5 min at 37°C. Subsequently, the dissociation reagent was removed and the cell clumps were resuspended and mechanically disrupted with E8 medium. The resulting clumps of cells were plated in a ratio of 1:6, 1:10 or 1:20, depending on the cell line

For given experiments such as cardiomyocyte differentiation or flow cytometry analysis, hiPSCs were preferably seeded in single cells so that they could be counted and quantified. For this procedure, Accutase ® was added to the cells and incubated at 37°C for 5 min. Accutase ® was diluted with twice the volume of medium and cells suspensions were centrifuged at 300xg for 5 min. The supernatant was discarded and the pellet was re-suspended in medium containing 10 µM ROCK-inhibitor. Cells were then seeded at the specified density and maintained in medium containing ROCK-inhibitor for 24 h to prevent cell death.

### 2.2.1.3 hCMPC and iCPC$^{Sca-1}$

Fetal hCMPCs (donor 15 HFH17.1) were obtained from the Gouman's laboratory (Leiden, the Netherlands). iCPC$^{Sca-1}$ and hCMPCs were grown in hCPC medium (**Table 10**) and on 0.1% gelatin coated plates. Cells were fed three times a week and typically passaged once to twice a week when cells had reached 70-80% confluence. Cells were detached with TrypLE Express for 5 min at 37°C. Trypsinization was stopped by adding medium to

the cells, and cell suspensions were centrifuged for 5 min at 300xg at room temperature (RT). Thereafter, cells pellets were resuspended and typically plated in ratio of 1:6 to 1:8.

iCPC$^{Sca-1}$ passages were re-named after MACS starting from passage 0. iCPC$^{Sca-1}$ between passage 5-10 and hCMPCs no older than passage 20 were used in this thesis.

### 2.2.1.4 Human cardiac fibroblasts

Human cardiac fibroblasts (306-05a- Cell applications Inc., lot no: 2827) were cultured in DMEM. Cells were typically passaged twice a week using TryplE express and plated at a cell density of 10,000 cells/cm$^2$.

### 2.2.1.5 Cell growth monitoring

To monitor cell growth over passaging, cells were split when 80% confluent, counted and seeded always at a density of 5,000 cells/cm$^2$ in T25 flasks. The population doubling time (PDT) was calculated, according to the following formula:

$$\text{PDT} = \left(\frac{\ln 2}{\ln \frac{c2}{c1}}\right) \text{x } (t1 - t2)$$

where, c1 is the starting cell number, c2 cell number at the harvesting time, and t1 and t2 represent the time difference in hours between seeding and harvesting.

In turn, the cumulative population doublings were calculated by adding up the population doubling level (PDL) from passage 2 until passage 15. The PDL refers to the total number of times the cells in the population have doubled since their primary isolation *in vitro* and is calculated as followed: PDL= 3.32 x (log c2 - log c1).

### 2.2.1.6 Cryopreservation of cells

The procedure for freezing hiPSCs is identical to that of cluster passaging of these cells until resuspension. Briefly, after incubation with 0.5 mM EDTA the detaching solution was removed and cell clumps were resuspended in 1 ml of cold Bambanker$^{TM}$ freezing medium and transferred to a cryovial.

HeLa, hCMPC, iCPC$^{Sca-1}$, and human cardiac fibroblasts were cryopreserved in homemade freezing medium (10% DMSO and 50% FBS). Typically, 1x10$^6$ cells were resuspended in 400 µl culture medium and transferred to pre-cooled cryovials containing 500 µl FBS and 100 µl DMSO.

All cryovials were transferred to a freezing container and stored at -80°C overnight until moved to liquid nitrogen for long-term storage.

## 2.2.2 Differentiation protocols

### 2.2.2.1 hiPSC differentiation into CMs

For CM differentiation, hiPSC at a confluence lower than 80% were seeded in single cells at a density of 10,000-20,000 cells/cm$^2$ and 10 µM ROCK inhibitor. The day after, medium was replaced with E8 medium without ROCK inhibitor. Daily medium changes were perfomed for two to three days, until cells reached 70-80% confluence and were ready for differentiation. CM differentiation was induced based on a published protocol (94), which was optimized by the BIH Stem cell core facility. Briefly, mesoderm differentiation was induced by adding cardiac priming medium to induce Wnt signaling for two days. Thereafter, basal medium was added for one day. Subsequently, cardiac lineage was induced by adding cardiac induction medium to inhibit Wnt signaling for two days. Daily medium changes with basal medium were subsequently performed for two days. Eventually, cells were kept in CMM. See media formulations in **Table 10**. Cell seeding density as well as the CHIR99021 concentration was titrated for each cell line.

### 2.2.2.2 hiPSC differentiation into iCPC$^{Sca-1}$

Three different hiPSC donors provided by the BIH Stem cell core facility were used to obtain iCPC$^{Sca-1}$ (**Table 14**)

***Table 14. Origin and reprogramming strategy of the hiPSC lines used in this study.*** *Information kindly provided by the BIH iPS core.*

| Name | Cell line | Origin | Reprogramming strategy | CHIR99021 |
|---|---|---|---|---|
| Donor A | BIHi001-B | Human Foreskin Fibroblast (HFF; ATCC; CRL-2429); male | mRNA reprogramming (Milteny Biotec) | 5 µM |
| Donor B | BIHi004-A | Normal human dermal fibroblasts (NHDF, Lonza CC2511); female | Epi5™ Episomal Kit (Life Technologies) | 4 µM |
| Donor C | BIHi005-A | Stanford Cardiovascular institute 111 (SCVI 111); male | Sendai Virus | 5 µM |

Differentiation into iCPC$^{Sca-1}$ started equally as for cardiomyocyte differentiation until cardiac induction. At day 4 (early) and day 5 (late), cardiomyocyte differentiation was halted by culturing the cells in hCPC medium in two sequential medium changes: 25% and 50% hCPC medium, on the first and second day, respectively. Thereafter, at day 6 (early) and day 7 (late), cells were trypsinized with TryplE Express for 5 min at 37°C, and Sca-1 positive cells were subsequently isolated using magnetic activated cell sorting (MACS) according to published protocols (80). Shortly, on the isolation day cells were trypsinized with TryplE Express for 5 min at 37°C. Subsequently, cells were washed in cold MACS buffer, centrifuged for 5 min at 300xg and RT and resuspended in 450 µl cold MACS buffer. Cells were incubated with 50 µl of anti-Sca-1 microbeads under rotation for 2 h at 4°C. After incubation with the microbeads, the cell solution was washed with cold MACS buffer, centrifuged for 5 min at 300xg and RT and resuspended in 1ml of cold MACS buffer, ensuring that there were no clumps. Thereafter, the cell suspension was run through a 40 mm-strainer, to avoid column clogging. The filtered cell solution was transferred to the pre-wet MS separation column held onto a MiniMACS™ Separator. During column washing with cold MACS buffer the unbound cell fraction (flow-through,

FT) was collected. Finally, the Sca-1 positive fraction was collected in MACS buffer after the MS column was removed from the magnets. Both, FT and the Sca-1 positive fraction were centrifuged for 5 min at 300xg and resuspended in MACS buffer. Live cells were counted in the flow cytometer by discrimination with propidium iodide staining solution. Upon isolation, early and late Sca-1 positive cells (iCPC$^{Sca-1}$) and the correspondent FT fraction were expanded in hCPC medium with 10 ng/ml FGF-2 until passage 3.

#### 2.2.2.3 iCPC$^{Sca-1}$ differentiation into cardiomyocytes

For cardiomyocyte differentiation, iCPC$^{Sca-1}$ were seeded into Geltrex-coated plates at a density of 40,000 cells/cm$^2$ in hCPC medium. When cells were 80% confluent, cardiac differentiation was induced by adding CDM for 3 days and cultured in CMM for up to 14 days in total. During cardiac induction, CDM was changed daily and IWR-1-endo was added fresh. Once the cells were cultured in CMM, the medium was changed three times a week.

### 2.2.3 Flow cytometry analysis

Antibodies were titrated on control cells depending on the recommended concentrations suggested by the manufacturer. The lower concentration leading to the best discrimination between positive and negative populations was selected as the optimal antibody concentration. Typically, 10,000 events per sample were analyzed in MACS Quant® VYB.

After obtaining a single cell suspension the protocol differed depending on the nature of the analyzed proteins. For endogenous fluorescent proteins, half to one million cells per sample were resuspended in cold FACS buffer and transferred to a FACS tube. Live dead staining was done before measuring by adding DAPI (1:100).

For extracellular epitopes, typically, 0.5-1x10$^6$ cells/sample in blocking buffer were transferred to V-bottom 96-well plates or 1.5 ml Eppendorf tubes and incubated for 15 min on ice. Conjugated antibodies were added directly to the samples and incubated for 15-30 min on ice. Thereafter, samples in plates or tubes were centrifuged, at 450xg or 300xg, respectively, for 5 min. The staining solution was removed and the cells were

washed with FACS buffer. Live dead staining with DAPI was performed as described above.

For intracellular epitopes, cells suspensions in PBS+ were stained with Aqua Live/Dead® Fixable Dead Cell Stain working solution for 30 min on ice in the dark. Thereafter, cells were washed with PBS+ twice and fixed and stained following Foxp3/Transcription factor staining buffer set instructions. Briefly, cells were incubated in fixation/permeabilization solution for 30 min at RT in the dark. Then, cells were washed twice with 1x permeabilization buffer and resuspended in 1x permeabilization buffer with 1% BSA, where they were incubated for 15 min at RT for blocking. Primary antibodies were added directly to the samples, mixed by pipetting, and incubated for 1 h at RT. Thereafter, wells were washed twice with 1x permeabilization buffer. If primary antibodies were not conjugated, secondary antibodies were added in 1x permeabilization buffer with 1% BSA and incubated for 30 min at RT in the dark. After the final washing step, samples were resuspended in FACS buffer and analyzed directly by MACS Quant® VYB or kept at 4°C until measurement. Unstained and secondary antibody controls were always measured in parallel.

## 2.2.4 Genetic engineering

### 2.2.4.1 Puromycin knockout in HeLa d2eGFP cells

In order to apply antibiotic selection in HeLa d2eGFP cells obtained from Wang *et al.* (95), puromycin resistance gene was knocked out with CRISPR-Cas9 technology (**Figure 6**). Crispr RNA (crRNA) sequences were designed using the *Benchling CRISPR tool* developed by the Zhang lab (96). The algorithm retrieved four 20-bp guides next to the protospacer adjacent motif (PAM) sequences. PAM sequences with the minimal off-target effects were selected (**Table 7**).

crRNA sequences were ordered from IDT Inc. and resuspended to 100µM stock solution. To complex crRNA:tracrRNA (sgRNA), 1 µl of PURO crRNA and 1 µl of tracrRNA (100 µM) were mixed with 98 µl Nuclease-free duplex buffer, heated at 95°C for 5 min and cooled down to RT. The Cas9 working solution (1 µM) was prepared in OptiMEM. To prepare the ribonucleoprotein complexes (RNPs) 6 µL of crRNA:tracrRNA complex, 6 µl of Cas9 (1 µM) and 88 µl of OptiMEM medium were mixed per well. Finally, the

transfection mix was prepared by adding 3 µl of Lipofectamine RNAiMax reagent, and 87 µl of OptiMEM to each RNP reaction. After incubation for 20 min at RT, 200 µl of transfection mix was added to the cells. Cells were kept at 37°C for 48 h before medium was changed.

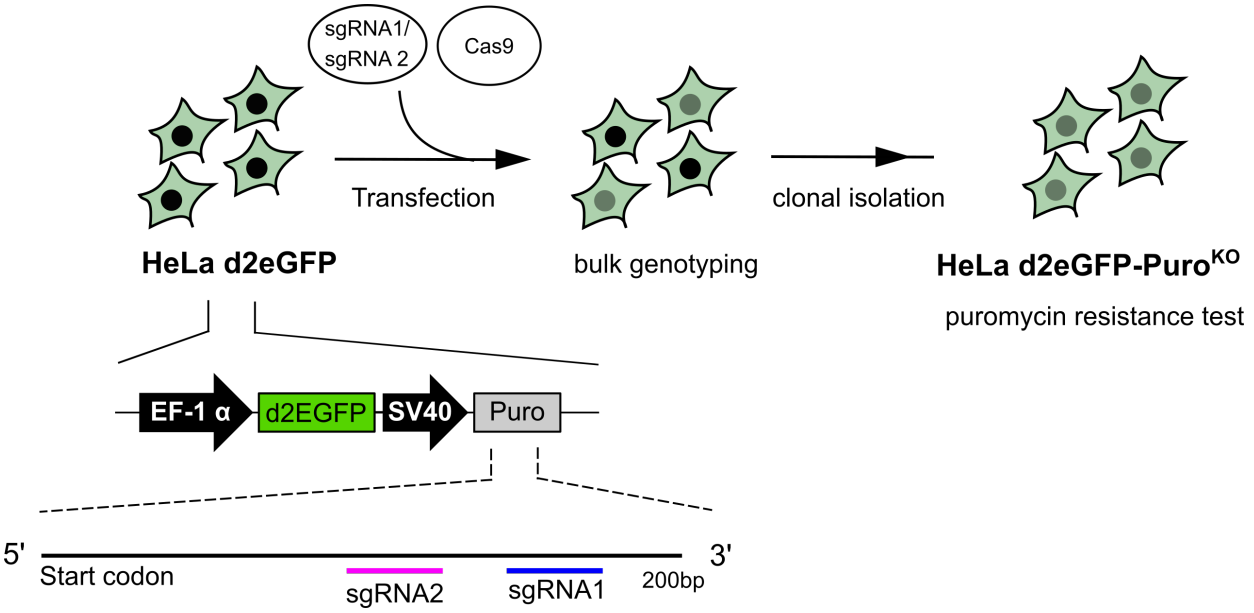


***Figure 6. Puromycin cassette knockout in HeLa d2eGFP using CRISPR-Cas9.*** *EF-1α: Human elongation factor-1 alpha promoter; d2eGFP: destabilized 2-hour enhanced green fluorescent protein; SV40: Simian virus 40 promoter; Puro: puromycin resistance cassette.*

Genomic DNA of the transfected cells was isolated for a preliminary assessment of the sgRNAs cleavage efficiency. The puromycin gene region was PCR-amplified using the GFP c-ter and SV40pA-R-156-175 primers and the PCR products were sequenced. Subsequently, single cells from cell pools modified with sgRNA2 were seeded in 96-well plates using the limiting dilution strategy. Colony-like growth was monitored for two weeks and wells containing more than one colony were discarded. Approximately 10 single-cell clones per sgRNA were expanded in parallel wells with or without puromycin (2 µg/ml), to determine puromycin sensitivity. Puromycin sensitive clones were expanded and used for subsequent experiments.

### 2.2.4.2 miRE design and cloning

shRNA 97-mer sequences to silence *CTNNB1* gene, coding for β-catenin, were obtained from shERWOOD database http://sherwood.cshl.edu:8080/sherwood/. Sequences with the highest score, indicating high specificity and low off-targets, were selected. shRNA sequence d2eGFP was designed using the shERWOOD web-tool, which is based on the algorithm described by Knott *et al*. (97).

Subsequently, 0.05 ng of shRNA oligonucleotides (**Table 8**) were PCR amplified with miRE‐Xho‐fw and miRE‐EcoRI‐rv primers to flank the shRNA of interest with Xho I and EcoRI restriction sites using Taq polymerase 2x Master Mix. Cycling parameters were 95°C for 5 min, 30 cycles of 95°C for 25 s, 56°C for 30 s, and 68°C for 10 s, and a final elongation round at 68°C for 5 min.

Following amplification, recipient Tet-ON-all-in-one vectors featuring the mCherry fused with the miRE backbone and the shRNAs of interest (**Figure 7** A,B) were digested with XhoI and EcoRI, and ligated using the Quick ligase kit. Quick ligation reactions were carried out with 50 ng of vector and a 3-fold molar excess of insert. The ligation product was transformed in *DH5*α competent bacteria using standard protocols. Single cell clones were expanded and the amplified vectors were control sequenced using mCherry-C Seq.

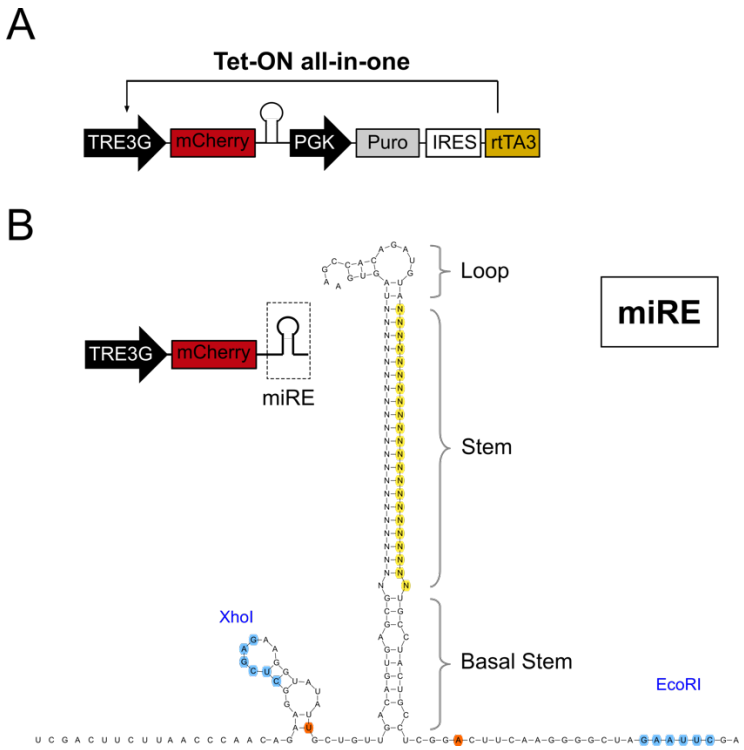


***Figure 7. Tet-ON-all-in-one construct and shRNA cloning strategy. A*** *Depiction of Tet-ON all-in-one construct used in this thesis. TRE3G is the tetracycline-response element (Tet promoter), which controls the expression of mCherry-coupled miRE, a short hairpin RNA (shRNA). Downstream, a second transcriptional unit with the constitutive phosphoglycerate kinase promoter (PGK), induces the expression of a puromycin resistance cassette (Puro), the internal ribosomal entry site (IRES), and the reverse tetracycline-controlled transactivator (rtTA3). IRES promotes the co-expression of both genes under the same promoter.* ***B*** *Detailed scheme of the shRNA used in this study. This so-called miRE is an enhanced version of the synthetic miR30 published by Fellmann et al.* (91)*. The shRNA containing the target-specific guide strand (yellow) is flanked by two restriction enzyme cutting sites (blue), XhoI and EcoRI, to virtually clone any sequence. The shRNA sequence is delimited by the orange nucleotides. shRNA characteristic secondary structures: loop, stem, and basal stem are indicated. Adapted from Fellmann et al.* (91)*.*

### 2.2.4.3 Lentiviral particles packaging

HEK293TN cells cultured in DMEM were used to generate viral particles. A day before transfection, cells were seeded in 150 mm dishes and transfected the day after. A mixture of 10µg of plasmid of interest (LT3GEPIR_mCherry-miRE), 6.7 µg of the gag/pol plasmid (psPAX2), and 3.3 µg of the envelope plasmid (pMD2.G) was added to each dish using standard protocols. Cells were incubated overnight. The morning after, medium was

added to the cells and after 7 h the first viral particle harvest was performed. Thereafter, two subsequent harvests were performed every 24 h. Supernatants were filtered with 0.45 µm diameter filters and kept at 4°C. The harvested supernatants were pooled together and ultracentrifuged at 22,000 rpm for 3 h and 30 min at 4°C. Viral pellets were resuspended in PBS and temporarily stored at 4°C for viral particle titration. Long term storage was at -80°C.

Virus titer was calculated by transducing HT1080 cells with 1, $10^{-1}$, $10^{-2}$, $10^{-3}$, and $10^{-4}$ µl of the concentrated vector. At day 1 after transduction, medium was replaced with fresh medium containing 1 µg/ml DOX. At day 2, cells were harvested and the number of reporter positive cells was determined by flow cytometry. Titer was calculated by using the following formula:

$$\mathbf{Titer} = \frac{\mathbf{Number\ of\ target\ cells\ (count\ at\ transduction\ day)x}\left(\frac{\mathbf{\%GFP\ positive\ cells}}{\mathbf{100}}\right)}{\mathbf{Concentrated\ vector\ volume\ (ml)}}$$

### 2.2.4.4 Single vector Tet-system transfer to HeLa d2eGFP Puromycin KO cells

To transduce HeLa d2eGFP cells with lentiviral particles, 50,000 cells/$cm^2$ were seeded in 6-well plates. Next day, at 70-80% confluency cells were transduced with a multiplicity of infection equal to 2 in 2 ml medium containing 3 µg/ml polybrene and incubated overnight at 37°C and 5% $CO_2$. The day after, the viral particles were removed and depending on cell density cells were split 1:6 and seeded without antibiotics. The next day, selection with 2 µg/ml puromycin was started for at least 10 days.

To modify HeLa d2eGFP cells with transposons, cells were seeded at a density of 25,000-40,000 cells/$cm^2$. The following day, cells were co-transfected with the Piggybac transposase vector (pPB_transposase) and the donor transposon plasmid (pPB-TRE_mCherry_miRE_PGK_Puro _rtTA3_pA). For a 6-well-plate well a total of 2.5 µg DNA at a ratio 1 to 10 (1:10, PB transposase:transposon) was mixed with 6 µl Lipofectamine 2000 Reagent in Opti-MEM® reduced serum medium. The DNA lipid complexes were added to cells drop-wise and incubated for 48 h at 37°C and 5% $CO_2$. Thereafter, cells were split 1:6-1:8 and cultured in medium containing 2 µg/ml puromycin as explained above. mCherry expression upon culturing with 0.5 µg/ml DOX for 3 days was used to monitor transgene integration.

### 2.2.4.5 rtTA3 rescue in the ROSA26 locus

HeLa cells were seeded one day before transfection. The next day, DNA-lipid complexes were formed using Lipofectamine 3000 Reagent. Briefly, 3.75 µl of Lipofectamine 3000 reagent in Opti-MEM® reduced serum medium was mixed with a plasmid DNA solution in Opti-MEM with 4 µl of P3000 reagent. A total of 2 µg of plasmid DNA consisting of: (i) 0.5 µg ROSA26-guideA_Cas9n, (ii) 0.5 µg ROSA26-guideB_Cas9n, and (iii) 1 µg puC-ROSA26-CAG-rtTA3G or rtTA3 was used per reaction. DNA-lipid complexes were added to the cells dropwise and incubated for 24 h. Thereafter cells were cultured in DMEM with neomycin (1000 µg/ml) and puromycin (2 µg/ml).

### 2.2.4.6 Targeted integration of the Tet-ON-miRE transgene in hiPSC

OPTi-OX® cells were kindly provided by the Kotter lab, Cambridge. These cells, hereafter named hiPSC-rtTA, constitutively express the rtTA3G protein under the control of the CAG promoter, which is integrated in the *ROSA26* safe harbor locus (93).

To integrate the Tet-ON-miRE transgene in the AAVS1 locus, hiPSC-rtTA were cultured in mTESR1 medium before transfection. When the cells had reached 70-80 % confluence, single cells were plated 12,500 cells/cm$^2$ in mTESR1 supplemented with 10 µM ROCK inhibitor. The next day, mTESR1 medium without ROCK inhibitor was added. DNA-lipid complexes were formed following Lipofectamine 3000 Reagent instructions. A total of 2 µg of plasmid DNA consisting of: (i) 0.5 µg pZFN-AAVS1-L-ELD, (ii) 0.5 µg pZFN-AAVS1-R_KKR, and (iii) 1 µg pUC-AAVS1-miRE mock or pUC-AAVS1-miRE CTNNB1 was used per reaction. DNA-lipid complexes were added to the cells dropwise and incubated for 24h. The next day, medium was removed and replaced with mTESR1 medium. After 24 h, cells were split in single cells in two wells at a density of 100,000 cells/well, in mTESR1 with 10 µM ROCK inhibitor. After one day of recovery, mTESR1 medium with 1 µg/ml puromycin with or without 1 µg/ml DOX was added to the wells. Selection was carried out for at least three days, until all cells were dead in non-transfected controls. Presence of the transgene was visualized in the wells with doxycycline. After selection, cells were recovered for at least 6 days in mTESR1 medium until normal cell growth was re-established and there were no signs of spontaneous differentiation.

To isolate single cell clones, antibiotic resistant hiPSCs were dissociated in single cells and plated in limiting dilution in Geltrex-coated 6-well plates with 10 µM ROCK inhibitor. For up to a week, daily medium changes were performed and colonies growing close to each other were scrapped out. At least four individual colonies per cell line were mechanically detached, and manually transferred to Geltrex-coated 24-well plates containing mTESR1 medium supplemented with 10 µM ROCK inhibitor. When 24-well plates were repopulated, single cell passaging and subsequent expansion of the cells in 6-well plates was performed. Cells were expanded for at least 2 passages until cell growth was established without spontaneous differentiation.

To genotype the cells, genomic DNA from one well of a 6-well plate was isolated for each monoclonal cell line using NucleoSpin® Tissue. The genomic DNA was eluted in two steps of 40 µl elution buffer each, and 50-100 ng per reaction was used as template. The genotyping strategy followed was published by Palowski *et al*. (93). Primers and the PCR strategy followed are summarized in **Table 15**.

***Table 15. AAVS1 locus Tet-miRE-mCherry genotyping primers***

| PCR name | Primer binding site | Primer name | Band size |
|---|---|---|---|
| Locus PCR | Genome (5') | hAAVS1-genome (5') | WT: 1692 bp<br>Insert: no band |
| | Genome (3') | hAAVS1-genome (3') | |
| 5'-INT PCR | Genome (5') | hAAVS1-genome (5') | WT: no band<br>Insert: 991 bp |
| | Puromycin N-terminal | Puro-N-ter rv | |
| 3' -INT PCR | mCherry C-terminal | mCherry-C-ter genotyping | WT: no band<br>Insert: 1601bp |
| | Genome (3') | hAAVS1-genome (3') | |
| 3'-BB PCR | mCherry C-terminal | mCherry-C-ter genotyping | WT: no band<br>Vector: 1622 bp |
| | Vector Backbone (3') | pUC-AAVS1- vector BB (3') | |

## 2.2.5 Immunohistochemistry

For staining cells growing on culture plates, cells were washed twice with PBS and fixed with 4% PFA in PBS for 15 min at RT. Afterwards, the fixative was removed and cells were washed with PBS+ twice. To stain intracellular proteins, cells were incubated with permeabilization/blocking buffer for 30 min at RT. Thereafter, primary antibodies were

diluted to the working concentration in permeabilization and blocking buffer added to the cells, and incubated for 60 min in the dark at RT or overnight at 4°C. Thereafter, cells were washed twice PBS+ and incubated with fluorescently labeled secondary antibodies for 30-60 min at RT. Subsequently, cells were washed two times with PBS+ to remove excess of secondary antibodies. Finally, cell nuclei were counterstained with DAPI (0.1 µg/ml) for 15 min at RT in the dark, washed once with PBS+ and stored at 4°C in the dark until imaging. The cells were imaged with Operetta™ High-Content Imaging System for image analysis and Opera Phenix™ High-Content screening system for confocal images.

### 2.2.6 High content screening image analysis

For high content image analysis purposes, cells were stained with CellMask Blue reagent diluted 1:5000 to delineate the cells cytoplasm or DAPI for nuclear staining.

Images for analysis were acquired using the Operetta™ High-Content Imaging System at a magnification of 10x. Image analysis was done using the Columbus image data system developed for high content screening analysis. A total of 25 fields were analyzed per well leading to an average of 10,000 analyzed objects per well. Two and three technical replicates were analyzed for differentiation and cell morphology, respectively.

Cells were identified based on CellMask or DAPI channel using the Find Nuclei method B function using the following parameters: common threshold: 0.55, area > 50 $\mu m^2$, splitting coefficient: 7.0, individual threshold: 0.4, contrast > 0.1. Morphology parameters such as cell area and α-actinin mean fluorescent intensity were calculated on the generated cell masks. Using the same mask, cTNI positive cells were quantified by counting the Alexa647 positive cells. Nuclear expression of NKX 2-5 was calculated by counting the Alexa488 positive nuclei using the function “Find Cells” following method B with the same parameters described above despite the common threshold, set to 0.4, and the area > 100 $\mu m^2$.

## 2.2.7 Transcriptome analysis by real time PCR (RT-PCR)

For RNA isolation and purification, pellets of 0.5-1 x$10^6$ cells were snap frozen with liquid nitrogen and stored at -80°C until further processing. RNA purification was performed with the NucleoSpin® RNA Kit by MACHEREY-NAGEL and the purified RNA was eluted in 40 µl of RNase-free $H_2O$ and immediately kept on ice.

cDNA was synthesized according to Thermo Scientific RevertAid H Minus First Strand cDNA Synthesis Kit manufacturer's instructions. The RNA input ranged between 600-1000 ng RNA per sample. Briefly, if oligo (dT)18 primers were used, samples were incubated for 60 min at 42°C followed by 70°C for 5 min. For random hexamer primers, samples were incubated for 5 min at 25°C, followed by 60 min at 42°C and terminated by 70°C for 5 min. The cDNA product was either directly used for qPCR or stored at -20°C.

For RT-PCR reactions, cDNA samples were diluted in DNAse/RNAse free water to a concentration of 2.5 ng/ml. Forward and reverse primer working mixtures for RT-PCR were prepared by diluting primer stocks to 1.5 µM in DNAse/RNAse free water. For RT-PCR reactions in 384-well plates, 6 µl of cDNA dilution or non-template control (water), 3 µl of primer working mixture and 9 µl of SYBR Green was added per well. All samples were analyzed in triplicates. Standard RT-PCR program consisting of 2 min at 50°C, 10 min at 95°C, followed by 40 cycles of 15 s at 95°C and 1 min at 60°C, each, was run in QuantStudio 6 Flex Real-Time PCR System. The melting curve for each sample was calculated at the end.

Finally, the delta Ct method (ΔCt) was used to calculate the relative gene expression. Only genes with Ct values lower than the water controls were included in the calculation. Next, the average Ct values of GAPDH and ß-actin was calculated for each sample ($Ct_{housekeeping}$) and subtracted to each gene to obtain the ΔCt. Thereafter, the mRNA expression was calculated using the following formula $2^{-\Delta Ct}$.

## 2.2.8 Statistics

Every experiment was performed at least three times or using three biological replicates unless otherwise stated. Data are shown as mean ± standard deviation. The statistical method was defined for each experiment individually. Generally, unpaired and paired t tests were performed to test differences between two unrelated or related groups. One-

way ANOVA and two-way ANOVA were performed when more than two groups were compared in order to test the effect of one or two variables, respectively. Multiple comparisons were assessed using a Bonferroni post-test correction. A p value of less than 0.05 was considered significant. GraphPad Prism versions 6.0 and 8.0 were used to plot and analyze the data.

# 3 RESULTS

# 3.1 Conditional expression of miRE to modulate the Wnt signaling pathway

Several studies have shown that inhibition of the canonical Wnt signaling pathway promotes differentiation of mesoderm cells into CMs (85,98). In order to have a cell-specific and inducible Wnt signaling inhibition, miRE targeting the Wnt key mediator β-catenin was combined with Tet-ON system.

In this chapter, different gene delivery strategies and transgene configurations were tested first in a reporter cell line to optimize the gene engineering strategy and later applied during CM differentiation of hiPSCs *in vitro*.

## 3.1.1 Single vector Tet-system in HeLa cells

Tet-ON single vector constructs, also known as “Tet-ON-all-in-one” systems, have been designed to introduce the elements necessary for conditional gene expression, namely the reverse tetracycline-controlled transactivator (rtTA) and the Tet promoter, in one single vector. This configuration simplifies the gene engineering process and increases safety as reduces the risk of insertional mutagenesis or gene disruption. However, it has been reported that insertion of transgenes with several promoters in tandem can lead to bimodal expression of Tet promoter regulated genes (99).

### 3.1.1.1 Characterization in a reporter HeLa cell line

Transgene expression in engineered cells can be lost over time due to transgene erasure from the genome or by transcriptional and post-transcriptional related mechanisms. To evaluate these two aspects, a customized reporter cell line was designed to visualize transgene transcription and translation, simultaneously.

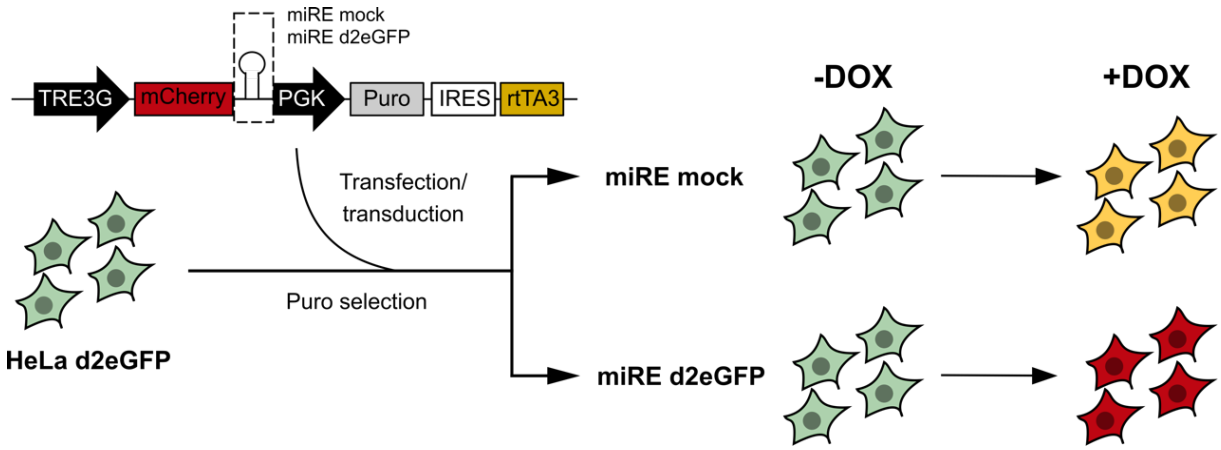


***Figure 8. Customized HeLa reporter cell line.*** *Tet-all-in-one construct was integrated in the genome of clonally expanded HeLa-d2eGFP cells. Upon conditional activation of transgene expression by adding doxycycline (DOX), miRE mock cells will co-express d2GFP and mCherry, and miRE d2eGFP cells will only express mCherry. TRE3G: Tet-response element 3rd generation. PGK: phosphoglycerate kinase promoter, IRES: internal ribosomal entry site. rtTA3: third generation reverse tetracycline controlled transactivator.*

Briefly, a HeLa cell line constitutively expressing a destabilized 2-hour enhanced green fluorescent protein- short-lived eGFP (d2eGFP) subjected to a puromycin resistance cassette knockout (HeLa d2eGFP) was used as a starting cell. Once Tet-ON-all-in-one transgenes with a mock (miRE mock) or a miRE silencing d2eGFP (miRE d2eGFP) are integrated in the cells' genome, Tet promoter-driven expression and miRE function can be visualized. In the absence of DOX, all cells are green. When cells are cultured in DOX, miRE mock cells co-express d2eGFP and mCherry, thereby becoming yellow, whereas miRE d2eGFP cells become mCherry positive (**Figure 8**). In the miRE d2eGFP, post-transcriptionally related silencing mechanisms can be observed if double negative cells arise, which would depict correct miRE functionality but lack of mCherry translation.

### 3.1.1.2 Bimodal transgene expression is independent of transgene delivery strategy

DNA transposons and retroviruses integrate exogenous DNA in the genome in a random fashion. However, both show preferential integration in certain DNA regions of the genome, depending on structural features associated with DNA flexibility (100).

To assess the effect of the chromatin environment on the activation of Tet promoter mediated gene expression, the Tet-all-in-one miRE mock and miRE d2eGFP constructs were delivered either by transfection with the *Piggybac* transposon system (virus-free) or by transduction with lentivirus. Immediately after transduction or transfection, cells were selected with puromycin to ensure that cells carrying at least one copy of the transgene are analyzed. After DOX treatment for 3 days, both lentivirus and *Piggybac*-mediated miRE d2eGFP cells showed remaining green cells, suggesting lack of Tet promoter-mediated miRE d2eGFP expression, which highly correlated with mCherry reporter absence. Similarly, the mock controls had a high percentage of mCherry negative cells (**Figure 9** A,B).

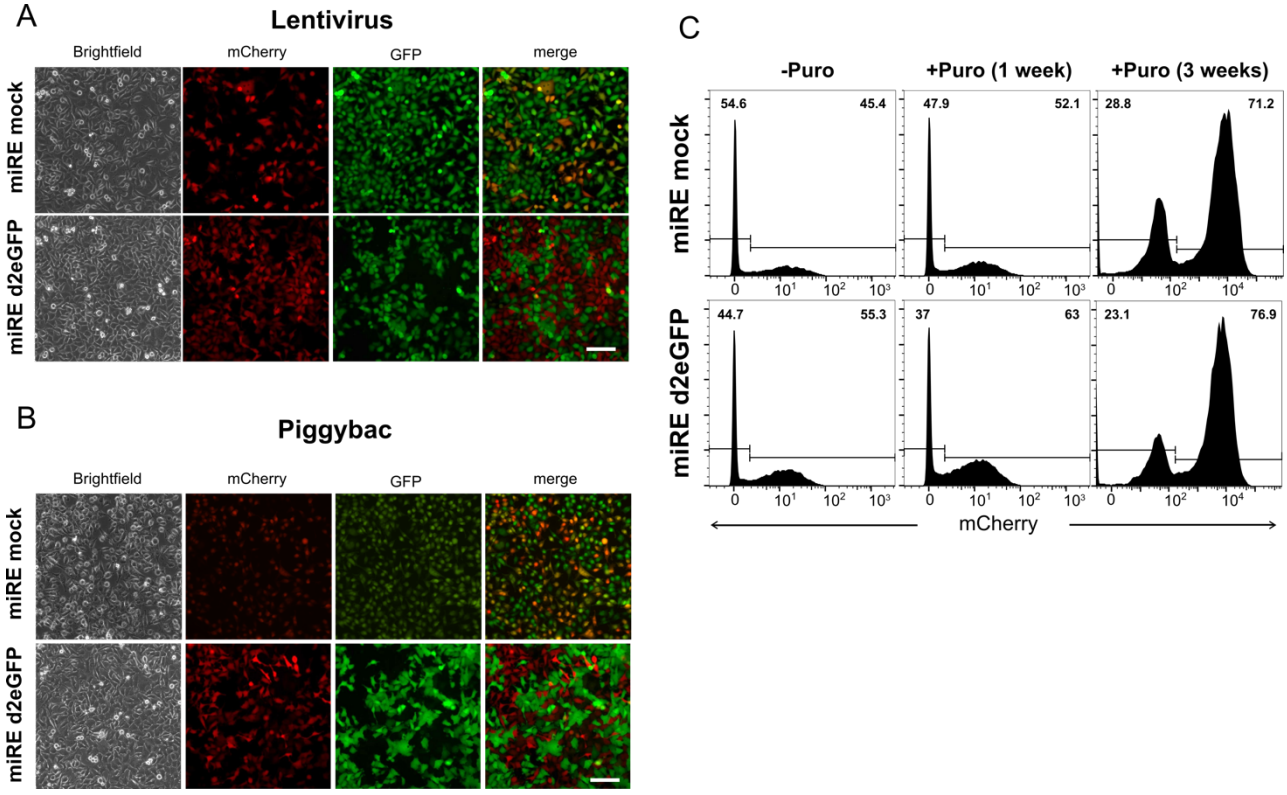


***Figure 9. Tet promoter-driven gene expression in HeLa d2eGFP miRE is independent of gene delivery strategy.*** *mCherry and GFP pictures of* ***A****. lentivirus-transduced cells 3-days after DOX treatment (1 µg/ml) and* ***B****. Piggybac-transfected cells, both using miRE mock and miRE d2eGFP constructs. miRE d2eGFP cells were previously fixed with 4% paraformaldehyde. Scale bars: 100 µM* ***C.*** *Flow cytometry histograms showing the percentage of mCherry positive cells in lentivirus-transduced cells during subculturing with high Puromycin concentration (2 µg/ml) for 3 weeks.*

Flow cytometry quantification in lentivirus-transduced cells under constant high selective pressure (2-fold puromycin concentration) for 1 week showed that Tet promoter-driven expression is only restored by 6.7% and 7.7% for miRE mock and miRE d2eGFP, respectively, as compared with unselected cells (-Puro). In turn, prolonged selection for 3 weeks, contributed to a partial increase of mCherry positive cells but did not fully restore expression in all cells. Almost a fourth of the cells, 28.8% and 23.1% of the selected miRE mock and miRE d2eGFP, respectively, were mCherry negative under prolonged selective pressure (**Figure 9** C).

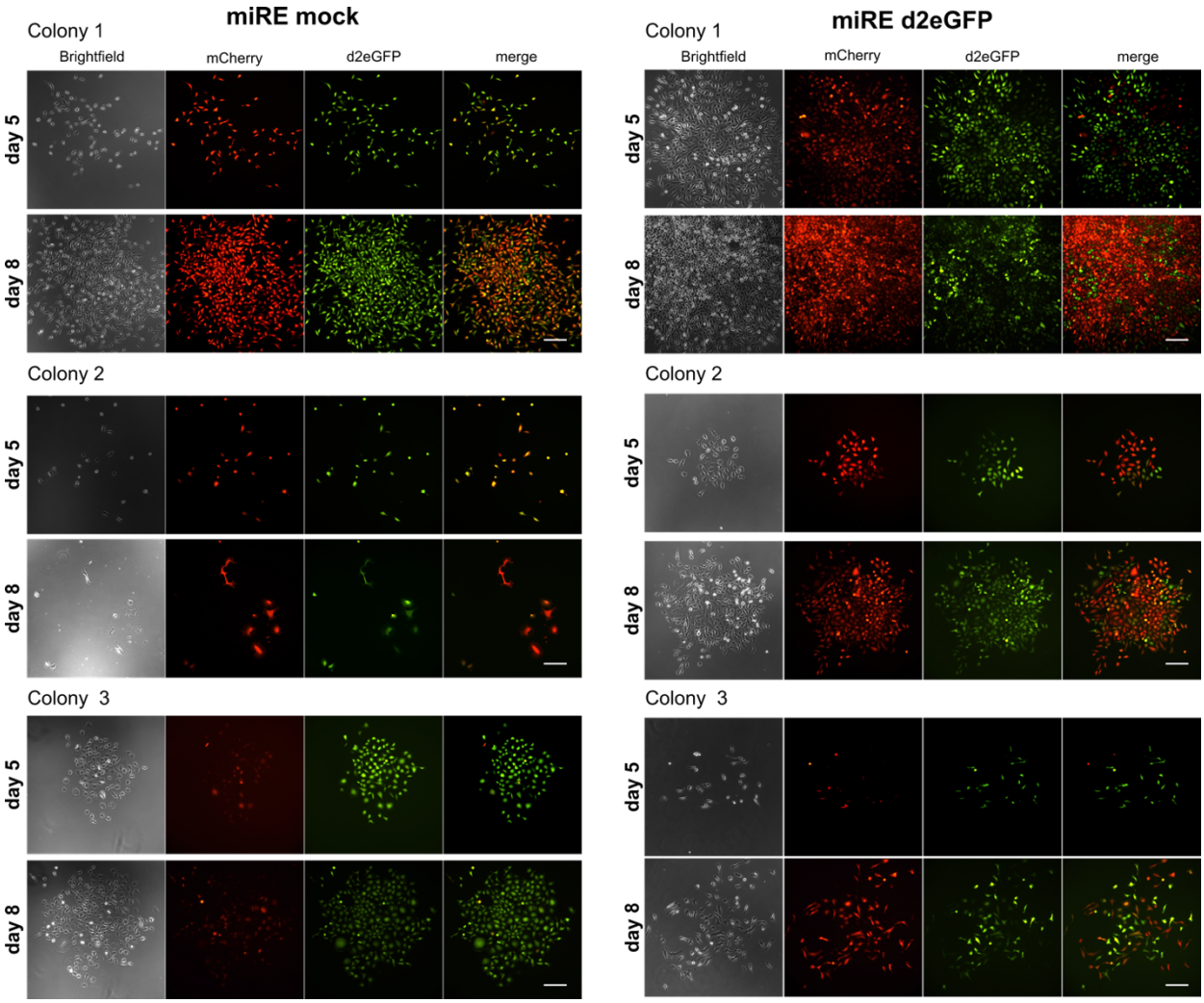


***Figure 10. Mosaicism in puromycin resistant single cell HeLa d2eGFP miRE mock and d2eGFP clones occurs early during expansion.*** *Expression of mCherry reporter protein and endogeneous d2eGFP in single cell HeLa clones carrying miRE mock or miRE d2eGFP constructs at day 5 and day 8 after transfection with Piggybac transposons. Cells were cultured with doxycycline (1 µg/ml) and puromycin (2 µg/ml). Scale bars: 100 µm.*

In addition, single cell colonies growing under selective pressure and continuous induction with doxycycline showed mosaic expression of mCherry positive and negative cells early after transfection with Piggybac in three independent clones for each miRE. No differences were observed between the two miREs (**Figure 10**).

The rapid loss of transactivation ability and the antibiotic selection time needed to achieve 75% of transcriptional activation in polyclonal cell populations is suboptimal for hiPSCs, the target cell line. hiPSCs are stress-sensitive and can only be exposed to antibiotics for a few days before they undergo apoptosis or spontaneously differentiate.

### 3.1.1.3 Epigenetic modifiers partially restore Tet promoter driven gene expression in mosaic cells

Based on the described results, whether the transgene remained in the cells genome and is repressed by epigenetic gene regulatory mechanisms such as DNA methylation or histone deacetylation remained unanswered.

To investigate this, lentivirus-transduced miRE mock isogenic cells showing mosaicism were cultured with epigenetic modifiers: 5'azacytidine, a DNA methylation inhibitor, and Trichostatin A (TSA), a class I and II mammalian histone deacetylase inhibitor. As expected, higher doses and long exposure of these epigenome modifiers led to a certain degree of cell toxicity, from mild in cells treated to 5'Azacytdine to high in those treated with TSA (**Figure 11** A,B). Quantification of mCherry and GFP positive cells using flow cytometry showed no significant increase in transgene activation after treatment for 48 h with 5' Azacytidine or TSA. However, treatment with TSA for 48 h showed a concentration-dependent increase in double mCherry-GFP positive cells (**Figure 11** C,D). This trend became significant when isogenic cell lines were treated with TSA for 72h although at the expense of high cell toxicity, as assessed by a decrease in cell number in groups treated with TSA concentrations higher than 20 ng/ml (**Figure 11** B,D). Likewise, treatment with 5' Azacytidine for 72h partially reverted gene silencing in all isogenic clones in a concentration-dependent manner although to a lesser extent than TSA; whereas 5' Azacytidine (2 μM) treatment for 72h led to 47.67 ± 13% mCherry-GFP positive cells (2.6-fold increase of double positive cells compared with untreated cells), TSA treatment (30 ng/ml) for 72h led to 74.17 ± 10.8% mCherry-GFP positive cells in the same clonal cells achieving an average 8.66-fold increase (**Figure 11** C,D).

Interestingly, exposure to the analyzed epigenetic modifiers had a different effect in clones with similar baseline silencing degree. For instance, treatment with TSA for 72h induced an 18-fold increase of mCherry-GFP positive cells in clone 3, and 9.1-fold in clone 1, which had an initial 4.5% and 6.8% mCherry-GFP positive cells, respectively.

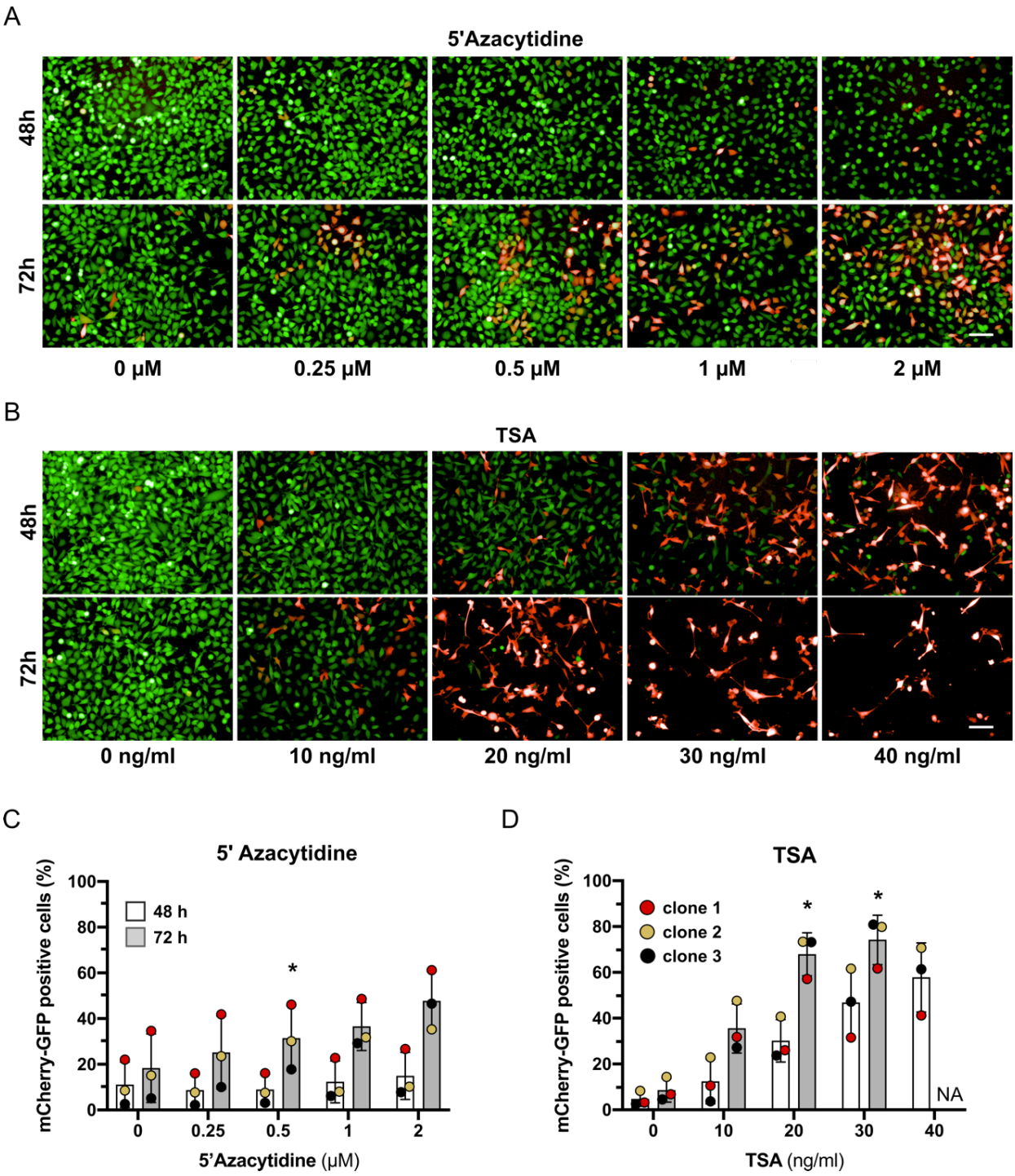


***Figure 11. Treatment with epigenetic modifiers in HeLa d2eGFP-miRE mock cells partially rescues transgene expression. A.*** *Representative merged mCherry and GFP fluorescence images of HeLa d2eGFP miRE mock clonal cells (clone 3) cultured with 1*

*µg/ml Doxycycline and treated with different concentrations of 5' Azacytidine or* ***B.*** *Trichostatin A (TSA) for 48 h or 72 h. Scale bars: 100 µm* ***C.*** *Flow cytometry quantification of the percentage of double mCherry-GFP positive cells after treatment with 5' Azacytidine and* ***D.*** *TSA represented as mean values ± SD (n=3, isogenic clones). NA: not applicable. two-way ANOVA followed by a multiple comparison Bonferroni test using untreated cells as the reference sample (* p<0.05).*

### 3.1.1.4 rtTA overexpression in a safe harbor locus rescues miRE expression

Next, to test whether the rtTA is responsible for the observed mosaicism, the effect of overexpressing rtTA in another genome locus was evaluated.

To that end, the rtTA3G gene was integrated into the *ROSA26* locus (rtTA3G$_{ROSA26}$), a genomic safe harbor locus, of HeLa d2eGFP miRE cells showing bimodal Tet-dependent gene expression (**Figure 12**).

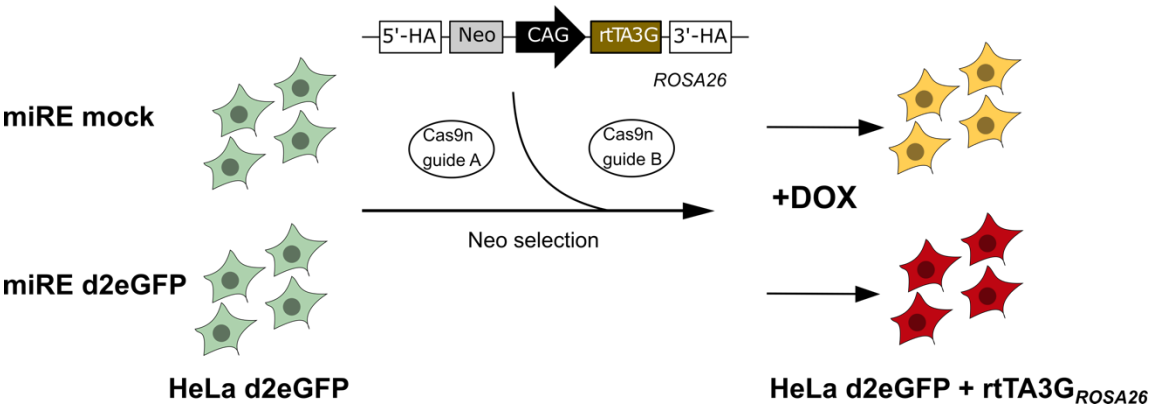


***Figure 12. rtTA3G rescue in the safe harbor locus ROSA26 of HeLa d2eGFP miRE cells.*** *Workflow for targeting the ROSA26 locus of HeLa d2eGFP-miRE mock and miRE d2eGFP cells using CRISPR/Cas9 to provide the rtTA3G to the Tet system in trans. 5' HA and 3' HA (5' and 3' homology arm), Neo (neomycin resistance cassette) and CAG (CMV enhancer, chicken beta-Actin promoter and rabbit beta-Globin splice acceptor site).*

After selection with neomycin, rtTA3G$_{ROSA26}$ rescued cell pools showed highly homogeneous mCherry expression when cultured with DOX for 3 days (**Figure 13** A,B). In addition to reporter gene expression, the phenotype in rtTA3G$_{ROSA26}$ rescued cells showed miRE specific functionality in 97.8 ± 0.3% and 96.2 ± 1.7% of the cells, for miRE mock and miRE d2eGFP, respectively (**Figure 13** B). This increase was statistically significant in both cell lines as compared with non-rescued cells (**Figure 13** C).

In contrast to the rtTA3 included in the Tet-all-in-one vector, the rtTA3G used in these rescue experiments, also known as third-generation rtTA, has three aminoacidic modifications: G12S, F67S and R171K. These modifications increase rtTA sensitivity to the DOX effector, thereby resulting in a higher transcriptional activity (101). To rule out the possibility that the enhanced transcription activation is due to the intrinsic higher rtTA3G affinity for the Tet promoter, a comparative rescue experiment was performed. First, the rtTA3G was replaced by the rtTA3 gene in the Tet-all-in-one vector in order to keep the genetic context identical. Then, like in the previous experiment, HeLa d2eGFP miRE mock cells were genetically modified either with rtTA3 or rtTA3G in the *ROSA26* safe harbor locus (**Figure 14** A).

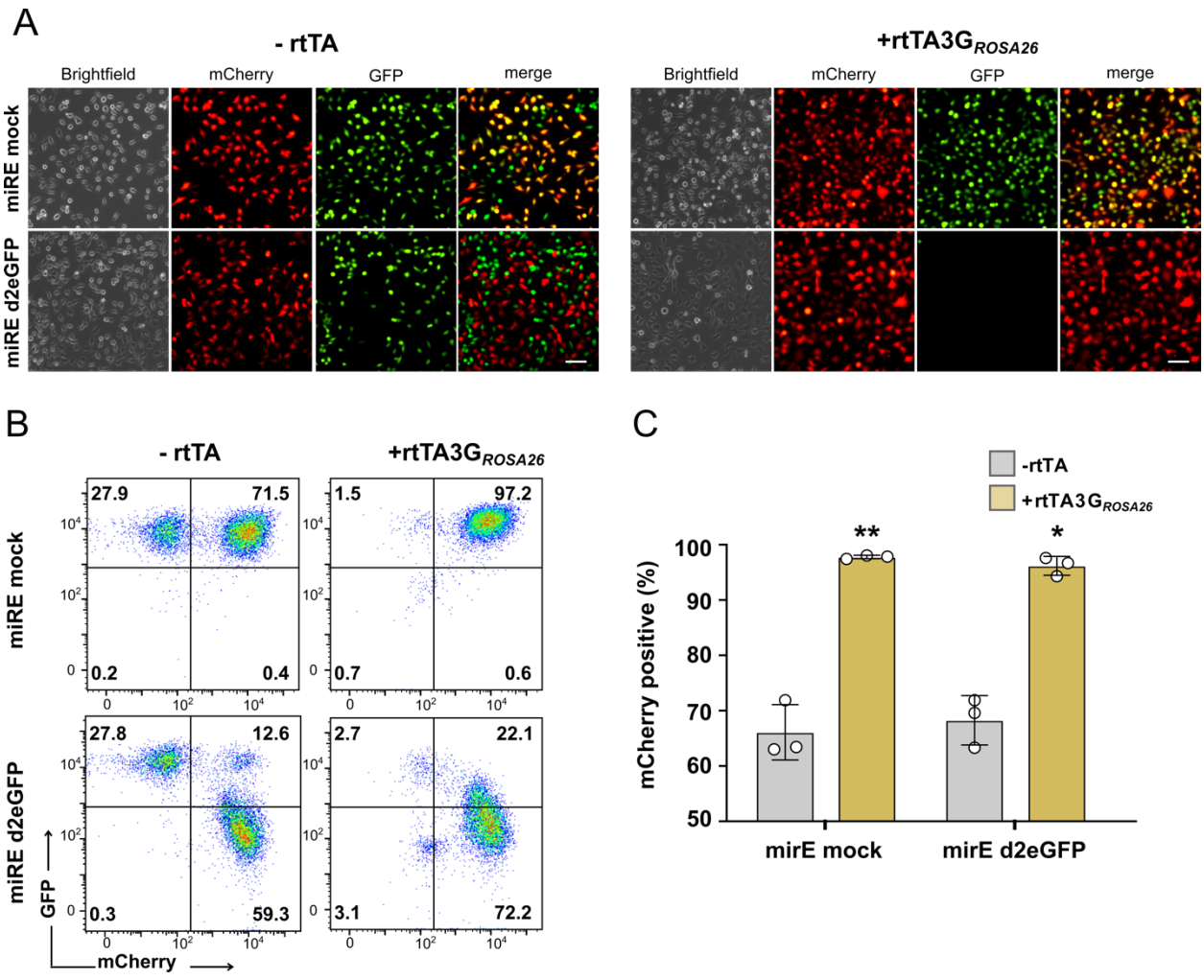


***Figure 13. Overexpression of rtTA3G in the ROSA26 locus rescues transgene expression in selected pools that previously exhibited bimodal expression. A.*** *mCherry and GFP expression in HeLa d2eGFP miRE mock and miRE d2eGFP cells after 3-day DOX treatment. Left: expression in unmodified cells (-rtTA); right: expression in cells overexpressing the rtTA3G in the ROSA26 locus (+rtTA3G$_{ROSA26}$). Cas9n: Cas9 nuclease.*

*Scale bars: 100 µm.* ***B.*** *Representative flow cytometry plots of HeLa d2eGFP-miRE mock and d2eGFP cells with or without rtTA3G$_{ROSA26}$ overexpression.* ***C.*** *Flow cytometry quantification of the percentage of mCherry positive cells in three independent experiments represented as mean values ± SD (n=3). Statistical differences between -rtTA and + rtTA3G$_{ROSA26}$ were analyzed using a paired t-test for each cell line (* p<0.05 ** p<0.01).*

Both rescue strategies led to a significant increase in the percentage of mCherry expressing cells as compared with cells in the -rtTA group. As assessed by flow cytometry, the nature of rtTA protein did not affect the overall rescue efficiency, as both rtTA3$_{ROSA26}$ and rtTA3G led to 96.8 ± 0.9% and 98.4 ± 0.3% of mCherry-expressing cells for rtTA3 and rtTA3G$_{ROSA26}$, respectively (**Figure 14** B,C). Finally, both rescue strategies were highly reproducible as evaluated by the small variations between replicates (**Figure 14** B,C). Therefore, delivery of Tet system elements in separate constructs fully restored Tet promoter-driven gene expression, thereby reverting mosaicism.

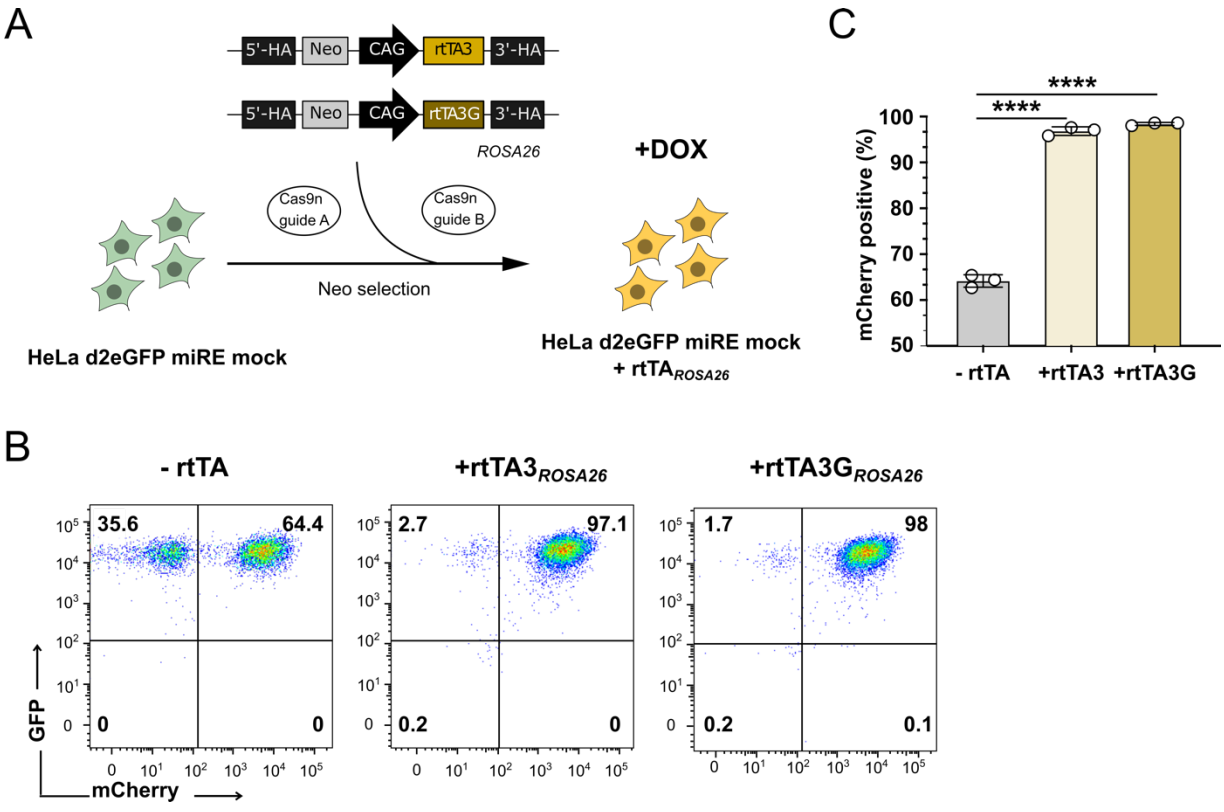


***Figure 14. Both rtTA3$_{ROSA26}$ and rtTA3G$_{ROSA26}$ can rescue transgene expression in bimodal cell populations when delivered in another genome location.*** ***A.*** *Workflow for targeting the ROSA26 locus of HeLa d2eGFP-miRE mock cells using CRISPR/Cas9 to provide either the rtTA3 or the rtTA3G to the Tet system in trans.* ***B.*** *Representative flow cytometry plots of HeLa d2eGFP-miRE mock and d2eGFP cells without (-rtTA) or with rtTA3*

*in the ROSA26 locus (+rtTA3$_{ROSA26}$) or rtTA3G (+rtTA3G$_{ROSA26}$) overexpression in trans after transgene expression induction with DOX.* ***C.*** *Flow cytometry quantification of the percentage of mCherry positive cells in three independent experiments represented as mean values ± SD (n=3). Statistical differences were analyzed using a one-way ANOVA followed by a multiple comparison Bonferroni test (**** p<0.0001).*

### 3.1.1.5 rtTA3G overexpression in trans led to sustained Tet promoter-mediated expression during subculturing

To test whether the recovery of Tet promoter-mediated expression was stable over cell division, clonal cell lines were generated from HeLa d2eGFP miRE mock rescued with rtTA3G (+rtTA3G$_{ROSA26}$) and compared to clones derived from polyclonal cells before the rescue experiment (-rtTA cells). Transgene expression was analyzed in isogenic cells at passage 3 (low passage) and passage 13 (high passage) after treatment with DOX for 3 days. Each isogenic cell line derived from pools rescued with rtTA3G$_{ROSA26}$ showed homogeneous mCherry expression, reaching a mean average of 96.8 ± 2.7% mCherry-GFP positive cells (**Figure 15**).

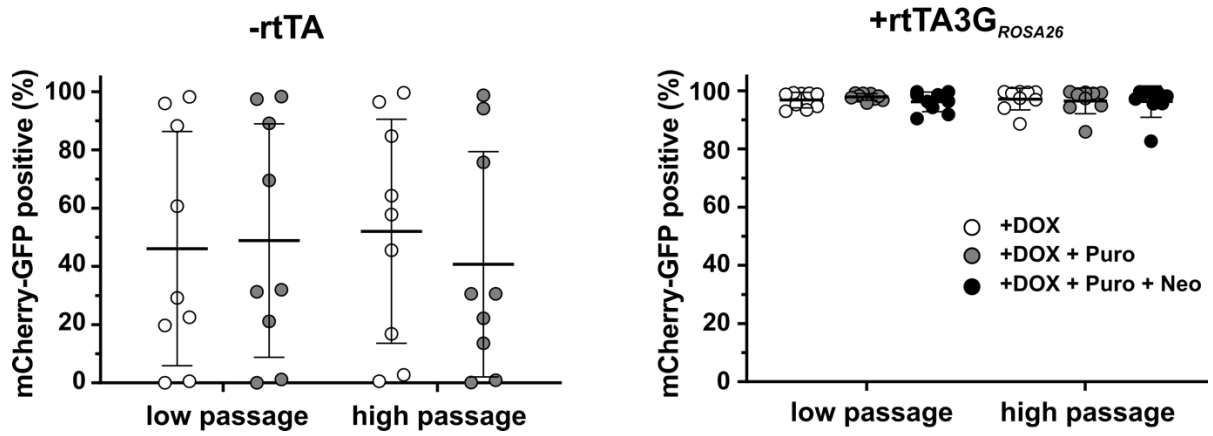


***Figure 15. rtTA3G overexpression in trans led to sustained Tet promoter-mediated expression during subculturing.*** *Flow cytometry quantification of the percentage of mCherry-GFP positive cells in isogenic clones derived from HeLa d2eGFP miRE mock cells (-rtTA, left) and HeLa d2eGFP miRE mock rescued with rtTA3G$_{ROSA26}$ (+rtTA3G $_{ROSA26}$, right) at low and high passage, cultured with DOX: doxycycline, Puro: puromycin and Neo: neomycin. Each dot represents an isogenic clone, bars display mean values ± SD (n=9 clones). A two-way ANOVA followed by a multiple comparison Bonferroni test showed no statistical differences between low and high passage for any groups.*

Furthermore, homogeneous expression was sustained for at least 13 passages after clonal isolation as assessed by an average expression of 97.1 ± 3.7% mCherry-GFP positive at high passage (**Figure 15**). Importantly, sustained selection with antibiotics was not required to achieve that figure, which is crucial for application in highly sensitive cells (**Figure 15**). In contrast, out of 9 isogenic cells in the -rtTA group only 3 showed over 75% mCherry-GFP positive cells, 4 clones exhibited bimodal expression at low passage, and 2 clones revealed less than 10% mCherry-GFP expressing cells (**Figure 15**). Interestingly, the average percentage of mCherry-GFP positive cells did not improved when -rtTA cells were cultured under continuous selective pressure with puromycin (46.1 ± 40.2% versus 48.9 ± 40.1%, respectively) (**Figure 15**). Based on these data, the two-vector Tet system leads to a more robust and stable inducibility in the majority of isogenic clones as compared with the single vector system.

## 3.1.2 Two-vector Tet-system in hiPSC

In view of the previous results, Wnt modulation experiments in hiPSCs were conducted in the OPTi-OX® cell line, a commercially available hiPSC line that constitutively expresses rtTA3G in the *ROSA26* locus under the control of the CAG promoter, hereafter named hiPSC-rtTA (93).

To analyze the miRE functionality in this cell platform, the Tet promoter-mCherry-miRE gene unit was transferred to the *AAVS1* safe harbor locus of hiPSC-rtTA cells using zinc-finger nucleases (ZFN) (**Figure 16**). In these experiments, miRE mock and miRE targeting the canonical Wnt signaling pathway mediator β-catenin (miRE β-cat) were used. After puromycin selection, isogenic cell lines were isolated, expanded and genotyped (**Figure 17** A).

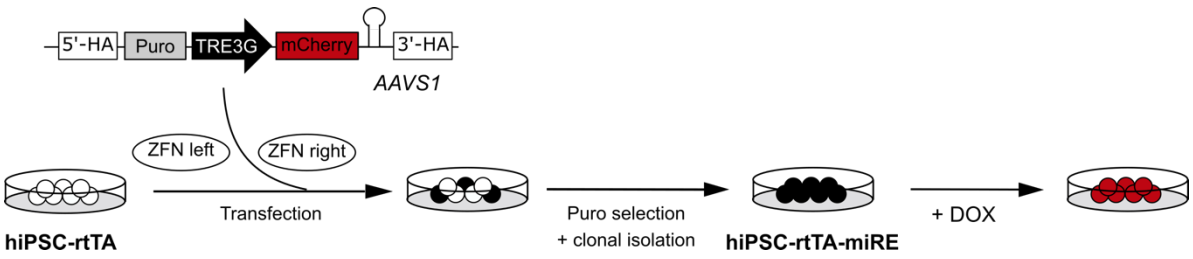


***Figure 16. Knockdown of β-catenin in hiPSC-rtTA cells using miRE technology.*** *Workflow to engineer hiPSC-rtTA cells with the Tet promoter controlling miRE expression in the AAVS1 locus using zinc-finger nucleases (ZFN).*

All the genotyped clones despite miRE mock clone 2 were heterozygous for Tet promoter-mCherry-miRE gene (**Figure 17** B). hiPSC-miRE mock clones 1, 3, 5, and miRE β-cat clones 5, 6, and 7 were used for the experiments in this thesis. Finally, differences in mCherry reporter expression between heterozygous and homozygous clones were shown by flow cytometry, thereby validating the genotyping strategy (**Figure 17** C).

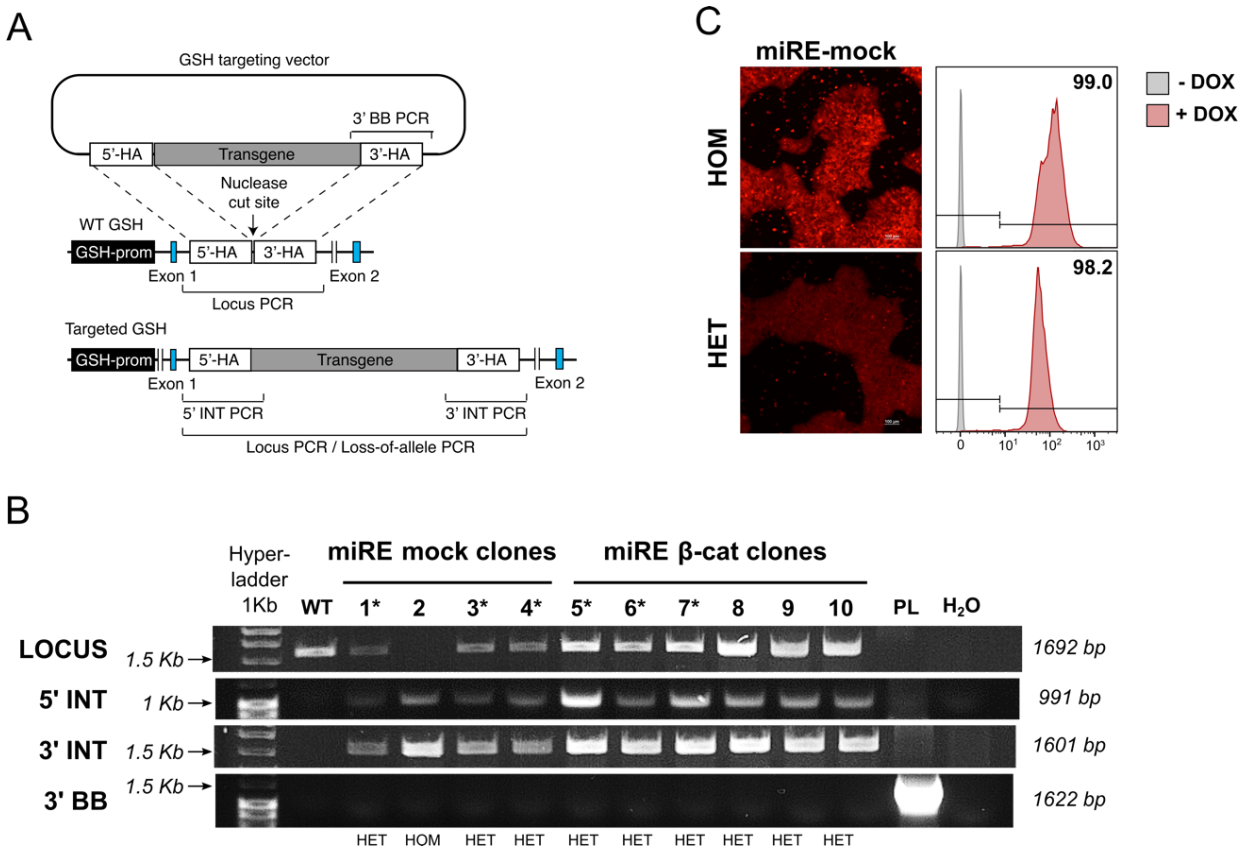


***Figure 17. Genotypic and phenotypic characterization of hiPSC isogenic lines. A.*** *PCR genotyping strategy. Figure adapted from* (93)*. The amplicons for the different genotyped reactions are indicated as locus PCR, 5'INT, 3'INT and 3'BB. GSH-prom: genomic safe harbor promoter.* ***B.*** *Results of genotyping PCR of 4 miRE mock clones and 6 miRE β-cat clones. Plasmid (PL) and water ($H_2O$) are the control samples. Below, HET and HOM indicate whether the clones are heterozygous or homozygous, respectively. Clones marked with an asterisk (*) were used for the experiments shown in this thesis* ***C.*** *mCherry expression after 3 days DOX treatment in homozygous and heterozygous miRE mock clones as shown by flow cytometry on live cells. Scale bars: 100 μm.*

### 3.1.2.1 Transgene expression characterization in hiPSC

Induction of gene expression in clonally expanded heterozygous cell lines showed homogeneous reporter mCherry expression in all cells and correlated with miRE functionality in terms of β-catenin knockdown efficiency (**Figure 18** A,B). Interestingly, miRE β-cat showed less reporter gene expression. Also, miRE mock cell lines had a lower β-catenin baseline expression (**Figure 18** B). In this configuration, a single copy of miRE β-cat led to 85% total β-catenin reduction after 4-day doxycycline treatment (**Figure 18** C).

In order to apply this conditional expression system during hiPSC differentiation, the kinetics and reversibility were analyzed. To that end, mCherry and β-catenin expression were monitored in hiPSC miRE β-cat isogenic lines during DOX treatment and subsequent withdrawal. Decreased mCherry expression and increased total β-catenin protein revealed that miRE β-cat induction was fully reverted 4 days after DOX withdrawal (**Figure 18** D**,** red and green histograms, respectively). Total β-catenin peaked at day 5 corresponding to 1.85-fold baseline β-catenin expression. Thereafter, β-catenin expression fluctuated from 1- to 1.85-fold as compared to day -4 and showed a decreasing trend towards baseline expression by day 9 (**Figure 18** E).

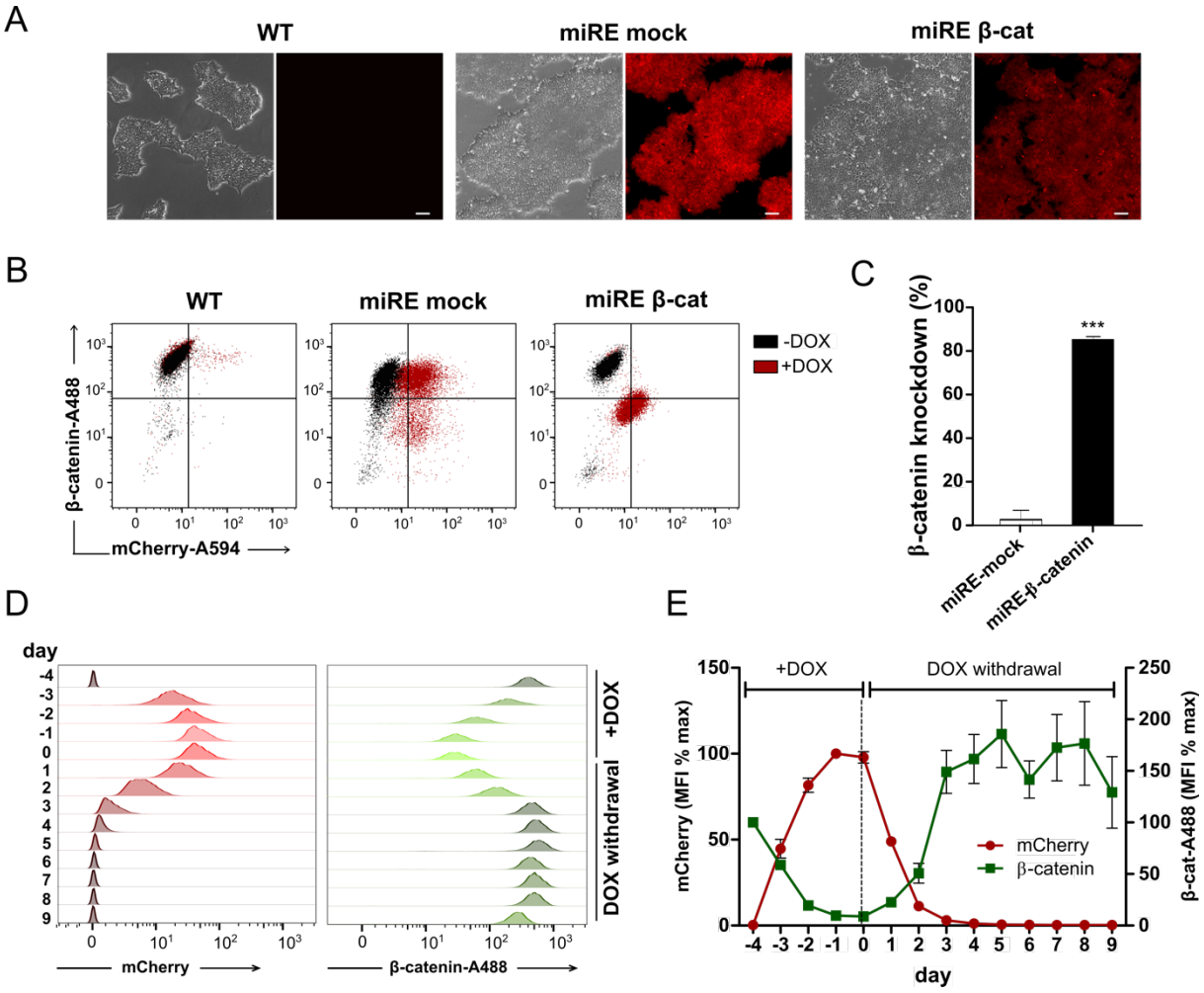


***Figure 18. Induction and reversibility of Tet promoter-driven miRE expression in hiPSC-rtTA.*** ***A****. Representative images of wild type (WT) and clonal engineered cells showing mCherry expression after 4-day doxycycline treatment (1 µg/ml). Scale bar: 100 µm* ***B****. Representative flow cytometry plots on fixed cells at day 4 of dox-treatment, co-stained for β-catenin and mCherry* ***C****. Quantification of the β-catenin knockdown efficiency percentage by subtraction of Alexa Fluor 488 mean fluorescence intensity (A488 MFI) in DOX-treated cells from untreated (-DOX) controls, divided by A488 MFI in -DOX controls multiplied by 100 (n=3 clonal cells). Unpaired t-test showed significant differences between miRE mock and miRE β-cat (*** p<0.001).* ***D****. Representative flow cytometry histograms of a time course analysis of mCherry expression (live measurement, left) and β-catenin expression (stained on fixed cells, right) during transgene expression induction with doxycycline, day -4 to day 0, and subsequent endogenous β-catenin expression recovery, day 0-9, after doxycycline withdrawal* ***E.*** *Quantification of β-catenin-A488 and mCherry MFI as a percentage of maximal baseline and maximal induction fluorescence, respectively*

*(day -1 for mCherry and day -4 for β-catenin). Represented as mean values ± SD (n=3 clonal cells).*

### 3.1.2.2 Induction of miRE expression during cardiomyocyte differentiation *in vitro*

The modulation of Wnt/β-catenin is central and sufficient to drive cardiac lineage specification of hiPSC *in vitro*. Firstly, the WNT-on-state is necessary to induce mesoderm cell commitment, followed by a WNT-off-state to further modulate differentiation of mesoderm cells into CMs. The exogenous modulation of this pathway is usually brought by using small molecule inhibitors such as CHIR to inhibit GSK3β, protein involved in destruction of β-catenin the Wnt master mediator, leading thus to a WNT-on state. Thereafter, IWR-1, which stabilizes the β-catenin destruction complex, is usually used to temporarily induce the WNT-off state needed for terminal differentiation into CMs. Consequently, it was hypothesized that miRE mediated knockdown of β-catenin could potentially promote differentiation of cardiac mesoderm cells into CMs following the same mechanism as IWR-1.

To determine the optimal DOX treatment window to induce sufficient β-catenin silencing and promote CM differentiation in mesoderm cells, hiPSC-miRE β-cat cells were differentiated into cardiac mesoderm cells and cardiac induction was brought by 1 µg/ml doxycycline treatment for 2, 3 or 4 days instead of IWR-1 (**Figure 19** A). At day 11, quantification of cTNT positive cells showed a correlation between cTNT positive cells and treatment length (**Figure 19** B). A 4-day-DOX-treatment was sufficient to achieve the same differentiation efficiency as in the control group (14.25 ± 3.5% and 13.6 ± 2.3% cTNT positive cells, respectively) (**Figure 19** B).

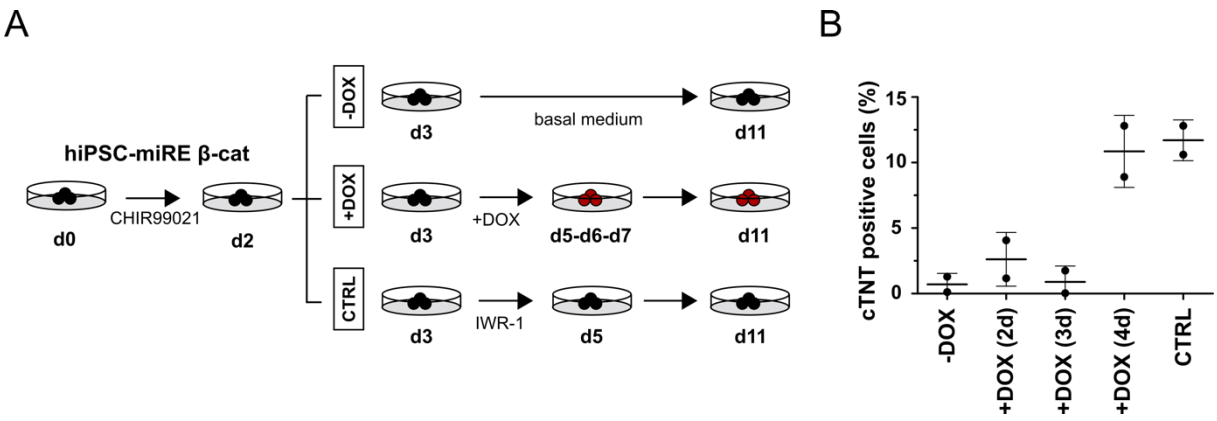


***Figure 19. Doxycycline incubation time titration to induce CM differentiation in hiPSC-miRE β-cat-derived mesoderm cells. A.*** *Schematic overview of the different groups and differentiation procedures.* ***B.*** *Quantification of the percentage of cTNT positive cells measure by flow cytometry and represented in means ± SD (n=2).*

To analyze the specificity of miRE β-cat, clonal hiPSCs miRE mock and miRE β-cat cells were differentiated into mesoderm cells and divided into 3 groups for further differentiation towards CMs: (i) untreated group (-DOX), (ii) treated with doxycycline for 4 days (+DOX) and (iii) treated with IWR-1 for 2 days (CTRL). Successful induction of miRE expression after DOX treatment during *in vitro* differentiation was confirmed by the residual presence of mCherry positive cells at day 11, 4 days after DOX withdrawal (**Figure 20** A). Interestingly, beating cell sheets were observed in all groups including the -DOX group (**Figure 20** A). In addition, all hiPSC-miRE mock groups differentiated more efficiently into CMs, 82.95 ± 5.75%, than hiPSC-miRE β-cat, 10.85 ± 7.95% cTNT positive cells at day 11 in the CTRL group (**Figure 20** B,C). Although no statistically significant differences were detected, DOX treatment in miRE β-cat led to an average 2.74-fold increase of cTNT positive cells at day 11 as compared with -DOX group, and this was similar to the 2-fold increase in the CTRL group. In contrast, mock controls did not show doxycycline-dependent differences in the percentage of cTNT positive cells as the fold change was approximately 1 in +DOX compared with the 1.43-fold reported in the CTRL group (**Figure 20** B,C,D). Of note, cTNT mean fluorescence intensity was conserved across groups at day 11, indicating a similar degree of CM maturity in all groups and cells (**Figure 20** B). Therefore, although the lower differentiation efficiency of cells harboring the miRE β-cat requires further investigation, conditional β-catenin silencing increases the conversion rate of mesoderm cells into cTNT positive cells by nearly 3-fold as compared with untreated cells.

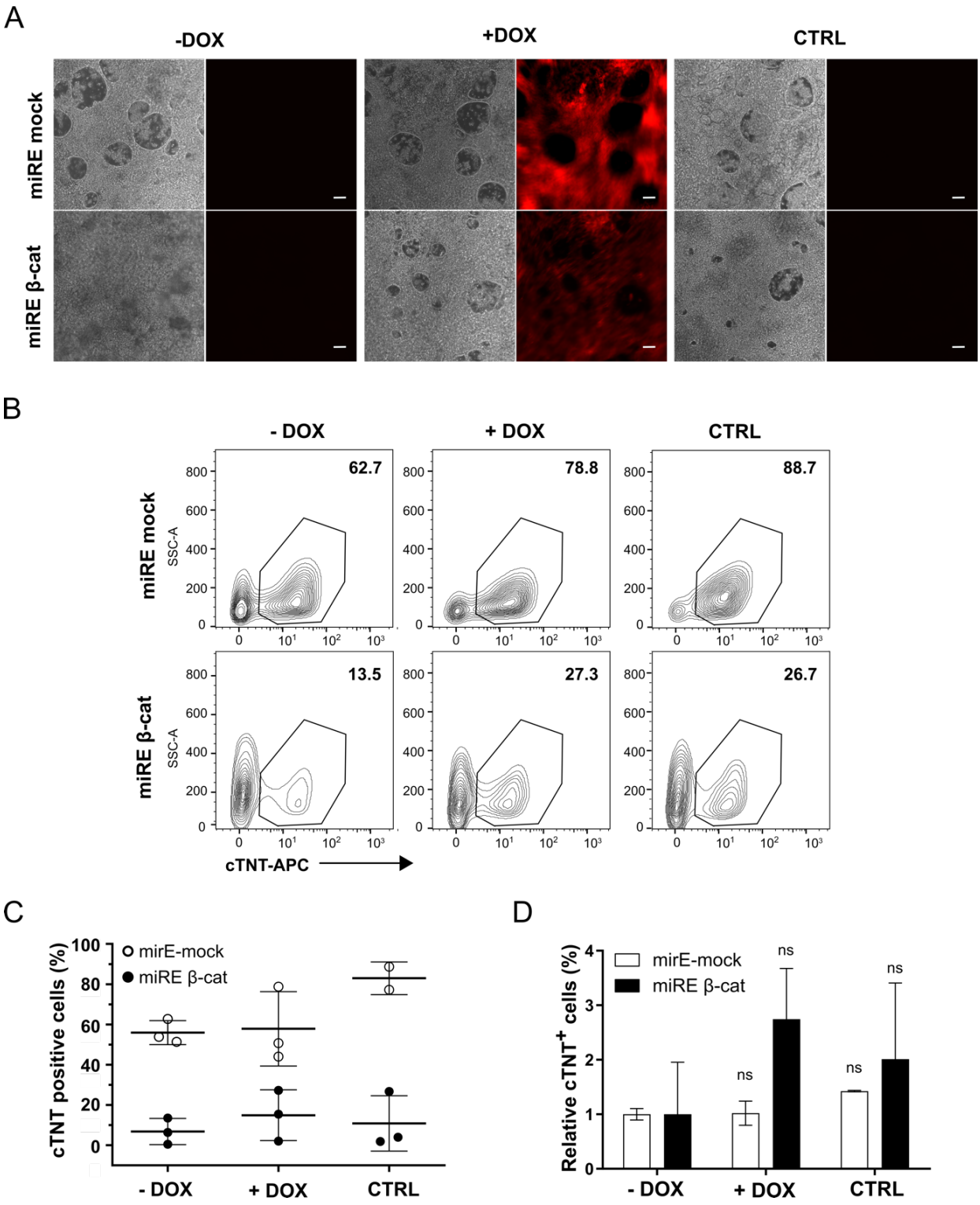


***Figure 20. Inducible Wnt signaling inhibition leads to an increase of cTNT positive cells in doxycycline-treated hiPSC mirE β-cat cells as compared with non-treated controls.*** ***A.*** *Representative pictures of miRE mock and miRE β-cat hiPSC lines at day 11 of cardiomyocyte differentiation showing beating cell sheets in different conditions: untreated (-DOX), doxycycline-mediated (+DOX) and small molecule or IWR-1-mediated (CTRL). Scale bars: 100 µm* ***B.*** *Scatter plots of cTNT-APC stained cells at day 11 of*

*differentiation.* ***C.*** *Flow cytometry quantification of the percentage of cTNT positive cells in biological replicates, shown as mean ± SD (n=3, different clones).* ***D****. Relative percentage of cTNT positive (cTNT+) cells normalized to -DOX baseline control shown as means ± SD (n=3). Two-way ANOVA followed by Bonferroni multiple comparison test showed no statistical differences between +DOX and CTRL groups when compared with -DOX (ns, p>0.05).*

# 3.2 Expandable Sca-1-positive cardiac progenitor-like cells from hiPSCs

In the previous chapter, the idea of inducing differentiation after cardiac mesoderm differentiation was explored with the aim of promoting CM differentiation in this multipotent cell population. However, it was shown that cells that have initiated differentiation into mesoderm cells tend to spontaneously differentiate into fetal-like beating CM *in vitro*. This phenomenon represents one of the main challenges when establishing protocols to generate *de novo* CPCs from hiPSCs (70).

In this chapter, it was hypothesized that a well-characterized non-beating human cardiomyocyte progenitor cell population based on Sca-1 expression (hCMPC) could be isolated from hiPSCs undergoing differentiation to CMs. Also, the proliferative and cardiomyogenic potential of the hiPSC-derived hCMPC ($iCPC^{Sca\text{-}1}$) was assessed.

## 3.2.1 Determining the optimal cardiac progenitor isolation time

hiPSCs can recapitulate cardiac development *in vitro* and thus represent a source of potentially expandable CPCs. To determine the optimal time for hCMPC-like cell isolation, gene expression of second heart field cardiac progenitor markers such as GATA4, NKX 2-5, and Isl-1 was monitored from day 0 to day 6 of *in vitro* CM differentiation. Expression of these markers occurred in two waves: first, GATA4 and Isl-1 expression started at day 5 and was further upregulated at day 6, followed by cardiac specification as shown by NKX 2-5 upregulation at day 6 (**Figure 21** A,B). hCMPCs isolated from human fetal hearts were used as reference cells. These cells technically are an independent CPC population from Isl-1 CPC but express NKX 2-5 and GATA-4 (**Figure 21** B). Based on this gene expression pattern, hCMPC-like cells are expected to occur between day 5 to 6 of CM differentiation.

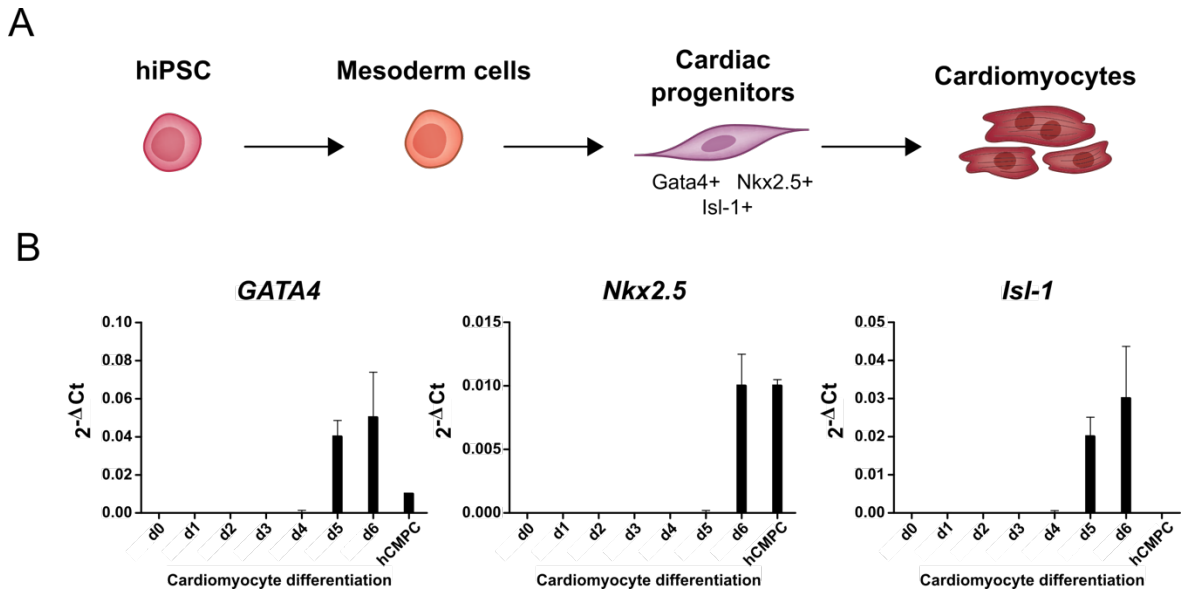


***Figure 21. Gene expression of cardiac progenitor markers during hiPSCs differentiation to cardiomyocytes.*** ***A****. Schematic overview of the intermediate cells during hiPSC differentiation into cardiomyocytes and specific markers used to identify them.* ***B****. Time course real-time PCR analysis of GATA4, NKX 2-5 and Isl-1 depicted as delta Ct values normalized to GAPDH (n=3, technical replicates). hCMPCs: fetal Sca-1 positive cardiomyocyte progenitor cells. This data was kindly provided by Janita Maring.*

### 3.2.2 Differentiation protocol and expandability of the isolated cells

As mentioned before, one of the reported challenges in obtaining hCPC-like cells from hiPSCs is to slow down the very rapid transition from mesoderm cells to beating CMs. Here, a protocol to hinder CM differentiation by sequentially withdrawing cardiac differentiation inducing factors while adding cardiac progenitor supportive medium was tested in three independent hiPSC lines. Firstly, cells were differentiated into mesoderm cells using the previously described cardiomyocyte differentiation protocol. Based on the onset of GATA4 and NKX2-5 expression, differentiation was hindered for 2 days at day 3, 4, 5 and 6 of differentiation. After two days, Sca-1 cell isolation was subsequently performed using MACS (**Figure 22**). Only the Sca-1 fraction isolated at day 4 (early) and day 5 (late) showed proliferative capacity and were, thus, selected for further experiments.

Flow cytometry analysis after MACS showed that although heterogeneous, the isolated Sca-1 positive fraction, hereafter named induced cardiac progenitor based on Sca-1 expression (iCPC$^{Sca\text{-}1}$), contains smaller and less complex cells than the unbound or flow-

through fraction (FT) (**Figure 23** A). Both early and late iCPC$^{Sca-1}$ showed a non-beating phenotype and heterogeneous morphology at passage 0. In turn, FT contained a mixed population of cells that included beating CM clusters also in the early group, wherein beating cells were not abundant before MACS (**Figure 23** B).

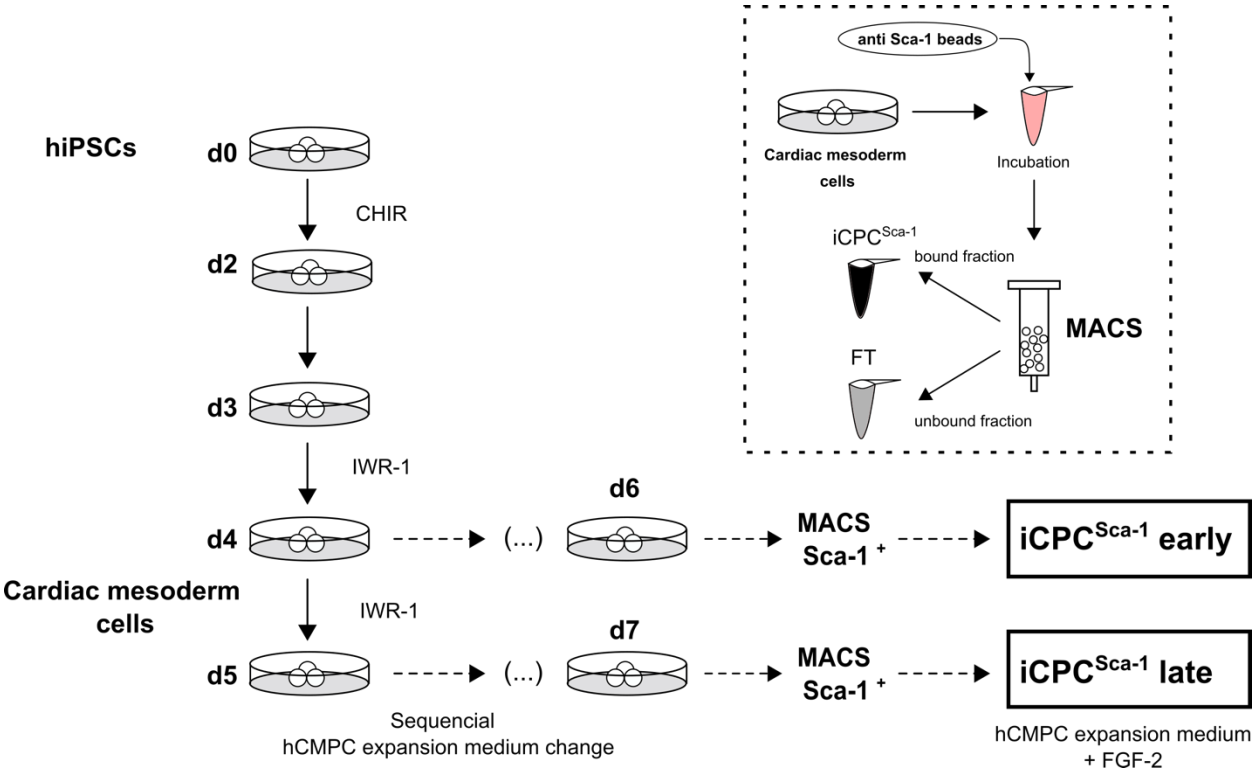


***Figure 22. iCPC$^{Sca-1}$ differentiation protocol.*** *Schematic overview of iCPC$^{Sca-1}$ differentiation protocol day by day. Within the dashed square detailed scheme of the magnetic cell sorting (MACS) strategy followed to isolate the bound fraction (iCPC$^{Sca-1}$) and the unbound fraction or flow-through (FT) for each timepoint. CHIR: CHIR99021, FT: Flow-through.*

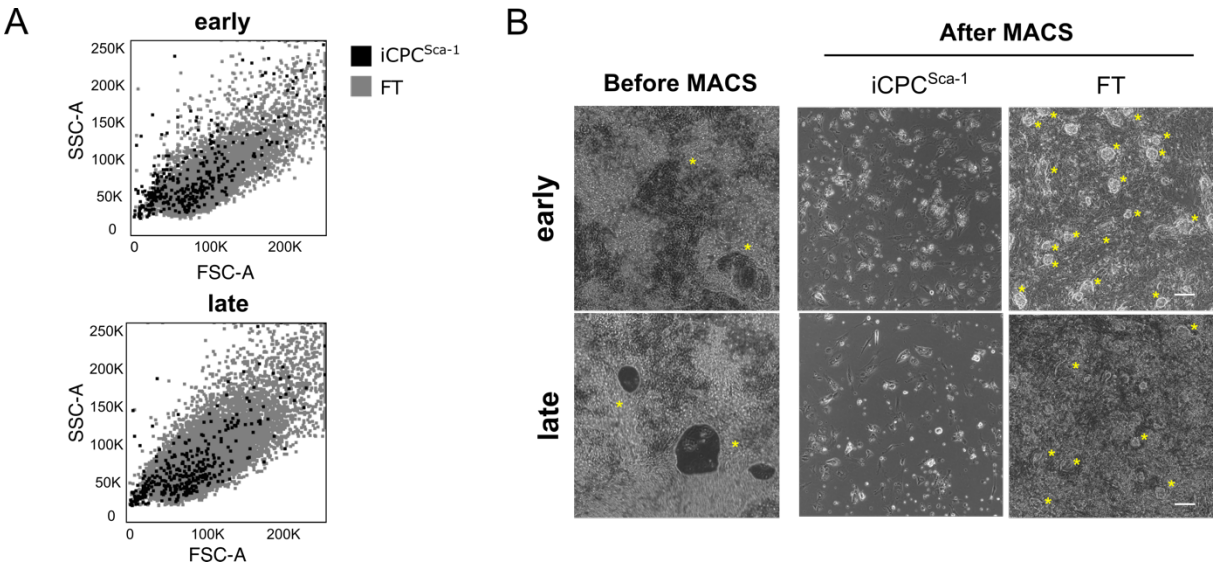


***Figure 23. Differentiation protocol and Sca-1 positive fraction isolation strategy.*** ***A.*** *Flow cytometry superimposed forward, and side scatter plots of iCPC$^{Sca-1}$ (black dots) and flow-through cells (FT) (grey dots) isolated at day 6 (iCPC$^{Sca-1}$ early) and day 7 (iCPC$^{Sca-1}$ late) of differentiation.* ***B.*** *Representative pictures showing the morphological characteristics of differentiated cells before and iCPC$^{Sca-1}$ and the FT after MACS, 4 and 3 days after sorting, for early and late groups, respectively. Yellow asterisks (*) indicate beating clusters. Scale bars: 100 µm*

After isolation, early and late iCPC$^{Sca-1}$ were cultured in hCMPC medium with fibroblast growth factor 2 (FGF-2) to induce cell growth for three passages as described for isolated hCMPC from fetal hearts (80). To analyze the effect of FGF-2 on cell growth after three passages, iCPCs$^{Sca-1}$ were cultured with or without FGF-2 for three days and counted daily. Cell growth curves showed no difference between both groups, and thus cells were expanded without FGF-2 after passage 3 (**Figure 24**).

Both early and late iCPC$^{Sca-1}$ were expanded for at least 10 passages without FGF-2 and showed a stable and similar morphology as hCMPC (**Figure 25** A, B). The proliferation capacity was monitored by calculating the population doubling time (PDT) during 10 passages. The PDT remained constant in all iCPC$^{Sca-1}$ groups until passage 10, when it was 49 ± 9.1 and 43.8 ± 15.2 h for early and late iCPC$^{Sca-1}$, respectively. In contrast, both early and late FT cells showed recurrent fluctuations and a higher average PDT than iCPC$^{Sca-1}$ (**Figure 26** A).

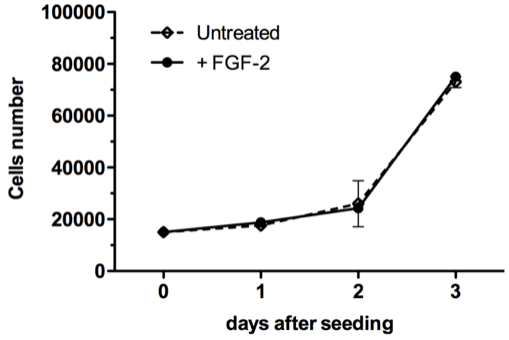


***Figure 24. Effect of FGF-2 in the proliferation of iCPC$^{Sca-1}$.*** *Cell counts of iCPC$^{Sca-1}$ cultured with or without FGF days after passaging represented as means ± SD (n=2, technical replicates).*

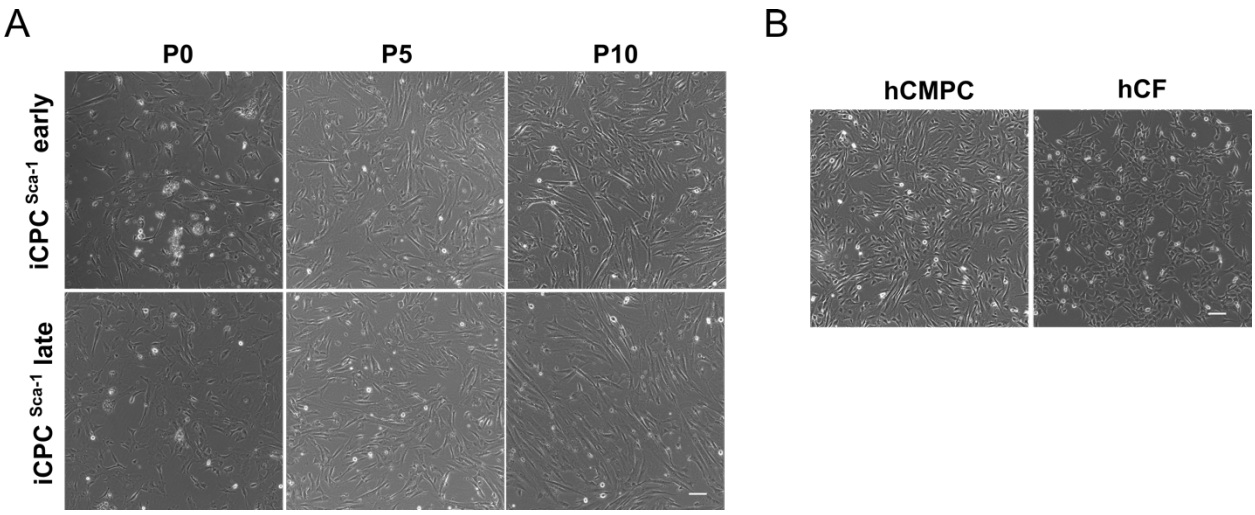


***Figure 25. iCPC$^{Sca-1}$ morphology during subculture. A.*** *Representative brightfield pictures of induced cardiomyocyte progenitor cell based on Sca-1 expression (iCPC$^{Sca-1}$) early and late cells at different passages (0, 5 and 10)* ***B.*** *Brightfield pictures of human fetal cadiomyocyte progenitor cells (hCMPCs) and human cardiac fibroblasts (hCF) at passage 11. Scale bars: 50 µm*

In addition, when compared to fetal hCMPCs (31.5 ± 6.5 h) and human cardiac fibroblasts (hCF) (8.5 ± 1.6 h) at matched passage, *i.e.*, passage over 10, both early (62 ± 39.1 h) and late iCPCs$^{Sca-1}$ (50 ± 35.9 h) had a higher PDT (**Figure 26** B). Yet, these differences were not statistically significant. Notably, PDTs in iCPC$^{Sca-1}$ were more variable as seen by high standard deviations between the biological replicates. Next, cumulative population doublings showed that late iCPC$^{Sca-1}$ had a higher proliferative potential than early iCPC$^{Sca-1}$ as assessed by comparing the PDT slopes *i.e.,* proliferation rate (**Figure**

**26** C). The overall cumulative population doublings were 33 and 39.14 for early and late iCPC$^{Sca-1}$, respectively (**Figure 26** C).

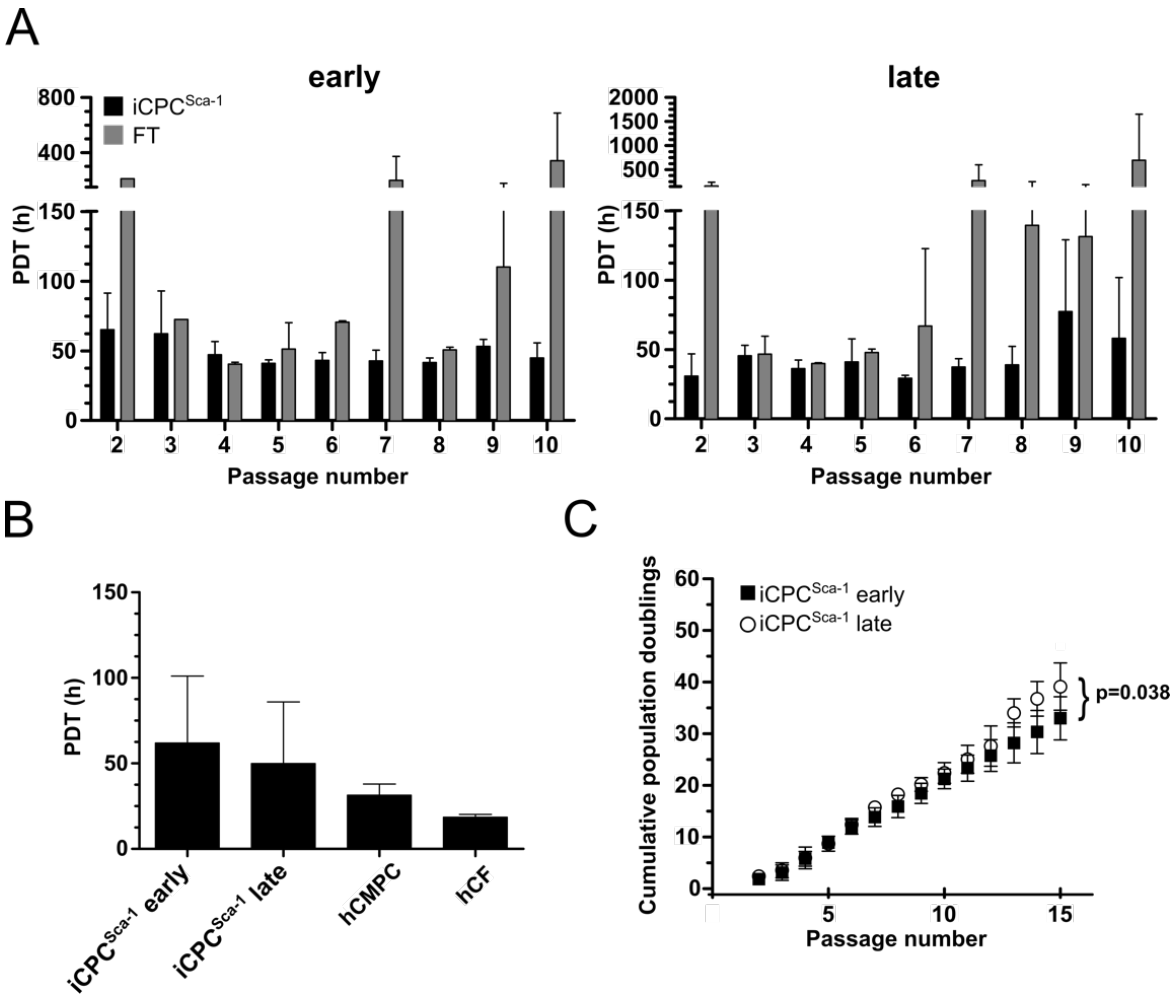


***Figure 26. Characterization of iCPC$^{Sca-1}$ and FT proliferative potential. A.*** *Population doubling time (PDT) in hours of early and late iCPC$^{Sca-1}$ and the correspondent flow-through fraction (FT) during subculturing for 10 passages after isolation. PDT calculation is done after passage 2 when proliferation has already been induced by FGF-2. (n=2-3, different hiPSC donors).* ***B.*** *Population doubling time (PDT) average of early iCPC$^{Sca-1}$, late iCPC$^{Sca-1}$, hCPCs and hCFs at matched passages (n= 3). One-way ANOVA showed no statistical differences.* ***C.*** *Cumulative population doubling comparison between early and late iCPC$^{Sca-1}$ for 15 passages after isolation (n=3, hiPSC donors). Linear regression test, slopes are significantly different.*

## 3.2.3 Phenotypic characterization

### 3.2.3.1 Immunophenotype

Mirroring development, iCPCs$^{Sca-1}$ are derived from the mesodermal germ layer during *in vitro* differentiation of hiPSCs. To discard the presence of other mesoderm-derived populations such as hematopoietic or endothelial progenitor cells, the immunophenotype of iCPC$^{Sca-1}$ was characterized during subculturing.

Flow cytometry analysis confirmed that iCPCs$^{Sca-1}$ did not express endothelial or hematopoietic progenitor markers, such as CD34 and CD45 positive cells, respectively (**Figure 27** A, B). This trend was conserved during cell expansion. In addition, the expression of Endoglin (CD105), considered a cell surface hCMPC population marker (80), while sparse and heterogeneous at low passages was acquired during subculturing, and became predominantly expressed at high passages (**Figure 27** A,B). Interestingly, the same trend was observed in the FT cells (**Figure 27** C). In addition, FT groups were similarly free from other mesoderm progenitors, suggesting that most of the cells had committed to the cardiac mesoderm lineage by the isolation day (**Figure 27** C).

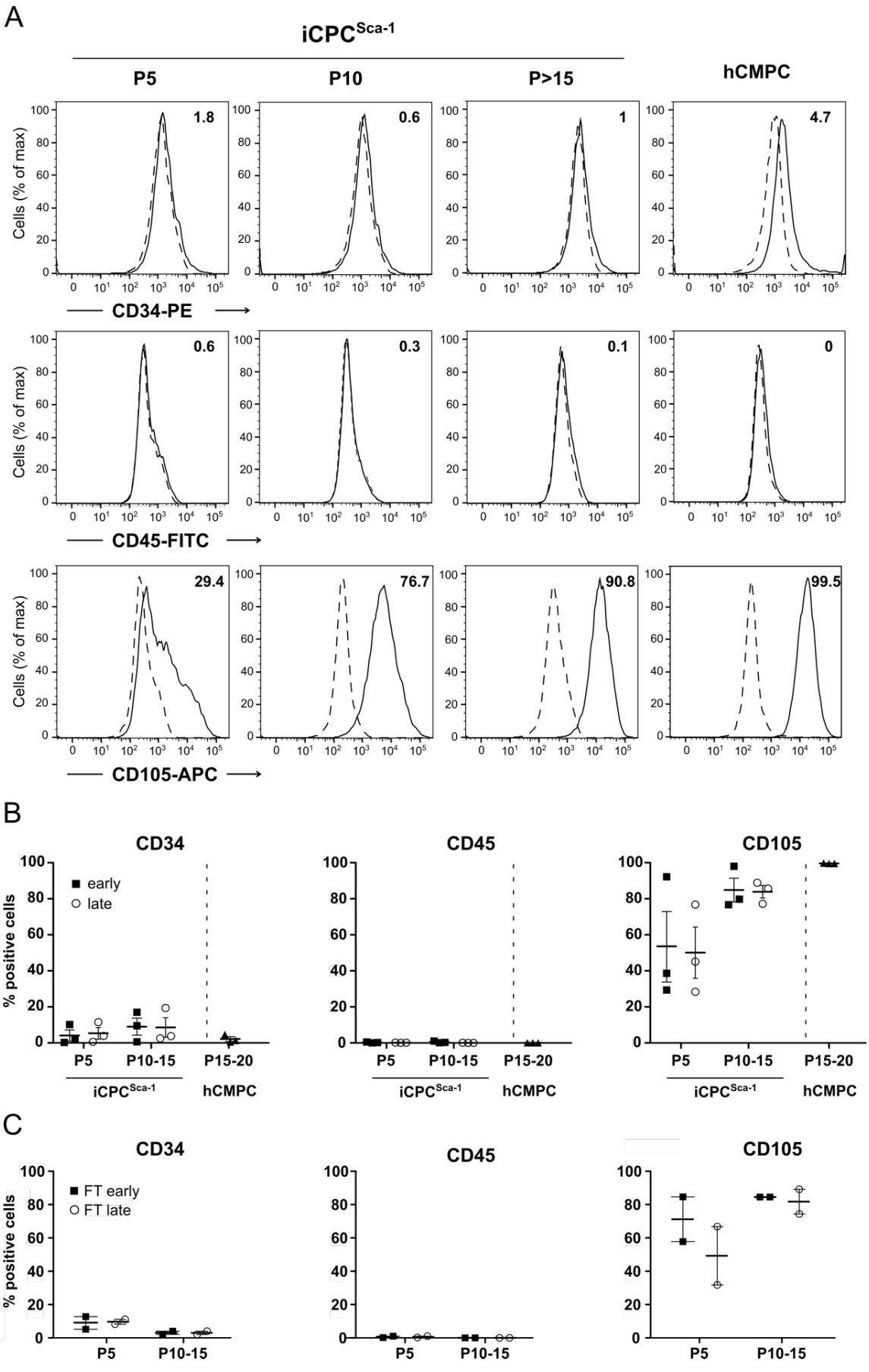
A
iCPC^Sca-1
P5
P10
P>15
hCMPC
Cells (% of max)
1.8
0.6
1
4.7
CD34-PE
0.6
0.3
0.1
0
CD45-FITC
29.4
76.7
90.8
99.5
CD105-APC
B
CD34
CD45
CD105
% positive cells
early
late
P5
P10-15
P15-20
iCPC^Sca-1
hCMPC
C
FT early
FT late

***Figure 27. Immunophenotypic characterization of the iCPC$^{Sca-1}$ at different passages.*** ***A.*** *Representative histograms of iCPC$^{Sca-1}$ early cells stained for CD34, CD45, and CD105 at different passages, 0, 5 and higher than 15, as well as hCMPC at passage 11. Dashed-lined histograms are unstained controls and numbers indicate the percentage of positive cells.* ***B.*** *Quantification of the percentage of iCPC$^{Sca-1}$ positive cells and hCMPCs for each cluster of differentiation, CD34, CD45 and CD105 during subculturing at passages 5, passage 10-15 for iCPCs and passage 15-20 for hCMPCs, the control cells (n=3 biological replicates).* ***C.*** *Quantification of the percentage of flowthrough CD34, CD45 and CD105 positive cells during subculturing at passage 5 and 10-15. (n=2 biological replicates). Values are represented as means ± SD.*

### 3.2.3.2 Cardiac signature

To discern whether these highly proliferative iCPC$^{Sca-1}$ were committed to the cardiac lineage, the expression of cardiac troponin I (cTNI) and NKX 2-5 was analyzed. cTNI is a structural cardiac regulatory protein that control the calcium mediated interaction between actin and myosin (102). In turn, NKX 2-5 is a transcription factor expressed by early cardiac progenitor cells during embryogenesis that continues to be expressed in the heart during adulthood (103).

cTNI was uniformly expressed across donors and was comparable to hCMPCs (**Figure 28** A). In contrast, different NKX 2-5 expression levels were found in iCPC$^{Sca-1}$ in a donor and time-dependent fashion (**Figure 28** B). Interestingly, donor A-derived late iCPC$^{Sca-1}$ showed higher expression of NKX 2-5 in early cells as compared with late cells. Donor B-derived iCPC$^{Sca-1}$ were NKX2-5 positive in early and late, and only late iCPC$^{Sca-1}$ were NKX2-5 positive in donor C (**Figure 28** B).

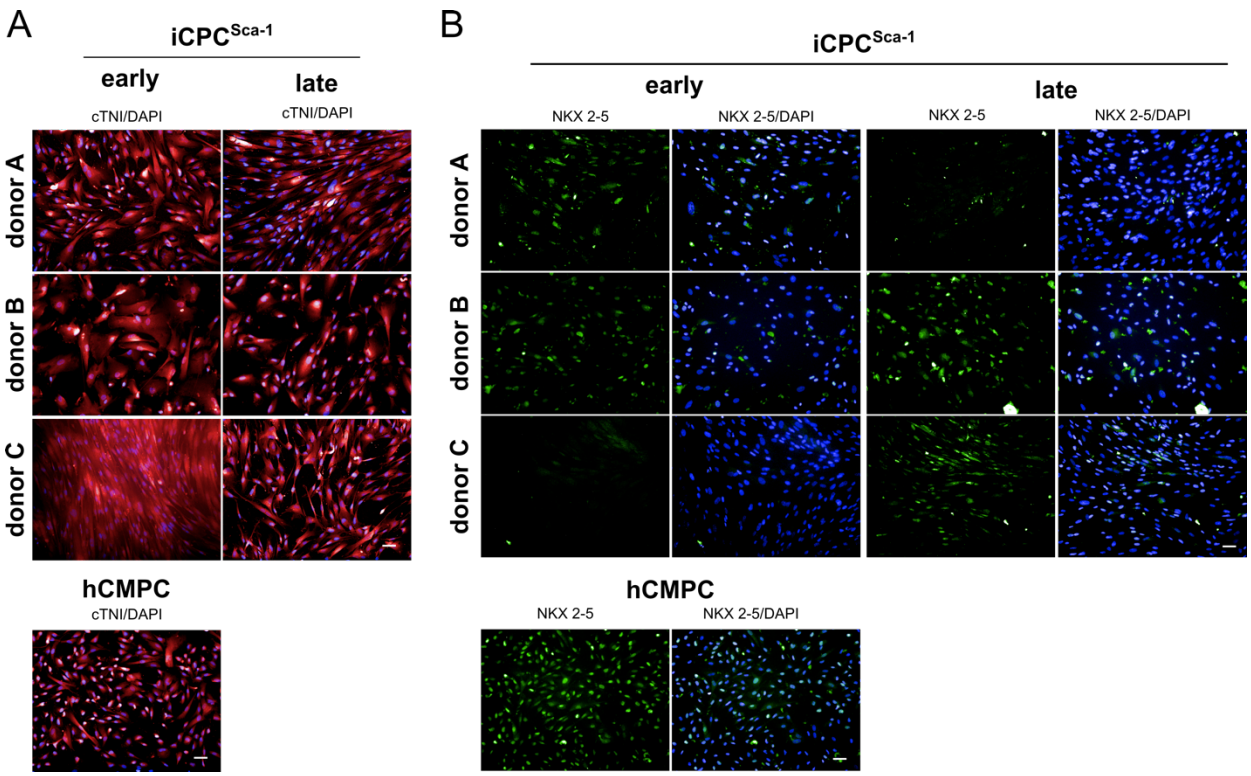


***Figure 28. Cardiac troponin I and NKX 2-5 expression in iCPC$^{Sca-1}$ and hCMPC. A.*** *cTNI (red) merged with DAPI (blue) in iCPC$^{Sca-1}$ early and iCPC$^{Sca-1}$ late from different hiPSC donors (A,B and C) at passage 5 and fetal hCMPCs passage 11.* ***B.*** *NKX 2-5 expression (green) and NKX 2-5 merged with DAPI (blue). Scale bars: 50 µm*

## 3.2.4 Cardiomyogenic potential

The ability to differentiate into cardiac cells is a hallmark of cardiac progenitor cells. To discern whether iCPC$^{Sca-1}$ differentiate into CMs, undifferentiated iCPC$^{Sca-1}$ and hCMPC cells were cultured with cardiomyocyte differentiation medium (CDM). Since previously frozen iCPC$^{Sca-1}$ were used for this experiment, the expression of cardiac progenitor markers was quantified before differentiation to corroborate that hCMPC-like phenotype was maintained. The majority of cells preserved an hCMPC-like phenotype as seen by 83.7 and 92.6% cTNI positive cells in iCPCs$^{Sca-1}$ and hCMPCs, respectively (**Figure 29** A,B). In addition, 15.1% of iCPC$^{Sca-1}$ and 30.5% hCMPC were NKX 2-5 positive (**Figure 29** C,D).

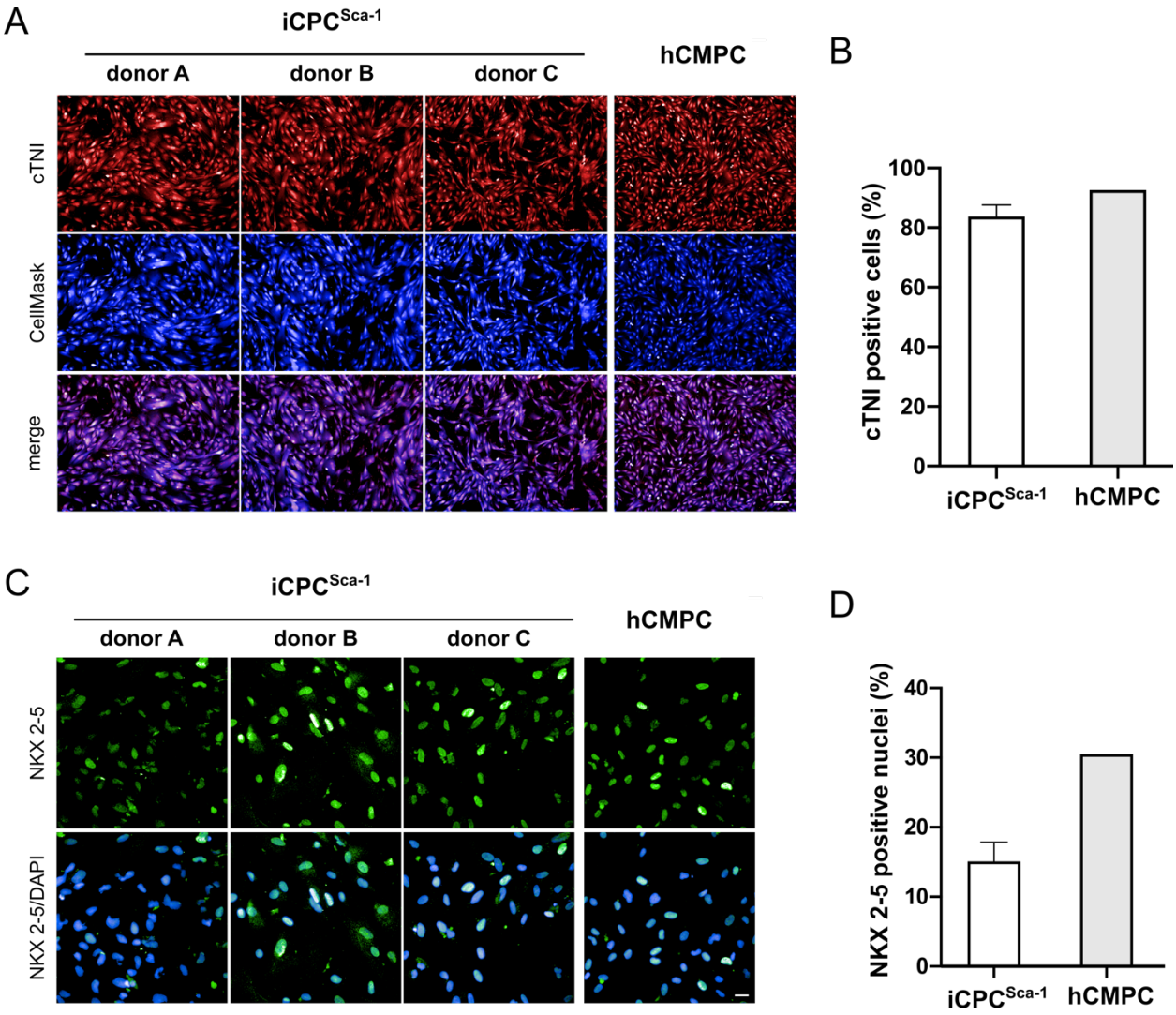


***Figure 29. Quantification of cardiac progenitor markers in thawed cells.*** ***A.*** *Representative pictures of iCPC$^{Sca-1}$and hCMPCs stained for cardiac troponin I (red), CellMASk (blue) and both (merge) at passage 6. Scale bar: 100 µm.* ***B.*** *Quantification of cTNI positive cells is represented as mean values ± SD (n=3 donors for iCPC$^{Sca-1}$ and n=1 for hCMPC).* ***C.*** *Representative pictures of iCPC$^{Sca-1}$and hCMPCs nuclei stained for NKX 2-5 (green) and merged with DAPI (blue) after thawing. Scale bar: 20 µm.* ***D.*** *Quantification of NKX 2-5 positive nuclei represented as mean values ± SD (n=3 donors for iCPC$^{Sca-1}$ and n=1 for hCMPC).*

In order to stimulate cardiomyogenesis, iCPC$^{Sca-1}$ and hCMPC were shortly cultured in CDM for 3 days and kept in cardiomyocyte maintenance medium (CMM) without induction factors for 11 days. Interestingly, a lot of cell death was observed during day 2 and 3 after CM differentiation induction (data not shown). Remarkably, this phenomenon was not compensated by cell proliferation after differentiation induction and generally led to scarcely populated wells by the experiment endpoint. After 14 days of differentiation,

analysis of cell morphology using CellMask revealed that donor B and C-derived iCPC$^{Sca-1}$ had significantly enlarged after culture in CDM similarly to hCMPCs and were as big as hiPSC-derived CMs (hiPSC-CMs) (**Figure 30** A,B,C). In contrast to hCMPCs, all iCPC$^{Sca-1}$ lines showed increased α-actinin expression at day 14 as compared with day 0. The latter was significant in donor B and C (**Figure 30** A,D). Despite α-actinin fluorescent intensity in iCPCs$^{Sca-1}$ was comparable to hiPSC-CMs cultured in CMM, no presence of beating cells nor CM-specific striated sarcomere structures were detected in iCPCs$^{Sca-1}$ after cardiomyogenic induction (**Figure 30** B).

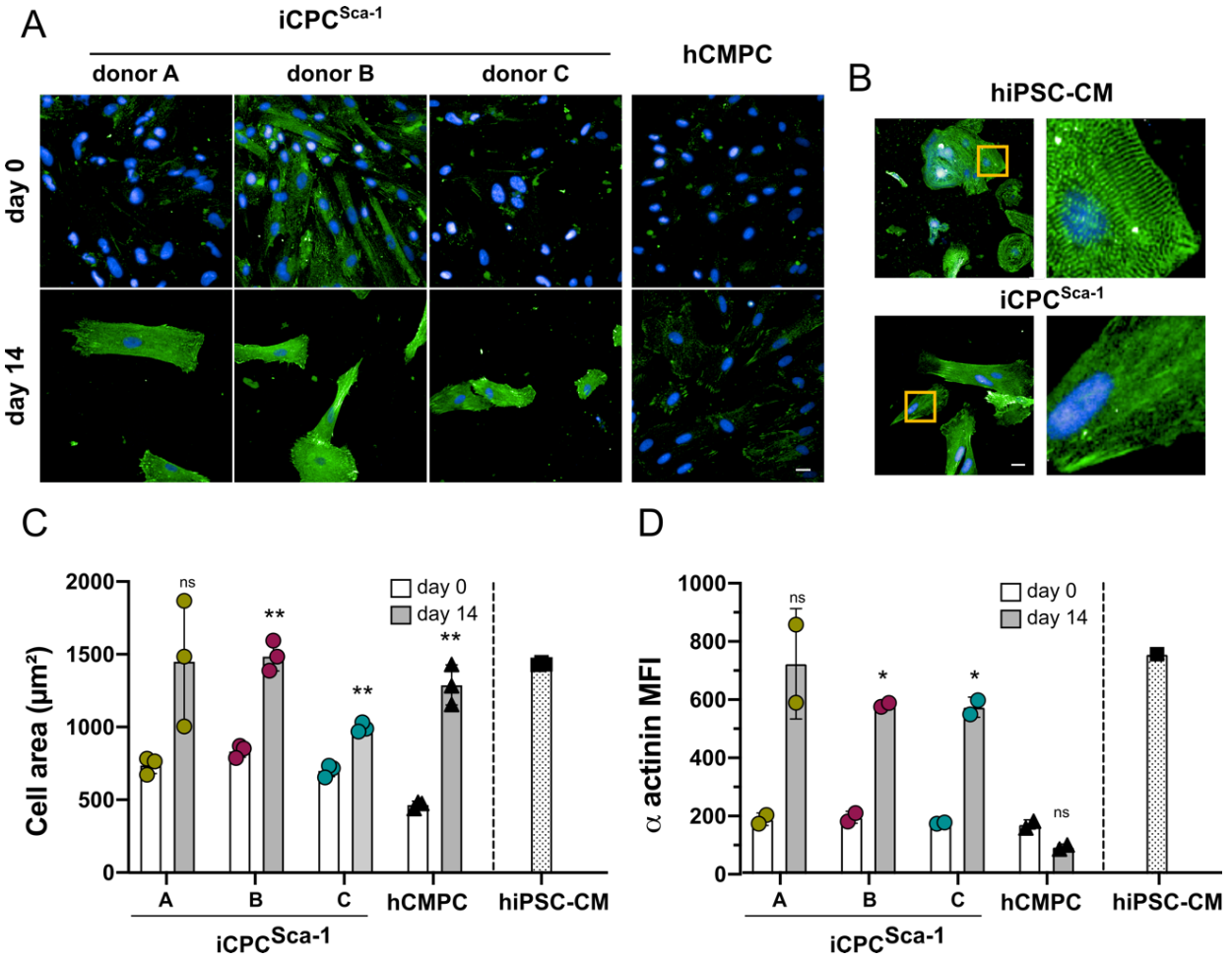


***Figure 30. Analysis of iCPC$^{Sca-1}$ and hCMPC cardiomyocyte phenotype upon culture in cardiomyocyte differentiation medium for 14 days. A*** *α-actinin (green) expression merged with DAPI (blue) in three iCPC$^{Sca-1}$ donors and hCMPCs before (day 0) and after culture in cardiomyocyte differentiation medium for 14 days (day 14).* ***B.*** *hiPSC-CM and iCPC$^{Sca-1}$ from donor A stained for α-actinin (green) and DAPI (blue). On the right, magnified images of the orange-squared area. Scale bars: 20 µm.* ***C.*** *Quantification of the average cell area and* ***D.*** *α-actinin mean fluorescence intensity (MFI) of iCPC$^{Sca-1}$ and hCMPCs at day 0 (white bar) and day 14 (grey bar) of cardiomyocyte differentiation. The three different*

*iCPC$^{Sca-1}$ donors are indicated as "A", "B" and "C" in the graphs. hiPSC-CMs cultured in cardiomyocyte maintenance medium and stained in parallel (dotted bar) were used as a reference value. Values are represented as mean ± SD (n=2-3 technical replicates). Paired t-tests were used to evaluate differences between day 0 and day 14 within each group (p<0.01 **, p<0.05 *, p>0.05 ns). hiPSC-CMs were not included in the statistical analysis.*

# 4 Discussion

## 4.1 Tet-systems: the hurdle of impaired expression

Single vector Tet-systems are attractive for clinical applications because they simplify the genetic engineering process, thereby reducing time, cell stress and risks associated to insertional mutagenesis. However, bimodal expression of genes controlled by the Tet promoter was observed in a reporter cell line. Bimodal expression of transgenes is routinely observed in a small fraction of any genetically engineered bulk cell populations cultured without selective pressure. Expression of foreign genes reduces cell fitness; thus, it is not surprising that cells develop mechanisms to cope with the presence of foreign DNA. Bimodal expression is commonly attributed to epigenetic mechanisms and can be counteracted either by (i) continuous antibiotic selection or (ii) expansion of stable single cell clones (104). However, in this thesis, mCherry negative cells (non-expressing cells) notably represented almost half of the population. In addition, homogeneous expression in bulk populations could not be restored by continuous selective pressure and clonal expansion revealed mosaic transgene expression in genetically identical cells within days of expansion in selection medium. Also, continuous gene expression activation, often considered a strategy to prevent transgene expression loss (105), failed to prevent mosaicism in clonally expanded cells cultured with doxycycline (DOX) since transfection. All these findings suggest that the mechanism leading to bimodal expression is not prevented by the transgene's chromatin environment at the moment of cell division.

Lack of transgene expression can be due to loss of the transgene, gene silencing, as well as post-translational regulatory mechanisms (106). Various factors contribute to these phenomena ranging from: (i) nature of integration sites (107), (ii) transgene copy number (108), (iii) methylation in the promoter regions (109), (iv) deacetylation of histones (105), (v) interactions between subsequent genetic units as a result of construct design (101), and (vi) repeated sequences within the transgene cassettes, as for instance within the Tet promoter (110). All these variables underline the need to optimize the gene engineering strategy for each application.

The fact that the mosaic HeLa cells are antibiotic resistant suggests that non-expressing cells still contain at least one copy of the transgene that confers the antibiotic resistance. Therefore, the lack of expression might not be uniquely attributed to transgene loss but most likely also partially owed to other gene regulatory mechanisms. Nevertheless, PCR

or genome sequencing to confirm the presence of the transgene in the genome of non-expressing cells would be needed to experimentally corroborate this idea.

Employing retrovirus or transposons for gene engineering leads to random insertion of several copies of the transgene in the target cell. Both Lentivirus and *Piggybac* transposon-mediated integration is biased toward transcriptionally active loci and should ensure expression due to the open chromatin nature (111–114). However, although mosaic expression and transgene loss have been reported for both strategies, transposons have been granted with a more stable gene expression reputation over cell division, probably due to their more random integration patterns as compared with lentivirus, which are highly biased to intragenic regions (111,115). Unfortunately, Tet-ON-all-in-one integration into the genome using the *Piggybac* transposon system was insufficient to overcome the loss of expression in the HeLa reporter cell line.

Methylation in the promoter regions and deacetylation of histones can contribute to lack of transgene expression. Therefore, recovery of transgene expression was analyzed in genetically identical cell lines showing mosaicism using epigenetic modulators. 5' Azacytidine and trichostatin A (TSA) modify the entire epigenome in an unspecific manner by respectively preventing DNA methylation or histone deacetylation after cell division. These genome-wide modifications are unspecific and often lead to high cell toxicity when the expression of essential genes is changed, which explains the high cell death observed in the assay. Interestingly, 5' Azacytidine could only partially rescue mCherry expression to a maximum of 50% mCherry positive cells, suggesting that methylation within the promoter region is not the only cause of epigenetic silencing in the analyzed clonal cell lines. In turn, TSA-mediated deacetylation inhibition led to a maximum of 75% mCherry expressing cells, suggesting that histone deacetylation might be contributing to the observed gene silencing. Although high cell toxicity might be masking the overall transgene expression recovery, none of the treatments led to full transgene expression recovery. In line with these results, Pankiewicz *et al.* showed that neither TSA nor 5' Azacytidine circumvent the need for more specific cellular activators in isogenic lines experiencing gene silencing (106). Only targeted demethylation strategies by for instance, fusing the catalytic domain of Ten-eleven translocation (TET) hydroxylase 1, essential for cytosine demethylation, to the rtTA (TET1c-rtTA) are effective at rescuing expression (109). Unfortunately, this strategy does not offer a definitive solution as constant TET1c-rtTA expression must be sustained to preserve expression. All in all,

epigenetic arrays on isogenic clones are imperative to confirm the role of epigenetics in the loss of transgene expression in our cells. To prevent DNA methylation-mediated silencing, CpG-depleted Tet promoters or insulator sequences might be alternatives to reduce the impact of DNA methylation in the transgene expression stability. In turn, less cytotoxic strategies are needed to prevent histone deacetylation as treatment with TSA fails to recover transgene expression in concentrations that preserve cell integrity.

Apart from epigenetics, construct architecture can influence the transactivation ability (116). Consequently, several groups have studied the optimal promoter combinations and orientations to provide rtTA and Tet elements in single vectors while ensuring minimal disturbance amongst units and thus the highest gene expression induction. For instance, Kang *et al.* showed that promoters oriented in opposite directions lead to the highest Tet promoter transactivation in Tet-ON all-in-one vectors with PGK-mediated rtTA expression. Instead, expression cassettes in the same orientation lead to higher Tet promoter leakiness (101). Moreover, distinct degree of mosaicism and level of expression of the Tet promoter have been reported regardless of the direction of transcription relative to an endogenous promoter (109). While no obvious leaky expression was observed in our cells, the negative effect of subsequent promoters oriented in the same direction cannot be ruled out. To understand whether the construct architecture was affecting Tet promoter activity or rtTA availability, the effect of overexpressing rtTA in a different genomic locus was analyzed. Interestingly, cells rescued with either rtTA3 or rtTA3G showed gene expression recovery in over 95% of the cells previously showing bimodal expression. This is in contrast with previous reports suggesting that rtTA molecules are not the limiting factor for expression because they are no longer able to access DNA-binding sites at the closed chromatin locus of cells that have undergone transgene silencing (106). The main difference with Pankiewicz *et al.* rescue experiments is that they pre-select clones in which the loss of expression mechanism is clearly due to epigenetic silencing, *i.e.,* same number of transgene copies in the genome but loss of transgene expression. The authors showed that this stage can only be reverted in a biphasic process requiring the collaboration of transcription factors that remodel chromatin with others that subsequently act to activate transcription in the transgenic cells (106). However, based on the effect of 5' Azacytidine on the recovery of gene expression, it is unlikely that bimodal expression in our cells is purely driven by methylation of the Tet promoter. Moreover, different phases of epigenetic gene expression repression are

characterized by different combinations of DNA/histone modifications, such as DNA methylation, histone acetylation / methylation / phosphorylation / ubiquitination / sumoylation. Therefore, it is speculated that within a polyclonal cell population different non-expressing cells show distinct intermediary stages of chromatin packaging. In that case, some of these cells might not require the full action of epigenetic modulators before they can respond to an excess of rtTA, thereby shifting to an active chromatin state and activating transgene expression.

In addition, clonally expanded rtTA3G rescued cells maintained the homogeneous transgene expression over subculturing while only a low percentage of the isogenic cell lines with the Tet-ON single vector showed high percentage of mCherry expressing cells. Therefore, high expression levels could be achieved using Tet-all-in-one vectors but only in a low percentage of isogenic cells, while the two-vector Tet-system led to stable transgene expression in a higher number of clonal cells.

Based on these results, it is likely that the observed mosaic expression using the Tet-ON-all-in-one vector is not due to transgene loss, or neighboring chromatin context but is instead triggered by construct architecture. Nevertheless, detection of rtTA protein as well as characterization of methylation status of the Tet promoter in non-expressing HeLa cells before rtTA rescue are crucial experiments to fully understand the mechanisms leading to impaired gene expression in Tet-ON all-in-one vectors.

Remarkably, experiments in hiPSC lines using the two-vector Tet system further supported the construct architecture hypothesis. Isogenic hiPSC lines with a single copy of the transgene in the AAVS1 locus showed intact mCherry expression and miRE functionality after several passages without selective pressure as well as during CM differentiation. Poor discrimination of mCherry positive and negative populations observed during flow cytometry experiments is most likely due to mCherry quenching during fixation and permeabilization of cells before intracellular staining of β-catenin. This is further supported by a better negative-positive-population discrimination in the kinetics experiments wherein mCherry is measured in live cells. Notably, mCherry expression was lower in miRE β-catenin as compared with miRE mock. Since all the isogenic cells are heterozygous, *i.e.,* have a single copy of the transgene in the AAVS1 locus, these differences are hard to explain. Epigenetic silencing would have been suspected if the expression pattern followed a mosaic fashion, namely a discrete expression of mCherry.

However, since mCherry expression is homogeneous in all cells and β-catenin knockdown is high, it is suspected that different Tet promoter activation kinetics rather than gene regulatory mechanisms are responsible for the observed differences across groups. In fact, differences in Tet promoter activation onset have been reported in individual cells within an isogenic clonal population (117). Still, this phenomenon requires further investigation.

## 4.2 Conditional Wnt signaling modulation to promote cardiomyocyte differentiation in hiPSC-derived mesoderm cells

Wnt/β-catenin signaling plays a biphasic role in heart development: early Wnt activation stimulates mesoderm induction, and subsequent Wnt inhibition promotes cardiogenesis (118). Also, other signaling pathways largely depending on Wnt such as Nodal/activin and BMP4 signaling have been used to promote cardiogenesis *in vitro* (98). In this thesis, synthetic RNAi combined with Tet systems were used to downregulate Wnt signaling in the later stage of hiPSC differentiation towards cardiomyocytes (CMs). Unlike, other studies where this strategy was used for protocol development purposes (85), here the ultimate aim was to optimize a system to conditionally promote CM differentiation of the mesoderm cells.

Induction of the WNT-off-stage by activation of Tet promoter-mediated expression of miRE β-catenin (miRE β-cat) reached the knockdown peak at day 4 of DOX treatment in undifferentiated cells. Consistently, induction of miRE β-cat yielded comparable numbers of CMs as the chemically-induced controls after 96 h of DOX induction. Notably, this transactivation time is 24 h longer as compared with similar induction experiments by Lian *et al.* (85). Yet, these findings are not surprising as Lian *et al.* used lentivirus, hence yielding several copies of transgene per cell, which likely shortened the time needed to achieve sufficient knockdown levels. In fact, our findings are consistent with expression patterns reported with the OPTi-OX system in homozygous clones- *i.e.*, two copies of the transgene (93). Nonetheless, to harness the full Wnt inhibition potential of this strategy, it would be interesting to assess whether the induction time needed in this platform could be reduced using homozygous clones.

Besides, although the system showed reversibility upon doxycycline withdrawal, β-catenin protein levels were largely affected as shown by an almost 2-fold increase in β-catenin protein 4 days after DOX withdrawal, which was sustained for several days. Whether this phenomenon also occurs in differentiating cells, which might not be as dependent on Wnt signaling as hiPSCs, still remains to be assessed.

Low CM differentiation efficiencies were generally observed in the miRE β-cat isogenic cell lines, including the control. This was particularly remarkable when compared with the miRE mock cells, which achieved differentiation efficiencies in all groups including -DOX that were similar to previously reported with this differentiation protocol (85).

Several critical factors determine successful differentiation of hiPSC into CMs: (i) starting seeding cell density (94), (ii) time of expansion before differentiation and (iii) CHIR99021 (CHIR) dose and time course (119). All of these are cell line and passage dependent. Because both miRE cell lines were derived from the same parental hiPSC line at the same time, no major differences are expected based on the cell line. However, since clonal cells were expanded after gene editing, it cannot be excluded that individual clones with distinct genetic background could have been selected from the entire cell population. For that reason, starting seeding density, time of expansion before differentiation, as well as CHIR concentrations were titrated for each individual clone. Interestingly, both hiPSC miRE mock and miRE β-cat clones differentiated the best with the same starting cell density and CHIR concentration (data not shown). In addition, whereas miRE mock clones showed some level of basal differentiation in the suboptimal conditions, miRE β-cat clones did not differentiate into cTNT positive cells in any other condition. These observations suggest that introducing the miRE β-cat in the cells could be leading to an overall CM differentiation impairment.

Wnt/β-catenin signaling is essential for the maintenance of naive embryonic stem cells (ESCs), yet is not necessary for stemness maintenance in ESCs, which are equivalent to hiPSCs (120). Although, the role of canonical Wnt signaling in stemness and self-renewal has been controversial, the notion that hiPSC behave like primed ESC-like cells is supported by the fact that Wnt signaling is not necessary for the expansion and survival of hiPSCs (121). In the Wnt/β-catenin signaling pathway, the role of β-catenin is central and crucial for the activation of genes involved in cell cycle regulation and stemness

(122). Also, β-catenin is a component of cell-to-cell adherent junctions connecting classical cadherins to the actin cytoskeleton (123).

Notably, hiPSC miRE mock isogenic clones showed on average a lower expression of baseline β-catenin levels as compared with the hiPSC wildtype (WT) and miRE β-cat. While such scenario would be reasonable in the hiPSC miRE β-cat isogenic cell lines due to promoter leakiness or baseline activity of miRE β-catenin molecules, it is more complex to justify in the mock controls. As a result of the pleiotropic function of β-catenin, a distinct cell density across different cell lines at the experimental endpoint could be a rational explanation. It is reasonable to assume that high confluent cultures would express more β-catenin that will be contributing to the cell-to-cell adhesions, while lower confluent ones will have the opposite scenario. However, WT cultures had the same or even lower density that the mock controls at the endpoint. Moreover, WT cells showed β-catenin protein levels comparable to miRE β-cat indicating that the differences observed in total β-catenin protein are not influenced by the amount of β-catenin involved in cell-adhesion complexes.

Loss of Wnt activity and downregulation of β-catenin protein due to prolonged cell culture have been associated with an increased proliferation rate in mouse ESCs, general loss of DNA methylation, and impaired differentiation(122). As hiPSCs miRE mock and miRE β-cat were derived from the same parental cell line and were no more than 2-3 passages apart in the differentiation experiments, the effect of prolonged culturing in the Wnt signaling pathway between both groups is expected to be minimal. Nevertheless, during regular cell maintenance miRE mock cells showed slightly higher proliferative rates and less spontaneous differentiation than miRE β-cat cells, which in turned usually had less densely packed colonies (data not shown). While proliferation rates are consistent with the current understanding of Wnt activity on pluripotent stem cells, discrepancies in differentiation efficiencies still cannot be explained.

Activation of Wnt activity in PSCs induces mesoderm differentiation in hESCs and hiPSC (85,124) due to a direct transcription activation of Brachyury, a master mesoderm transcription factor, by β-catenin (125). In the differentiation protocol used in this thesis, activation of Wnt activity is exogenously promoted by CHIR, a small molecule that destabilizes the β-catenin degradation complex by potently inhibiting GSK3β. CHIR-mediated differentiation is characterized by a transient high cell death followed by cell

recovery. Recently, Laco *et al.* linked the inconsistences of CHIR-mediated differentiation in different cell lines, clones, and passage numbers to the cell cycle state. In a nutshell, highly proliferative cell lines maintained in <70% confluency, with a high percentage of cells in S/G2/M cell-cycle experience less CHIR-induced cell death and show a better recovery after CHIR. These cells also require lower CHIR concentrations and efficiently differentiate into CMs (50-90%) (119). Although this has never been reported, based on the existing evidence it is fair to speculate that the Wnt signaling status of a cell, which correlates with proliferation rates and therefore to cell cycle, could also be a predictor of how efficient CHIR-mediated CM differentiation will be. In that scenario, this hypothesis would correlate with our findings as follows: a cell with low Wnt signaling (*i.e.,* hiPSC miRE mock) with most likely a higher percentage of cells in S/G2/M cell-cycle phase- would react to lower CHIR concentrations and be able to recover faster due to less cell death and higher proliferative capacity. Instead, cells with high baseline Wnt signaling (*i.e*., hiPSC miRE β-cat) would need a higher CHIR dose sustained for a longer time in order to induce a significant shift in Wnt signaling and differentiate into mesoderm cells, yet at the expense of high cell death that they will fail to compensate for. Evaluation of mesoderm differentiation (*e.g*., quantification of Brachyury expressing cells) after CHIR treatment would be a key experiment to define CHIR and basal Wnt signaling as factors causing discrepancies in CM differentiation efficiencies.

Spontaneous differentiation into CMs has been reported after hiPSC have committed to the mesoderm lineage and are kept in the basal medium (85). Interestingly, basal CM differentiation was observed in the –DOX groups and correlated with the differentiation efficiency achieved after treatment with Wnt inhibitors, highlighting the importance of efficient initial mesoderm conversion. As expected, subsequent inhibition of Wnt signaling by IWR-1 (CTRL) in both groups, miRE mock and miRE β-cat, led to an increased percentage of cTNT positive cells as compared with untreated controls. As expected, only miRE β-cat induction showed a similar fold change.

Although the biological mechanisms leading to a lower CM differentiation potential observed in miRE β-cat hiPSCs still need to be understood, Tet promoter driven expression of miRE β-cat is a promising tool to conditionally increase the conversion of mesoderm cells into CMs.

Lastly, the two-vector Tet-ON system is not restricted to RNAis and could be used to conditionally overexpress genes that could be beneficial for the heart, *e.g.* pyruvate kinase muscle isoenzyme 2 to induce CM proliferation (126). A unique feature of this strategy is that it is directed to the therapeutic cells thereby reducing side-effects.

## 4.3 hiPSC-derived expandable cardiac progenitors as an alternative source of cells for cardiac cell therapy

Myocardial function is enhanced by adaptive transfer of human cardiac progenitor cells (hCPCs) into the injured heart (127). Typically, CPCs are isolated from heart biopsies of patients undergoing heart-related surgeries, expanded *in vitro*, and subsequently re-injected into the patients' heart. However, CPCs are severely impacted by co-morbidities and aging, which lead to an increased percentage of senescence cells, and thus limit CPCs' therapeutic potential. Alternative sources are limited and ethically charged as they involve the use of human fetal tissue. In fact, different differentiation potentials have been described within the Sca-1 positive CPC population (hCMPC) depending on origin (46). Consequently, hiPSC have arisen as an alternative to obtain young and healthy cardiac progenitor cells.

Based on the numerous reports showing that hiPSCs recapitulate early cardiac development *in vitro*, it was hypothesized that putative CPC populations such as hCMPC could be obtained from hiPSCs undergoing differentiation to CMs. Sca-1 positive cells isolated at different times during CM differentiation of hiPSC showed different proliferative profiles. Only cells isolated at day 4 (early iCPC$^{Sca\text{-}1}$) and day 5 (late iCPC$^{Sca\text{-}1}$) started proliferating shortly after isolation and continued during extended periods of subculturing. In agreement, cells isolated based on the C19 antigen, an alternative strategy to isolate hCMPC with similar characteristics to fetal hCMPCs, were isolated from day 4 until day 7 in hESC-derived embryoid bodies (128). Interestingly, the authors did not report different proliferation rates between different days. Therefore, comparison of the number of colony-forming units between iCPC$^{Sca\text{-}1}$ isolated at different time points would be a strategy to evaluate if the observed differences are directly linked to the self-renewal potential of each population.

Magnetic activated cell sorting (MACS) using an anti-Sca-1 antibody, which is feasible for clinical application, was the chosen strategy to isolate hCMPC-like cells from the

differentiating hiPSC pool. Clusters of beating cells were consistently observed in the flow-through fraction shortly after MACS, which were in turn more densely populated due to the inability to dissociate and accurately count beating clusters without compromising the non-beating cells survival. In contrast, the positive fraction (iCPC$^{Sca-1}$) contained predominantly non-beating cells that would proliferate shortly after isolation. Although this strategy is still highly controversial due to the nature of the recognized epitope (78), it seems to be effective at consistently isolating proliferative non-beating cells from different sources. In contrast to mouse cardiac development, wherein Lin negative/ Sca-1 positive cells were detected mainly from E17 and in postnatal hearts (82), Sca-1 expressing cells seem to arise very early in human cardiac development. Despite our findings correlate with previous reports (128), more stringent experiments based on single cell transcriptomics and proteomics right after isolation would be key to confirm the cardiac progenitor identity of iCPC$^{Sca-1}$.

Based on cell counts, the isolation efficiency and thus, indirectly the differentiation efficiency of hiPSC into Sca-1 positive cells was estimated to be 1%. As a matter of fact, similar isolation efficiencies have been reported elsewhere for isolations from heart biopsies (79). Such low efficiency is not surprising when using heart biopsies due to high cell heterogeneity *i.e.,* blood cells, endothelial cells, smooth muscle cells or CMs. Yet, if Sca-1 positive CPC would arise from early developmental stages as we hypothesized here, a higher efficiency should be expected when using hiPSCs-derived mesoderm cells, a comparatively pure cell population, as starting material. The relatively low isolation efficiencies would go in line with other reports suggesting that Sca-1 cells might be a small CPC subpopulation (82). It is currently accepted that developmental CPC arise from distinct populations marked by MESP1 expression (129). Therefore, it would be crucial to determine whether iCPC $^{Sca-1}$ express MESP1. Since MESP1 expression has not been reported in adult or fetal hCMPC, expression of MESP1 in iCPC $^{Sca-1}$ would point to a developmental origin common to other well-characterized developmental CPC populations such as NKX 2-5 or Isl-1. However, since hCMPCs do not express Isl-1, screening of Isl-1 cells in the FT cell fraction right after MACS would be key to evaluate whether hCMPCs originate in fact as a CPC subpopulation during hiPSC differentiation.

Alternatively, the low percentage of Sca-1 cells at the isolation day might be affected by the differentiation protocol. In order to hinder CM differentiation and preventing massive cell death, our differentiation protocol includes a sequential medium change to cardiac

progenitor supportive medium for 2 days. At this given point, the CPC medium, rich in growth factors, is expected to reinforce CPC proliferation (130). However, this approach lengthens the time the putative iCPC $^{Sca-1}$ are in contact with differentiating cells that might induce iCPC $^{Sca-1}$ differentiation into CMs, thereby reducing the overall yield. In fact, direct C19 antigen isolation strategy led to a 20% hCMPC isolation efficiency (128). Therefore, direct isolation of Sca-1 positive cells at day 4 and 5 should be considered during protocol optimization.

Early and late iCPCs$^{Sca-1}$ were expanded for 15 passages without reaching replicative senescence. Although donor-dependent differences were observed, late iCPC Sca-1 exhibited an overall higher proliferative rate as compared with early iCPC$^{Sca-1}$. In addition, iCPCs$^{Sca-1}$ population doubling time (PDT) was comparable to hCMPCs and human cardiac fibroblasts (hCF) at matched passages. Interestingly, late and early iCPC$^{Sca-1}$ PDTs were in the same range as previously reported PDTs for iPSC-derived CPC (73). Of note, early and late iCPCs$^{Sca-1}$ generally had a lower population doubling time as compared with FT cells. FT cells proliferation was fluctuating and generally marked by a long lag phase, most likely due to the remaining presence of non-proliferative CMs, followed by a short period of similar growth as the iCPC$^{Sca-1}$. After passage 7-9, all the cells showed replication arrest, as seen by persistently high PDTs (>100h). These findings are in line with previous reports (128) and highlight the superior proliferative capacity of iCPCs$^{Sca-1}$ as compared to FT cells under these growth conditions. Although the full proliferation potential of iCPCs$^{Sca-1}$ remains to be determined to estimate accurate cell yields per isolation, iCPCs$^{Sca-1}$ could be expanded $10^{11}$-fold by passage 15. Notably, iCPC$^{Sca-1}$ had a 10,000-fold higher proliferative capacity than previously reported expandable hiPSC-derived CPCs (73,75). Since those hiPSC-derived CPCs were not pre-sorted and, thus, represent a mixed population, these results suggest that sorting for Sca-1 might be selecting a highly proliferative progenitor subpopulation. However, the effect of serum-free medium, which is desirable for clinical translation, should be tested as the serum contained in the expansion medium largely influences cell proliferation. Besides, iCPCs$^{Sca-1}$ did not require Wnt, BMP and Activin/Nodal pathway modulators as described for other expandable *de novo* CPCs (73,75,131). The latter is an important factor for cost-effective scalability. Additionally, these cell yields would be suitable for clinical application as current clinical studies employing similar cell types have used approximately $10^7$ cells per heart (44,63).

The proliferation rate and the average replicative senescence has never been comprehensively reported for fetal and adult hCMPCs. Goumans and colleagues have stated that hCMPCs can be passaged for 25 passages (80) and have shown that cells that have undergone >100 population doublings have a stable karyotype (28). As differences exist depending on the origin, fetal hCPCs exhibit higher proliferation rates than adult cells (46), it is intricate to make fair comparisons. A plausible comparable figure is the lag phase right after MACS; while hCPCs need 2 weeks to colonize a 24-well (79), iCPC$^{Sca-1}$ can be expanded after 1 week. Considering that ageing negatively affects self-renewal, the latter figure seems reasonable.

All in all, although the replicative senescence was not determined in this thesis, iCPCs$^{Sca-1}$ could proliferate for more than 30 population doublings and yielded higher cell numbers than previously reported for other hiPSC-derived CPCs. Also, the average PDT of iCPCs$^{Sca-1}$ isolated from hiPSC is similar to that of fetal hCMPCs, although it was highly donor-dependent.

During development, embryonic cells go through different cell fate decision-making processes that are guided through spatial, temporal and chemical cues. Likewise, during *in vitro* differentiation protocols, hiPSCs have to commit to different cell developmental stages typically guided by chemical cues added in the medium. The heart develops from mesoderm cells that migrate antero-laterally from the primitive streak in the embryo to form the cardiac crescent (55). The crescent fuses to establish the primitive heart tube in the midline that is patterned with anterior-posterior axis to form distinct spatial poles, which contain progenitors that will give rise to different regions in the adult organ. *In vitro*, after committing to the mesoderm layer, cells develop further into late plate mesoderm-like cells that will give rise to the circulatory system including the heart, blood vessels, and blood cells (132). Immunophenotypic analysis confirmed the absence of lateral plate mesoderm-derived progenitors such as endothelial or hematopoietic progenitors in iCPCs$^{Sca-1}$. Importantly, pro-angiogenic factors present in the hCPC expansion medium, such as VEGF, did not stimulate endothelial lineage commitment neither at the beginning of cell expansion nor during subculturing. Equally crucial was to determine the absence of a hematopoietic progenitor cell signature (82). Interestingly, FT cells did not show traces of other hematopoietic or endothelial cells either, which indicates that the cells had committed to the cardiac mesoderm by the isolation day. Of note, expression of Sca-1 could not be detected after isolation in any of the cells (data not shown), indicating that

Sca-1 expression may be lost due to cell-culture-induced phenotypical changes. Importantly, Sca-1 expression has only been reported in clonally expanded cells from adult and fetal hearts (28) but to the best of our knowledge never shown after expansion of Sca-1 isolated cells.

Compelling evidence suggests that adult and fetal hCPCs experience phenotypical changes during subculturing that can alter their functionality (133). CD105 (endoglin) expression in iCPCs$^{Sca-1}$ was acquired during cell expansion and was homogeneously expressed in cells at passage 15, which correlated with fetal hCPCs at matched passages. Interestingly, CD105 is also uniformly expressed in cells that qualify as cardiac progenitor cells such as CDCs (134), Isl-1 positive cells (39), as well as adult and fetal hCMPCs (28). While Isl-1 positive cells co-express endoglin in human fetal hearts (42), whether hCMPCs and CDCs acquire endoglin as a result of subculturing has not been reported.

Endoglin is a co-receptor for transforming growth factor-β (TGFβ) family members. It is highly expressed in vascular endothelial cells and plays a key role in vasculogenesis (135) and the development of the cardiovascular system (136). In cardiac tissue, endoglin is expressed by cardiac fibroblasts (137,138). In addition, the role of endoglin in regulating cardiac remodeling in heart failure and MI has recently been shown (136). A decline in cardiac function as a result of ischemic injury activates signaling cascades that lead to CM hypertrophy and cardiac fibrosis. Among these, TGFβ1 signaling is increased, leading to a conversion of fibroblasts into myofibroblasts that will secrete extracellular matrix proteins and form scar tissue (139). In fact, loss-of-function *in vitro* studies have confirmed the dependence of TGFβ1 activity on endoglin expression in cardiac fibroblasts (136). Interestingly, injection of human mononuclear cells with normal endoglin expression partially rescued adverse cardiac remodeling in mice with one copy of endoglin gene while mononuclear cells harboring mutant endoglin failed to do so (140). It has been postulated that cells expressing endoglin might be acting as traps for ligands of the TGFβ superfamily like it has been described for soluble endoglin molecules (136), thereby reducing TGFβ1-induced cardiac fibrosis. In line with this, reduced circulating levels of soluble endoglin are considered a predictor of short- and long-term cardiovascular mortality (136). This could partially explain the observed benefits of CDCs and other endoglin-expressing cells at improving cardiac function. However, why is endoglin induced during subculturing?

Angiotensin II, TGFβ, hypoxia- inducible factor-1, hypercholesterolemia, are factors known to induce endoglin expression in different cell lines (136). However, the hCMPC cell culture medium does not contain any of these factors, thus there is no indication that the culture medium could be directly stimulating the expression of endoglin. Both hCMPCs and CDC maintenance medium contain epidermal growth factor (EGF) and fibroblast growth factor 2 (FGF-2) though at different concentrations (80,141). FGF-2 may stimulate fibroblast proliferation (142). Remarkably, FGF-2 is also pivotal to maintain iPSC-derived cardiac progenitors phenotype (70,71,73,75).

Whether the increase of endoglin expressing cells is governed by a mesenchymal transition, cardiac fibroblast-like overgrowth or a mere cell culture artifact remains to be investigated. Detection of markers associated with fibroblasts such as DDR2, FSP-1, PDGFR-α, periostin, CD90, vimentin, and ultimately type I collagen at low and high passages (142), would be crucial to determine to which extent iCPCs$^{Sca-1}$ and cardiac fibroblast phenotypes overlap as a result of subculturing.

In fact, hCMPCs feature cardiac fibroblast-like characteristics; (i) hCMPCs display the typical mesenchymal proteins CD90, CD44, and CD105 (28); (ii) adult hCMPCs are more prone to differentiate in smooth muscle actin-expressing cells (46); (iii) hCMPCs augment the production of extracellular matrix and matrix metalloproteinases following TGF-β stimulation (143); and (iv) hCMPCs play an important role in heart repair mainly by paracrine and pro-angiogenic effects (144). For that reason, the expression of CM specific markers and the ability of iCPC$^{Sca-1}$ to differentiate into CMs was further investigated.

NKX 2-5 is a highly conserved homeodomain transcription factor and a master regulator of cardiac development. NKX 2-5 has also a crucial role in preserving human CM identity and functionality (145). In turn, cardiac troponin I (cTNI) belongs to the troponin protein complex, where it has a structural and functional role, as it responds to calcium levels. Expression of NKX 2-5 and cTNI are thus indicative of cardiac signature. Undifferentiated iCPC$^{Sca-1}$ expressed NKX 2-5 and cTNI, similarly to fetal hCMPCs, and the expression was conserved after cryopreservation. NKX 2-5 expression in hiPS-derived CPCs has been linked to a ventricular phenotype progenitor that proliferates in the presence of FGF-2 and BMP4 (70). As these markers are generally absent in cardiac fibroblasts (146), it is tempting to conclude that iCPC$^{Sca-1}$ and hCMPCs represent a distinct cell population from hCF. Inclusion of other transcription factors will help to discern what exact CPC population

overlaps with Sca-1 expression during development. However, it is important to note that several of the markers widely used to define CPC populations, such as GATA4, MEF2C or PDGFR-A, largely overlap with cardiac fibroblasts in mouse and human (146,147).

Another important aspect that remains to be addressed is whether the number of NKX 2-5/cTNI positive iCPCs$^{Sca-1}$ remains constant or lowers when CD105 positive cells increase during subculturing. In addition, a direct comparison between iCPCs$^{Sca-1}$ and hCFs at the single cell level, combined with robust clonal assays to test iCPCs$^{Sca-1}$ stem cell activity are crucially needed to establish the functional and phenotypic differences of these populations *in vitro* and eventually *in vivo*.

Also, the expression of NKX 2-5 was affected by the isolation day in a donor dependent fashion. However, due to the limited number of screened hiPSC donors, it is not possible to conclude which, early or late, iCPCs$^{Sca-1}$ resemble hCMPCs the most. In addition, batch-to-batch differentiation differences could influence this parameter too. Therefore, it is likely that the isolation day must be determined for each individual donor. One strategy could be quantifying the percentage of NKX 2-5 positive cells at an early passage.

Functional CM differentiation is a hallmark of cardiac progenitor cells. CM differentiation of hCMPCs is induced by the use of demethylating agents (*e.g.,* 5' Azacytidine) and TGFβ1 signaling (28). However, the use of unspecific DNA demethylation to induce differentiation is problematic. For that reason, Wnt signaling inhibition, a recurrent differentiation strategy in the realm of iPSC-derived CPCs (70,73,76), was chosen to induce CM differentiation of iCPC$^{Sca-1}$ with the highest percentage of NKX 2-5 positive cells for each donor. Differentiation was quantified by differences in cell size and expression of α-actinin, a Z-disc protein that anchors myofibrillar actin thin filaments and titin to Z-discs. Inhibition of Wnt signaling during 2 days in iCPC$^{Sca-1}$ led to significant cell death as assessed by the low cell number by the experiment endpoint. The latter indicates that Wnt signaling is necessary for a subset of iCPC$^{Sca-1}$ survival and aligns with studies reporting CHIR as a key component to support iPSC-derived CPC self-renewal (73,75). Interestingly, the surviving subset of cells showed phenotypic changes as a result of the cardiac differentiation medium, including increase in cell size and up-regulation of α-actinin expression. Yet, no beating cells nor sarcomere structures indicative of mature CMs were observed. Based on these results, it is still unclear whether these cells hold true cardiomyogenic potential. Cao *et al.* reported 12 days were sufficient to induce

progenitors differentiation with this CM differentiation medium (73). However, fetal hCMPCs and C19 positive ESC-derived hCMPCs usually need 3-4 weeks to differentiate (80,128). Therefore, the differentiation time might be a major limiting factor in the observed differentiation outcome. Also, other reports combine Wnt signaling inhibition with Hedgehog, and/or TGFβ pathway modulation to induce CM differentiation (70,76). Thus, the contribution of these pathways to the successful iCPCs$^{Sca-1}$ differentiation into functional CMs still needs to be assessed. Alternatively, induction of iCPC$^{Sca-1}$ differentiation via co-culture with GFP-labeled CMs, as frequently used for other CPCs (148), would be a straightforward strategy to test the myogenic potential of these cells.

One limitation of this study is the use of polyclonal populations. As a result of the high heterogeneity reported for hCMPCs isolated with the Sca-1 antibody, stringent characterization at the clonal level would be necessary to obtain more conclusive data on whether iCPC$^{Sca-1}$ are *bona fide* cardiac progenitors. In addition, single transcriptomics or proteomics could be used to fully characterize the identity and the possible different subpopulations present in the iCPCs$^{Sca-1}$ and FT cells.

Moreover, the multipotent nature of iCPCs$^{Sca-1}$ as assessed by the ability to differentiate into other cells found in the heart such as endothelial and smooth muscle cells still remain to be evaluated.

In addition, other relevant aspects related to the indirect mechanisms of these cells such as paracrine signaling also remain to be investigated. Like in CDCs, the cardiomyogenic differentiation of Sca-1 cells seems to be a minor contributor to the improvement of cardiac function (144,149). In the last years, functional recovery and beneficial effects of cardiac cell therapies have been attributed to paracrine mediators, such as VEGF, HGF, IGF-1, and secreted extracellular vesicles (6). Therefore, the isolation and functional characterization of iCPC$^{Sca-1}$-derived extracellular vesicles in for instance organotypic models *in vitro* or in preclinical models would be key to predict the ultimate therapeutic potential of these cells. If iCPC$^{Sca-1}$–derived exosomes would benefit cardiac function *in vivo,* iCPC$^{Sca-1}$ could also represent a standardized and renewable platform for large-scale extracellular vesicle manufacturing.

## 4.4 Outlook

The route to clinical success is paved by the acquisition of profound biological knowledge and thorough pre-clinical and clinical testing. However, to bridge these two ends there is a necessary and often neglected painstaking optimization of production protocols. This study is a glimpse of that bridging work and essentially summarizes the complexity of cell biology systems in the field of cardiac cell therapy.

In this thesis, a reproducible protocol to differentiate cardiac progenitor-like cells from hiPSCs was developed. Importantly, the derived cells, which have cardiac progenitor characteristics, could be expanded to unprecedented numbers, which is essential to meet the clinical needs. In addition, a gene-based strategy was implemented to remotely modulate virtually any signaling pathway at the desired time. With this strategy, cellular products based on stem or progenitor cells can be improved by generating “smart cells” that could be remotely activated with DOX after implantation.

These technologies could ultimately be combined to overcome the complications associated with implanting beating cells into the heart. A visionary application would start with either a universal donor or patient- specific hiPSCs that could be generated by reprogramming skin, blood or urine-derived cells. Then, hiPSCs would be genetically engineered to introduce the Tet promoter-regulated miRE targeting β-catenin in genome safe harbor loci as described in this thesis. The engineered cells would be differentiated into iCPC$^{Sca\text{-}1}$ and subsequently expanded to achieve therapeutically relevant cell numbers. Finally, cells would be transferred to the infarcted myocardium within, for instance, a carrier patch. Differentiation of the transferred cells into CMs could be induced by local administration of small doses of DOX once they have settled into the heart muscle (**Figure 31**).

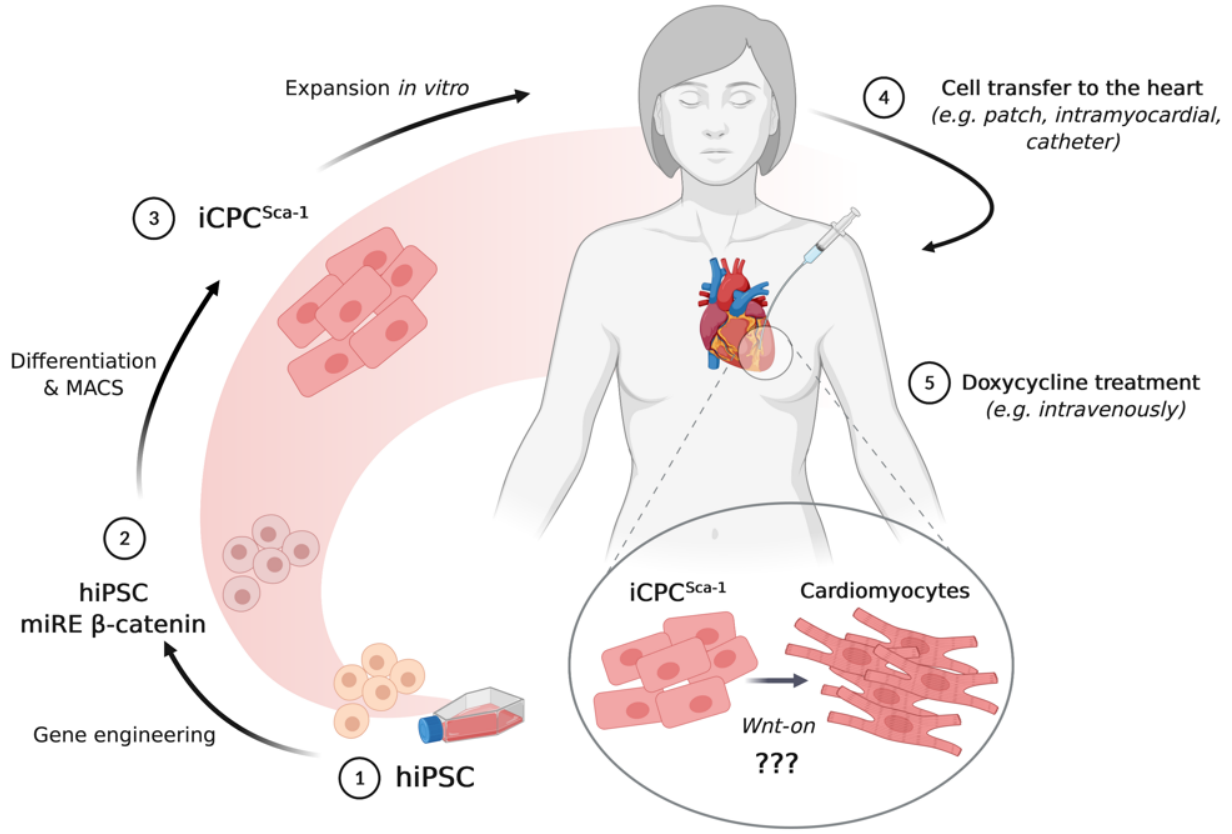


***Figure 31. A visionary application of iCPC$^{Sca-1}$ combined with conditional gene expression for cardiac cell therapy.*** *Created with BioRender.com*

# REFERENCES

1. World Health Organisation. Cardiovascular diseases (CVDs) [Internet]. 2017 [cited 2020 Feb 6]. Available from: https://www.who.int/news-room/fact-sheets/detail/cardiovascular-diseases-%28cvds%29

2. Wilkins E, Wilson L, Wickramasinghe K, Bhatnagar P, Leal J, Luengo-Fernandez R, Burns R, Rayner M, Townsend N. European Cardiovascular Disease Statistics 2017 edition. 2017.

3. World Health Federation. Cardiovascular risk factors [Internet]. 2020 [cited 2020 Apr 6]. Available from: https://www.world-heart-federation.org/resources/risk-factors/

4. World Health Organisation. Cardiovascular diseases [Internet]. 2020 [cited 2020 Apr 23]. Available from: http://www.euro.who.int/en/health-topics/noncommunicable-diseases/cardiovascular-diseases/cardiovascular-diseases2

5. Beffagna G. Zebrafish as a Smart Model to Understand Regeneration After Heart Injury: How Fish Could Help Humans. Front Cardiovasc Med. 2019;6:107.

6. Marbán E. A mechanistic roadmap for the clinical application of cardiac cell therapies. Nat Biomed Eng. 2018;2(6):353–61.

7. Menasché P, Alfieri O, Janssens S, McKenna W, Reichenspurner H, Trinquart L, Vilquin JT, Marolleau JP, Seymour B, Larghero J, Lake S, Chatellier G, Solomon S, Desnos M, Hagège AA. The myoblast autologous grafting in ischemic cardiomyopathy (MAGIC) trial: First randomized placebo-controlled study of myoblast transplantation. Circulation. 2008;117(9):1189–200.

8. Orlic D, Kajstura J, Chimenti S, Bodine DM, Leri A, Anversa P. Bone marrow stem cells regenerate infarcted myocardium. Nature. 2001;410:701–5.

9. Murry CE, Soonpaa MH, Reinecke H, Nakajima H, Nakajima HO, Rubart M, Pasumarthi KBS, Virag JI, Bartelmez SH, Poppa V, Bradford G, Dowell JD, Williams DA, Field LJ. Haematopoietic stem cells do not transdifferentiate into cardiac myocytes in myocardial infarcts. Nature. 2004;428(6983):664–8.

10. Fisher S, Doree C, Mathur A, Taggart. DP, Martin-Rendon E. Stem cell therapy for chronic ischaemic heart disease and congestive heart failure ( Review ). Cochrane Libr. 2016;(4).

11. Jeevanantham , Vinodh Afzal, Mohammad R. Zuba-Surma EK an, Dawn B. Clinical Trials of Cardiac Repair with Adult Bone Marrow- Derived Cells Vinodh. Cell cardiomzoplasty Methods Protoc. 2013;1036:179–205.

12. Nowbar AN, Mielewczik M, Karavassilis M, Dehbi HM, Shun-Shin MJ, Jones S, Howard JP, Cole GD, Francis DP. Discrepancies in autologous bone marrow stem cell trials and enhancement of ejection fraction (DAMASCENE): Weighted regression and meta-analysis OPEN ACCESS. BMJ. 2014;348(April):1–9.

13. Hare JM, Fishman JE, Gerstenblith G, DiFede Velazquez DL, Zambrano JP, Suncion VY, Tracy M, Ghersin E, Johnston P V, Brinker JA, Breton E, Davis-Sproul J, Byrnes J, George R, Lardo A, Schulman IH, Mendizabal AM, Lowery MH, Rouy D, et al. Comparison of Allogeneic vs Autologous Bone Marrow–Derived

Mesenchymal Stem Cells Delivered by Transendocardial Injection in Patients With Ischemic Cardiomyopathy: The POSEIDON Randomized Trial. JAMA. 2012 Dec 12;308(22):2369–79.

14. Henry TD, Pepine CJ, Lambert CR, Traverse JH, Schatz R, Costa M, Povsic TJ, David Anderson R, Willerson JT, Kesten S, Perin EC. The Athena trials: Autologous adipose-derived regenerative cells for refractory chronic myocardial ischemia with left ventricular dysfunction. Catheter Cardiovasc Interv. 2017;89(2):169–77.

15. Qayyum AA, Mathiasen AB, Mygind ND, Kuhl JT, Jorgensen E, Helqvist S, Elberg JJ, Kofoed KF, Vejlstrup NG, Fischer-Nielsen A, Haack-Sorensen M, Ekblond A, Kastrup J. Adipose-Derived Stromal Cells for Treatment of Patients with Chronic Ischemic Heart Disease (MyStromalCell Trial): A Randomized Placebo-Controlled Study. Stem Cells Int. 2017;2017:5237063.

16. Qayyum AA, Mathiasen AB, Helqvist S, Jørgensen E, Haack-Sørensen M, Ekblond A, Kastrup J. Autologous adipose-derived stromal cell treatment for patients with refractory angina (MyStromalCell Trial): 3-years follow-up results. J Transl Med. 2019 Nov;17(1):360.

17. Gyöngyösi M, Wojakowski W, Lemarchand P, Lunde K, Tendera M, Bartunek J, Marban E, Assmus B, Henry TD, Traverse JH, Moyé LA, Sürder D, Corti R, Huikuri H, Miettinen J, Wöhrle J, Obradovic S, Roncalli J, Malliaras K, et al. Meta-analysis of cell-based CaRdiac stUdiEs (ACCRUE) in patients with acute myocardial infarction based on individual patient data. Circ Res. 2015;116(8):1346–60.

18. Martin-Puig S, Wang Z, Chien KR. Lives of a Heart Cell: Tracing the Origins of Cardiac Progenitors. Cell Stem Cell. 2008;2(4):320–31.

19. Karsner HT, Saphir O, Todd TW. The State of the Cardiac Muscle in Hypertrophy and Atrophy. Am J Pathol. 1925 Jul;1(4):351-372.1.

20. Linzbach A. Heart failure from the point of view of quantitative anatomy. Am J Cardiol. 1960;5(3):370–82.

21. Kajstura J, Leri A, Finato N, Di Loreto C, Beltrami CA, Anversa P. Myocyte proliferation in end-stage cardiac failure in humans. Proc Natl Acad Sci U S A. 1998 Jul;95(15):8801–5.

22. Beltrami AP, Urbanek K, Kajstura J, Shao-Min Y, Finato N, Bussani R, Nadal-Ginard B, Silvestr F, Leri A, Beltrami A, Anversa P. Evidence that human cardiac myocytes divide after myocardial infarction. N Engl J Med. 2001;344(23):1750–7.

23. Bergmann O, Bhardwaj RD, Bernard S, Zdunek S, Barnabé-Heide F, Walsh S, Zupicich J, Alkass K, Buchholz BA, Druid H, Jovinge S, Frisén J. Evidence for cardiomyocyte renewal in humans. Science (80- ). 2009;324(5923):98–102.

24. Hsieh PCH, Segers VFM, Davis ME, MacGillivray C, Gannon J, Molkentin JD, Robbins J, Lee RT. Evidence from a genetic fate-mapping study that stem cells refresh adult mammalian cardiomyocytes after injury. Nat Med. 2007;13(8):970–4.

25. Quaini F, Urbanek K, Beltrami AP, Finato N, Beltrami CA, Nadal-Ginard B, Kajstura J, Leri A, Anversa P. Chimerism of the transplanted heart. N Engl J Med. 2002;346(1).

26. Beltrami AP, Barlucchi L, Torella D, Baker M, Limana F, Chimenti S, Kasahara H, Rota M, Musso E, Urbanek K, Leri A, Kajstura J, Nadal-Ginard B. Adult Cardiac Stem Cells Are Multipotent and Support Myocardial Regeneration. Cell. 2003;114:763–76.

27. Matsuura K, Nagai T, Nishigaki N, Oyama T, Nishi J, Wada H, Sano M, Toko H, Akazawa H, Sato T, Nakaya H, Kasanuki H, Komuro I. Adult Cardiac Sca-1-positive Cells Differentiate into Beating Cardiomyocytes. J Biol Chem. 2004;279(12):11384–91.

28. Goumans MJ, de Boer TP, Smits AM, van Laake LW, van Vliet P, Metz CHG, Korfage TH, Kats KP, Hochstenbach R, Pasterkamp G, Verhaar MC, van der Heyden MAG, de Kleijn D, Mummery CL, van Veen TAB, Sluijter JPG, Doevendans PA. TGF-β1 induces efficient differentiation of human cardiomyocyte progenitor cells into functional cardiomyocytes in vitro. Stem Cell Res. 2008;1(2):138–49.

29. Martin CM, Meeson AP, Robertson SM, Hawke TJ, Richardson JA, Bates S, Goetsch SC, Gallardo TD, Garry DJ. Persistent expression of the ATP-binding cassette transporter, Abcg2, identifies cardiac SP cells in the developing and adult heart. Dev Biol. 2004;265(1):262–75.

30. Laugwitz KL, Moretti A, Lam J, Gruber P, Chen Y, Woodard S, Lin LZ, Cai CL, Lu MM, Reth M, Platoshyn O, Yuan JXJ, Evans S, Chien KB. Postnatal isl1+ cardioblasts enter fully differentiated cardiomyocyte lineages. Nature. 2005;433(7026):647–53.

31. Wu SM, Chien KR, Mummery C. Origins and Fates of Cardiovascular Progenitor Cells. Cell. 2008;132(4):537–43.

32. Weinberger F, Mehrkens D, Friedrich FW, Stubbendorff M, Hua X, Müller JC, Schrepfer S, Evans SM, Carrier L, Eschenhagen T. Localization of islet-1-positive cells in the healthy and infarcted adult murine heart. Circ Res. 2012;110(10):1303–10.

33. Sultana N, Zhang L, Yan J, Chen J, Cai W, Razzaque S, Jeong D, Sheng W, Bu L, Xu M, Huang GY, Hajjar RJ, Zhou B, Moon A, Cai CL. Resident c-kit + cells in the heart are not cardiac stem cells. Nat Commun. 2015;6:1–10.

34. Bradfute SB, Graubert TA, Goodell MA. Roles of Sca-1 in hematopoietic stem/progenitor cell function. Exp Hematol. 2005 Jul;33(7):836–43.

35. Uchida S, De Gaspari P, Kostin S, Jenniches K, Kilic A, Izumiya Y, Shiojima I, Grosse Kreymborg K, Renz H, Walsh K, Braun T. Sca1-derived cells are a source of myocardial renewal in the murine adult heart. Stem Cell Reports [Internet]. 2013;1(November):397–410. Available from: http://dx.doi.org/10.1016/j.stemcr.2013.09.004

36. Van Berlo JH, Molkentin JD. An emerging consensus on cardiac regeneration. Nat Med. 2014;20(12):1386–93.

37. Bearzi C, Rota M, Hosoda T, Tillmanns J, Nascimbene A, De Angelis A, Yasuzawa-Amano S, Trofimova I, Siggins RW, LeCapitaine N, Cascapera S, Beltrami AP, D'Alessandro DA, Zias E, Quaini F, Urbanek K, Michler RE, Bolli R, Kajstura J, et

al. Human cardiac stem cells. Proc Natl Acad Sci U S A. 2007;104(35):14068–73.

38. Fuentes TI, Appleby N, Tsay E, Martinez JJ, Bailey L, Hasaniya N, Kearns-Jonker M. Human Neonatal Cardiovascular Progenitors: Unlocking the Secret to Regenerative Ability. PLoS One. 2013;8(10).

39. Serradifalco C, Catanese P, Rizzuto L, Cappello F, Puleio R, Barresi V, Nunnari CM, Zummo G, Di Felice V. Embryonic and foetal Islet-1 positive cells in human hearts are also positive to c-Kit. Eur J Histochem. 2011;55(4):229–34.

40. Messina E, De Angelis L, Frati G, Morrone S, Chimenti S, Fiordaliso F, Salio M, Battaglia M, Latronico MVG, Coletta M, Vivarelli E, Frati L, Cossu G, Giacomello A. Isolation and expansion of adult cardiac stem cells from human and murine heart. Circ Res. 2004;95(9):911–21.

41. Le T, Chong J. Cardiac progenitor cells for heart repair. Cell Death Discov. 2016 Dec 18;2(1):16052.

42. Smits AM, Van Laake LW, Den Ouden K, Schreurs C, Szuhai K, Van Echteld CJ, Mummery CL, Doevendans PA, Goumans MJ. Human cardiomyocyte progenitor cell transplantation preserves long-term function of the infarcted mouse myocardium. Cardiovasc Res. 2009;83(3):527–35.

43. Pagano F, Picchio V, Angelini F, Iaccarino A, Peruzzi M, Cavarretta E, Biondi-Zoccai G, Sciarretta S, De Falco E, Chimenti I, Frati G. The Biological Mechanisms of Action of Cardiac Progenitor Cell Therapy. Curr Cardiol Rep. 2018;20(10).

44. Malliaras K, Makkar RR, Smith RR, Cheng K, Wu E, Bonow RO, Marbán L, Mendizabal A, Cingolani E, Johnston P V., Gerstenblith G, Schuleri KH, Lardo AC, Marbán E. Intracoronary cardiosphere-derived cells after myocardial infarction: Evidence of therapeutic regeneration in the final 1-year results of the CADUCEUS trial (CArdiosphere-derived aUtologous stem CElls to reverse ventricular dysfunction). J Am Coll Cardiol. 2014;63(2):110–22.

45. Sano T, Ousaka D, Goto T, Ishigami S, Hirai K, Kasahara S, Ohtsuki S, Sano S, Oh H. Impact of Cardiac Progenitor Cells on Heart Failure and Survival in Single Ventricle Congenital Heart Disease. Circ Res. 2018;122(7):994–1005.

46. van Vliet P, Smits AM, de Boer TP, Korfage TH, Metz CHG, Roccio M, van der Heyden MAG, van Veen TAB, Sluijter JPG, Doevendans PA, Goumans MJ. Foetal and adult cardiomyocyte progenitor cells have different developmental potential. J Cell Mol Med. 2010;14(4):861–70.

47. Chong JJH, Yang X, Don CW, Minami E, Liu Y-W, Weyers JJ, Mahoney WM, Van Biber B, Cook SM, Palpant NJ, Gantz JA, Fugate JA, Muskheli V, Gough GM, Vogel KW, Astley CA, Hotchkiss CE, Baldessari A, Pabon L, et al. Human embryonic-stem-cell-derived cardiomyocytes regenerate non-human primate hearts. Nature. 2014;510(7504):273–7.

48. Shiba Y, Gomibuchi T, Seto T, Wada Y, Ichimura H, Tanaka Y, Ogasawara T, Okada K, Shiba N, Sakamoto K, Ido D, Shiina T, Ohkura M, Nakai J, Uno N, Kazuki Y, Oshimura M, Minami I, Ikeda U. Allogeneic transplantation of iPS cell-derived cardiomyocytes regenerates primate hearts. Nature. 2016;538(7625):388–91.

49. Marchianò S, Bertero A, Murry CE. Learn from Your Elders: Developmental Biology Lessons to Guide Maturation of Stem Cell-Derived Cardiomyocytes. Pediatr Cardiol. 2019;40(7):1367–87.

50. Barreto S, Hamel L, Schiatti T, Yang Y, George V. Cardiac Progenitor Cells from Stem Cells: Learning from Genetics and Biomaterials. Cells. 2019;8(12):1536.

51. Mummery CL, Zhang J, Ng ES, Elliott DA, Elefanty AG, Kamp TJ. Differentiation of human embryonic stem cells and induced pluripotent stem cells to cardiomyocytes: A methods overview. Circ Res. 2012;111(3):344–58.

52. Burridge PW, Keller GM, Gold JD, Wu JC. Production of de novo cardiomyocytes: human pluripotent stem cells differentiation and direct reprogramming. Natl Institutes Heal. 2013;10(1):16–28.

53. Bondue A, Lapouge G, Paulissen C, Semeraro C, Iacovino M, Kyba M, Blanpain C. Mesp1 acts as a master regulator of multipotent cardiovascular progenitor specification. Cell Stem Cell. 2008 Jul;3(1):69–84.

54. Saga Y, Kitajima S, Miyagawa-Tomita S. Mesp1 expression is the earliest sign of cardiovascular development. Trends Cardiovasc Med. 2000 Nov;10(8):345–52.

55. Buckingham M, Meilhac S, Zaffran S. Building the mammalian heart from two sources of myocardial cells. Nat Rev Genet. 2005;6(11):826–35.

56. Später D, Abramczuk MK, Buac K, Zangi L, Stachel MW, Clarke J, Sahara M, Ludwig A, Chien KR. A HCN4+ cardiomyogenic progenitor derived from the first heart field and human pluripotent stem cells. Nat Cell Biol. 2013;15(9):1098–106.

57. Domian IJ, Chiravuri M, van der Meer P, Feinberg AW, Shi X, Shao Y, Wu SM, Parker KK, Chien KR. Generation of functional ventricular heart muscle from mouse ventricular progenitor cells. Science. 2009 Oct;326(5951):426–9.

58. Cai CL, Martin JC, Sun Y, Cui L, Wang L, Ouyang K, Yang L, Bu L, Liang X, Zhang X, Stallcup WB, Denton CP, McCulloch A, Chen J, Evans SM. A myocardial lineage derives from Tbx18 epicardial cells. Nature. 2008;454(7200):104–8.

59. Tomescot A, Leschik J, Bellamy V, Dubois G, Messas E, Bruneval P, Desnos M, Hagege AA, Amit M, Itskovitz J, Menasche P, Puceat M. Differentiation in vivo of cardiac committed human embryonic stem cells in postmyocardial infarcted rats. Stem Cells. 2007 Sep;25(9):2200–5.

60. Blin G, ..., Menasché P, Pucéat M. A purified population of multipotent cardiovascular progenitors derived from primate pluripotent stem cells engrafts in postmyocardial infarcted nonhuman primates. J Clin Invest. 2010;120(4):1125–39.

61. Menasché P, Vanneaux V, Hagège A, Bel A, Cholley B, Cacciapuoti I, Parouchev A, Benhamouda N, Tachdjian G, Tosca L, Trouvin JH, Fabreguettes JR, Bellamy V, Guillemain R, Suberbielle Boissel C, Tartour E, Desnos M, Larghero J. Human embryonic stem cell-derived cardiac progenitors for severe heart failure treatment: First clinical case report. Eur Heart J. 2015;36(30):2011–7.

62. Bellamy V, Vanneaux V, Bel A, Nemetalla H, Emmanuelle Boitard S, Farouz Y, Joanne P, Perier MC, Robidel E, Mandet C, Hagège A, Bruneval P, Larghero J,

Agbulut O, Menasché P. Long-term functional benefits of human embryonic stem cell-derived cardiac progenitors embedded into a fibrin scaffold. J Hear Lung Transplant. 2015;34(9):1198–207.

63. Menasché P, Vanneaux V, Hagège A, Bel A, Cholley B, Parouchev A, Cacciapuoti I, Al-Daccak R, Benhamouda N, Blons H, Agbulut O, Tosca L, Trouvin JH, Fabreguettes JR, Bellamy V, Charron D, Tartour E, Tachdjian G, Desnos M, et al. Transplantation of Human Embryonic Stem Cell–Derived Cardiovascular Progenitors for Severe Ischemic Left Ventricular Dysfunction. J Am Coll Cardiol. 2018;71(4):429–38.

64. Lin B, Kim J, Li YY, Pan H, Carvajal-Vergara X, Salama G, Cheng T, Li YY, Lo CW, Yang L. High-purity enrichment of functional cardiovascular cells from human iPS cells. Cardiovasc Res. 2012;95(3):327–35.

65. Lu T-YY, Lin B, Kim J, Sullivan M, Tobita K, Salama G, Yang L. Repopulation of decellularized mouse heart with human induced pluripotent stem cell-derived cardiovascular progenitor cells. Nat Commun. 2013;4:1–11.

66. Kattman SJ, Witty AD, Gagliardi M, Dubois NC, Niapour M, Hotta A, Ellis J, Keller G. Stage-specific optimization of activin/nodal and BMP signaling promotes cardiac differentiation of mouse and human pluripotent stem cell lines. Cell Stem Cell. 2011;8(2):228–40.

67. Moretti A, Bellin M, Jung CB, Thies T-MT, Takashima Y, Bernshausen A, Schiemann M, Fischer S, Moosmang S, Smith AG, Lam JT, Laugwitz KK-L. Mouse and human induced pluripotent stem cells as a source for multipotent Isl1 + cardiovascular progenitors. FASEB J. 2010;24(3):700–11.

68. Bu L, Jiang X, Martin-Puig S, Caron L, Zhu S, Shao Y, Roberts DJ, Huang PL, Domian IJ, Chien KR. Human ISL1 heart progenitors generate diverse multipotent cardiovascular cell lineages. Nature. 2009;460(7251):113–7.

69. Soh BS, Ng SY, Wu H, Buac K, Park JHC, Lian X, Xu J, Foo KS, Felldin U, He X, Nichane M, Yang H, Bu L, Li RA, Lim B, Chien KR. Endothelin-1 supports clonal derivation and expansion of cardiovascular progenitors derived from human embryonic stem cells. Nat Commun. 2016;7:1–10.

70. Birket MJ, Ribeiro MC, Verkerk AO, Ward D, Leitoguinho AR, Den Hartogh SC, Orlova V V., Devalla HD, Schwach V, Bellin M, Passier R, Mummery CL. Expansion and patterning of cardiovascular progenitors derived from human pluripotent stem cells. Nat Biotechnol. 2015;33(9):970–9.

71. Schwach V, Gomes Fernandes M, Maas S, Gerhardt S, Tsonaka R, Van Der Weerd L, Passier R, Mummery CL, Birket MJ, Salvatori DCFF. Expandable human cardiovascular progenitors from stem cells for regenerating mouse heart after myocardial infarction. Cardiovasc Res. 2019;116(3):545–53.

72. Elliott DA, Braam SR, Koutsis K, Ng ES, Jenny R, Lagerqvist EL, Biben C, Hatzistavrou T, Hirst CE, Yu QC, Skelton RJP, Ward-van Oostwaard D, Lim SM, Khammy O, Li X, Hawes SM, Davis RP, Goulburn AL, Passier R, et al. NKX2-5(eGFP/w) hESCs for isolation of human cardiac progenitors and cardiomyocytes. Nat Methods. 2011 Oct;8(12):1037–40.

73. Cao N, Liang H, Huang J, Wang J, Chen Y, Chen Z, Yang HT. Highly efficient induction and long-term maintenance of multipotent cardiovascular progenitors from human pluripotent stem cells under defined conditions. Cell Res. 2013;23(9):1119–32.

74. Hu J, Wang Y, Jiao J, Liu Z, Zhao C, Zhou Z, Zhang Z, Forde K, Wang L, Wang J, Baylink DJ, Zhang XB, Gao S, Yang B, Chen YE, Ma PX. Patient-specific cardiovascular progenitor cells derived from integration-free induced pluripotent stem cells for vascular tissue regeneration. Biomaterials. 2015;73:51–9.

75. Vahdat S, Pahlavan S, Mahmoudi E, Barekat M, Ansari H, Bakhshandeh B, Aghdami N, Baharvand H. Expansion of Human Pluripotent Stem Cell-derived Early Cardiovascular Progenitor Cells by a Cocktail of Signaling Factors. Sci Rep. 2019;9(1):1–14.

76. Vahdat S, Pahlavan S, Aghdami N, Bakhshandeh B, Baharvand H. Establishment of a protocol for in vitro culture of cardiogenic mesodermal cells derived from human embryonic stem cells. Cell J. 2019;20(4):496–504.

77. van de Rijn M, Heimfeld S, Spangrude GJ, Weissman IL. Mouse hematopoietic stem-cell antigen Sca-1 is a member of the Ly-6 antigen family. Proc Natl Acad Sci U S A. 1989 Jun;86(12):4634–8.

78. Holmes C, Stanford WL. Concise review: stem cell antigen-1: expression, function, and enigma. Stem Cells. 2007 Jun;25(6):1339–47.

79. Smits A, van Oorschot A, Goumans M. Isolation and Differentiation of Human Cardiomyocyte Progenitor Cells into Cardiomyocytes. Methods Mol Biol. 2012;879:339–49.

80. Smits AM, van Vliet P, Metz CH, Korfage T, Sluijter JP, Doevendans PA, Goumans M-J. Human cardiomyocyte progenitor cells differentiate into functional mature cardiomyocytes: an in vitro model for studying human cardiac physiology and pathophysiology. Nat Protoc. 2009;4(2):232–43.

81. de Boer TP, van Veen TAB, Jonsson MKB, Kok BGJM, Metz CHG, Sluijter JPG, Doevendans PA, de Bakker JMT, Goumans MJ, van der Heyden MAG. Human cardiomyocyte progenitor cell-derived cardiomyocytes display a maturated electrical phenotype. J Mol Cell Cardiol. 2010;48(1):254–60.

82. Valente M, Nascimento DS, Cumano A, Pinto-Do-Ó P. Sca-1+cardiac progenitor cells and heart-making: A critical synopsis. Stem Cells Dev. 2014;23(19):2263–73.

83. Gossen M, Freundlieb S, Bender G, Moller G, Hillen W, Bujardt H. Transcriptional Activation by Tetracyclines in Mammalian Cells. Science (80- ). 1995;268(5218):1766–9.

84. Ozhan G, Weidinger G. Wnt/β-catenin signaling in heart regeneration. Cell Regen. 2015;4(1):3.

85. Lian X, Hsiao C, Wilson G, Zhu K, Hazeltine LB, Azarin SM, Raval KK, Zhang J, Kamp TJ, Palecek SP. Robust cardiomyocyte differentiation from human pluripotent stem cells via temporal modulation of canonical Wnt signaling. Proc Natl Acad Sci. 2012;109(27):E1848–57.

86. Chen B, Dodge ME, Tang W, Lu J, Ma Z, Fan C-W, Wei S, Hao W, Kilgore J, Williams NS, Roth MG, Amatruda JF, Chen C, Lum L. Small molecule–mediated disruption of Wnt-dependent signaling in tissue regeneration and cancer. Nat Chem Biol. 2009;5(2):100–7.

87. Filipowicz W, Bhattacharyya SN, Sonenberg N. Mechanisms of post-transcriptional regulation by microRNAs: Are the answers in sight? Nat Rev Genet. 2008;9(2):102–14.

88. Winter J, Jung S, Keller S, Gregory RI, Diederichs S. Many roads to maturity: microRNA biogenesis pathways and their regulation. Nat Cell Biol. 2009;11(3):228–34.

89. Carthew RW, Sontheimer EJ. Origins and Mechanisms of miRNAs and siRNAs. Cell. 2009;136(4):642–55.

90. Grimm D, Streetz KL, Jopling CL, Storm TA, Pandey K, Davis CR, Marion P, Salazar F, Kay MA. Fatality in mice due to oversaturation of cellular microRNA/short hairpin RNA pathways. Nature. 2006 May;441(7092):537–41.

91. Fellmann C, Hoffmann T, Sridhar V, Hopfgartner B, Muhar M, Roth M, Lai DY, Barbosa IAM, Kwon JS, Guan Y, Sinha N, Zuber J. An optimized microRNA backbone for effective single-copy RNAi. Cell Rep. 2013;5(6):1704–13.

92. Boudreau RL, Martins I, Davidson BL. Artificial MicroRNAs as siRNA shuttles: Improved safety as compared to shRNAs in vitro and In vivo. Mol Ther. 2009;17(1):169–75.

93. Pawlowski M, Ortmann D, Bertero A, Tavares JM, Pedersen RA, Vallier L, Kotter MRN. Inducible and Deterministic Forward Programming of Human Pluripotent Stem Cells into Neurons, Skeletal Myocytes, and Oligodendrocytes. Stem Cell Reports. 2017;8(4):803–12.

94. Lian X, Zhang J, Azarin SM, Zhu K, Hazeltine LB, Bao X, Hsiao C, Kamp TJ, Palecek SP. Directed cardiomyocyte differentiation from human pluripotent stem cells by modulating Wnt/β-catenin signaling under fully defined conditions. Nat Protoc. 2013;8(1):162–75.

95. Wang W, Balk M, Deng Z, Wischke C, Gossen M, Behl M, Ma N, Lendlein A. Engineering biodegradable micelles of polyethylenimine-based amphiphilic block copolymers for efficient DNA and siRNA delivery. J Control Release. 2016 Nov 28;242:71–9.

96. Guide design resources — Zhang Lab [Internet]. [cited 2020 Sep 2]. Available from: https://zlab.bio/guide-design-resources

97. Knott SR V, Maceli AR, Erard N, Chang K, Marran K, Zhou X, Gordon A, ElDemerdash O, Wagenblast E, Kim S, Fellmann C, Hannon GJ. A Computational Algorithm to Predict shRNA Potency. Mol Cell [Internet]. 2014;56(6):796–807. Available from: http://dx.doi.org/10.1016/j.molcel.2014.10.025

98. Paige SL, Osugi T, Afanasiev OK, Pabon L, Reinecke H, Murry CE. Endogenous wnt/β-Catenin signaling is required for cardiac differentiation in human embryonic stem cells. PLoS One. 2010 Jun;5(6):e11134.

99. Barde I, Zanta-Boussif MA, Paisant S, Leboeuf M, Rameau P, Delenda C, Danos O. Efficient control of gene expression in the hematopoietic system using a single Tet-on inducible lentiviral vector. Mol Ther. 2006;13(2):382–90.

100. Vrljicak P, Tao S, Varshney GK, Quach HNB, Joshi A, LaFave MC, Burgess SM, Sampath K. Genome-wide analysis of transposon and retroviral insertions reveals preferential integrations in regions of DNA flexibility. G3 Genes, Genomes, Genet. 2016;6(4):805–17.

101. Kang K, Huang L, Li Q, Liao X, Dang Q, Yang Y, Luo J, Zeng Y, Li L, Gou D. An improved Tet-on system in microRNA overexpression and CRISPR/Cas9-mediated gene editing. J Anim Sci Biotechnol. 2019;10(1).

102. Sharma S, Jackson PG, Makan J. Cardiac troponins. J Clin Pathol. 2004;57(10):1025–6.

103. Lints T, Parsons L, Hartley L, Lyons I, Harvey R. NKX-2.5: A novel murine homeobox gene expressed in early heart progenitor cells and their myogenic descendants. Development. 1993;119:969.

104. Welman A, Barraclough J, Dive C. Generation of cells expressing improved doxycycline-regulated reverse transcriptional transactivator rtTA2S-M2. Nat Protoc. 2006;1(2):803–11.

105. Oyer JA, Chu A, Brar S, Turker MS. Aberrant epigenetic silencing is triggered by a transient reduction in gene expression. PLoS One. 2009;4(3).

106. Pankiewicz R, Karlen Y, Imhof MO, Mermod N. Reversal of the silencing of tetracycline-controlled genes requires the coordinate action of distinctly acting transcription factors. J Gene Med. 2005;7(1):117–32.

107. Migliaccio AR, Bengra C, Ling J, Pi W, Li C, Zeng S, Keskintepe M, Whitney B, Sanchez M, Migliaccio G, Tuan D. Stable and unstable transgene integration sites in the human genome: extinction of the Green Fluorescent Protein transgene in K562 cells. Gene. 2000 Oct;256(1–2):197–214.

108. Kong Q, Wu M, Huan Y, Zhang L, Liu H, Bou G, Luo Y, Mu Y, Liu Z. Transgene expression is associated with copy number and cytomegalovirus promoter methylation in transgenic pigs. PLoS One. 2009 Aug;4(8):e6679.

109. Gödecke N, Zha L, Spencer S, Behme S, Riemer P, Rehli M, Hauser H, Wirth D. Controlled re-activation of epigenetically silenced Tet promoter-driven transgene expression by targeted demethylation. Nucleic Acids Res. 2017;45(16).

110. Garrick D, Fiering S, Martin DI, Whitelaw E. Repeat-induced gene silencing in mammals. Nat Genet. 1998 Jan;18(1):56–9.

111. Schroder ARW, Shinn P, Chen H, Berry C, Ecker JR, Bushman F. HIV-1 integration in the human genome favors active genes and local hotspots. Cell. 2002 Aug;110(4):521–9.

112. Staunstrup NH, Moldt B, Mátés L, Villesen P, Jakobsen M, Ivics Z, Izsvák Z, Mikkelsen JG. Hybrid lentivirus-transposon vectors with a random integration profile in human cells. Mol Ther. 2009;17(7):1205–14.

113. Galvan DL, Nakazawa Y, Kaja A, Kettlun C, Cooper LJ, Rooney CM, Wilson MH. Genome-wide mapping of Piggybac transposon integrations in primary human T cells. J Immunother. 2009;32(8):837–44.

114. Liang Q, Kong J, Stalker J, Bradley A. Chromosomal mobilization and reintegration of Sleeping Beauty and PiggyBac transposons. Genesis. 2009;47(6):404–8.

115. Vigdal TJ, Kaufman CD, Izsvak Z, Voytas DF, Ivics Z. Common physical properties of DNA affecting target site selection of sleeping beauty and other Tc1/mariner transposable elements. J Mol Biol. 2002 Oct;323(3):441–52.

116. Heinz N, Schambach A, Galla M, Maetzig T, Baum C, Loew R, Schiedlmeier B. Retroviral and transposon-based tet-regulated all-in-one vectors with reduced background expression and improved dynamic range. Hum Gene Ther. 2011;22(2):166–76.

117. Rand U, Riedel J, Hillebrand U, Shin D, Willenberg S, Behme S, Klawonn F, Köster M, Hauser H, Wirth D. Single-cell analysis reveals heterogeneity in onset of transgene expression from synthetic tetracycline-dependent promoters. Biotechnol J. 2015;10(2):323–31.

118. Naito AT, Shiojima I, Akazawa H, Hidaka K, Morisaki T, Kikuchi A, Komuro I. Developmental stage-specific biphasic roles of Wnt/beta-catenin signaling in cardiomyogenesis and hematopoiesis. Proc Natl Acad Sci. 2006;103(52):19812–7.

119. Laco F, Woo TL, Zhong Q, Szmyd R, Ting S, Khan FJ, Chai CLL, Reuveny S, Chen A, Oh S. Unraveling the Inconsistencies of Cardiac Differentiation Efficiency Induced by the GSK3β Inhibitor CHIR99021 in Human Pluripotent Stem Cells. Stem Cell Reports. 2018;10(6):1851–66.

120. Xu Z, Robitaille AM, Berndt JD, Davidson KC, Fischer KA, Mathieu J, Potter JC, Ruohola-Baker H, Moon RT. Wnt/β-catenin signaling promotes self-renewal and inhibits the primed state transition in naïve human embryonic stem cells. Proc Natl Acad Sci U S A. 2016;113(42):E6382–90.

121. Chen G, Gulbranson DR, Hou Z, Bolin JM, Probasco MD, Smuga-otto K, Howden SE, Nicole R, Propson NE, Wagner R, Lee GO, Teng JMC, Thomson JA. Chemically defined conditions for human iPS cell derivation and culture. Nat me. 2011;8(5):424–9.

122. Theka I, Sottile F, Cammisa M, Bonnin S, Sanchez-Delgado M, Di Vicino U, Neguembor MV, Arumugam K, Aulicino F, Monk D, Riccio A, Cosma MP. Wnt/β-catenin signaling pathway safeguards epigenetic stability and homeostasis of mouse embryonic stem cells. Sci Rep. 2019;9(1):1–18.

123. Kemler R. From cadherins to catenins: cytoplasmic protein interactions and regulation of cell adhesion. Trends Genet. 1993;9(9):317–21.

124. Rao J, Pfeiffer MJ, Frank S, Adachi K, Piccini I, Quaranta R, Araúzo-Bravo M, Schwarz J, Schade D, Leidel S, Schöler HR, Seebohm G, Greber B. Stepwise Clearance of Repressive Roadblocks Drives Cardiac Induction in Human ESCs. Cell Stem Cell. 2016;18(3):341–53.

125. Yamaguchi TP, Takada S, Yoshikawa Y, Wu N, McMahon AP. T (Brachyury) is a

direct target of Wnt3a during paraxial mesoderm specification. Genes Dev. 1999;13(24):3185–90.

126. Magadum A, Singh N, Kurian AA, Munir I, Mehmood T, Brown K, Sharkar MTK, Chepurko E, Sassi Y, Oh JG, Lee P, Santos CXC, Gaziel-Sovran A, Zhang G, Cai CL, Kho C, Mayr M, Shah AM, Hajjar RJ, et al. Pkm2 regulates cardiomyocyte cell cycle and promotes cardiac regeneration. Circulation. 2020;141(15):1249–65.

127. Zwetsloot PP, Végh AMD, Jansen Of Lorkeers SJ, Van Hout GPJ, Currie GL, Sena ES, Gremmels H, Buikema JW, Goumans MJ, Macleod MR, Doevendans PA, Chamuleau SAJ, Sluijter JPG. Cardiac stem cell treatment in myocardial infarction: A systematic review and meta-analysis of preclinical studies. Circ Res. 2016;118(8):1223–32.

128. Leung HW, Moerkamp AT, Padmanabhan J, Ng SW, Goumans MJ, Choo A. MAb C19 targets a novel surface marker for the isolation of human cardiac progenitor cells from human heart tissue and differentiated hESCs. J Mol Cell Cardiol. 2015;82:228–37.

129. Lescroart F, Chabab S, Lin X, Rulands S, Paulissen C, Rodolosse A, Auer H, Achouri Y, Dubois C, Bondue A, Simons BD, Blanpain C. Early lineage restriction in temporally distinct populations of Mesp1 progenitors during mammalian heart development. Nat Cell Biol. 2014;16(9):829–40.

130. Birket MJ, Mummery CL. Pluripotent stem cell derived cardiovascular progenitors - A developmental perspective. Dev Biol. 2015;400(2):169–79.

131. Cao N, Liu Z, Chen Z, Wang J, Chen T, Zhao X, Ma Y, Qin L, Kang J, Wei B, Wang L, Jin Y, Yang HT. Ascorbic acid enhances the cardiac differentiation of induced pluripotent stem cells through promoting the proliferation of cardiac progenitor cells. Cell Res. 2012;22(1):219–36.

132. Gilbert S. Paraxial and intermediate mesoderm. In: Associates S, editor. Developmental Biology. Sunderland (MA); 2000.

133. Mohsin S, Khan M, Nguyen J, Alkatib M, Siddiqi S, Hariharan N, Wallach K, Monsanto M, Gude N, Dembitsky W, Sussman MA. Rejuvenation of human cardiac progenitor cells with pim-1 kinase. Circ Res. 2013;113(10):1169–79.

134. Makkar RR, Smith RR, Cheng K, Malliaras K, Thomson LEJ, Berman D, Czer LSC, Marbán L, Mendizabal A, Johnston P V., Russell SD, Schuleri KH, Lardo AC, Gerstenblith G, Marbán E. Intracoronary cardiosphere-derived cells for heart regeneration after myocardial infarction (CADUCEUS): A prospective, randomised phase 1 trial. Lancet. 2012;379(9819):895–904.

135. Liu Z, Lebrin F, Maring JA, Van Den Driesche S, Van Der Brink S, Van Dinther M, Thorikay M, Martin S, Kobayashi K, Hawinkels LJAC, Van Meeteren LA, Pardali E, Korving J, Letarte M, Arthur HM, Theuer C, Goumans MJ, Mummery C, Ten Dijke P. ENDOGLIN is dispensable for vasculogenesis, but required for vascular endothelial growth factor-induced angiogenesis. PLoS One. 2014;9(1):1–12.

136. Kapur NK, Morine KJ, Letarte M. Endoglin: a critical mediator of cardiovascular health. Vasc Health Risk Manag. 2013;9:195–206.

137. Chen K, Mehta JL, Li D, Joseph L, Joseph J. Transforming growth factor β receptor endoglin is expressed in cardiac fibroblasts and modulates profibrogenic actions of angiotensin II. Circ Res. 2004;95(12):1167–73.

138. Shyu KG. The role of endoglin in myocardial fibrosis. Acta Cardiol Sin. 2017;33:461–7.

139. Leask A. TGFbeta, cardiac fibroblasts, and the fibrotic response. Cardiovasc Res. 2007 May;74(2):207–12.

140. Van Laake LW, Van Den Driesche S, Post S, Feijen A, Jansen MA, Driessens MH, Mager JJ, Snijder RJ, Westermann CJJ, Doevendans PA, Van Echteld CJA, Ten Dijke P, Arthur HM, Goumans MJ, Lebrin F, Mummery CL. Endoglin has a crucial role in blood cell-mediated vascular repair. Circulation. 2006;114(21):2288–97.

141. Smith RR, Barile L, Cho HC, Leppo MK, Hare JM, Messina E, Giacomello A, Abraham MR, Marbán E. Regenerative potential of cardiosphere-derived cells expanded from percutaneous endomyocardial biopsy specimens. Circulation. 2007;115(7):896–908.

142. Humeres C, Frangogiannis NG. Fibroblasts in the Infarcted, Remodeling, and Failing Heart. JACC Basic to Transl Sci. 2019;4(3):449–67.

143. Bax NAM, van Marion MH, Shah B, Goumans MJ, Bouten CVC, Van Der Schaft DWJ. Matrix production and remodeling capacity of cardiomyocyte progenitor cells during in vitro differentiation. J Mol Cell Cardiol. 2012;53(4):497–508.

144. Maring JA, Lodder K, Mol E, Verhage V, Wiesmeijer KC, Dingenouts CKE, Moerkamp AT, Deddens JC, Vader P, Smits AM, Sluijter JPG, Goumans MJ. Cardiac Progenitor Cell–Derived Extracellular Vesicles Reduce Infarct Size and Associate with Increased Cardiovascular Cell Proliferation. J Cardiovasc Transl Res. 2019;12(1):5–17.

145. Anderson DJ, Kaplan DI, Bell KM, Koutsis K, Haynes JM, Mills RJ, Phelan DG, Qian EL, Leitoguinho AR, Arasaratnam D, Labonne T, Ng ES, Davis RP, Casini S, Passier R, Hudson JE, Porrello ER, Costa MW, Rafii A, et al. NKX2-5 regulates human cardiomyogenesis via a HEY2 dependent transcriptional network. Nat Commun. 2018;9(1):1–13.

146. Furtado MB, Costa MW, Pranoto EA, Salimova E, Lam NT, Park A, Snider P, Chandran A, Richard P, Boyd R, Conway SJ, Pearson J, Kaye DM, Nadia A. Cardiogenic Genes Expressed in Cardiac Fibroblasts Contribute to Heart Development and Repair. Circ Res. 2014;114(9):1422–34.

147. Schaum N, Karkanias J, Neff NF, May AP, Quake SR, Wyss-Coray T, Darmanis S, Batson J, Botvinnik O, Chen MB, Chen S, Green F, Jones RC, Maynard A, Penland L, Pisco AO, Sit R V., Stanley GM, Webber JT, et al. Single-cell transcriptomics of 20 mouse organs creates a Tabula Muris. Nature. 2018;562(7727):367–72.

148. Zeng J, Wang Y, Wei Y, Xie A, Lou Y, Zhang M. Co-culture with cardiomyocytes induces mesenchymal stem cells to differentiate into cardiomyocyte-like cells and express heart development-associated genes. Cell Res. 2008;18(S1):S62–S62.

149. Jansen of Lorkeers SJ, Gho JMIH, Koudstaal S, Van Hout GPJ, Zwetsloot PPM, Van Oorschot JWM, Van Eeuwijk ECM, Leiner T, Hoefer IE, Goumans MJ, Doevendans PA, Sluijter JPG, Chamuleau SAJ. Xenotransplantation of human cardiomyocyte progenitor cells does not improve cardiac function in a porcine model of chronic ischemic heart failure. Results from a randomized, blinded, placebo controlled trial. PLoS One. 2015;10(12):1–19.

# APPENDICES

# Statutory declaration

I, Ana Garcia Duran, by personally signing this document in lieu of an oath, hereby affirm that I prepared the submitted dissertation on the topic “Strategien zur Nutzung des Potenzials menschlicher Herzvorläuferzellen für die Herzzelltherapie/ Strategies to harness the potential of human cardiac progenitor cells for heart cell therapy”, independently and without the support of third parties, and that I used no other sources and aids than those stated.

All parts which are based on the publications or presentations of other authors, either in letter or in spirit, are specified as such in accordance with the citing guidelines. The sections on methodology (in particular regarding practical work, laboratory regulations, statistical processing) and results (in particular regarding figures, charts and tables) are exclusively my responsibility.

Furthermore, I declare that I have correctly marked all of the data, the analyses, and the conclusions generated from data obtained in collaboration with other persons, and that I have correctly marked my own contribution and the contributions of other persons. I have correctly marked all texts or parts of texts that were generated in collaboration with other persons.

I declare that I have not yet submitted this dissertation in identical or similar form to another Faculty.

The significance of this statutory declaration and the consequences of a false statutory declaration under criminal law (Sections 156, 161 of the German Criminal Code) are known to me.”

Berlin, ……. ……..

Ana Garcia Duran

# Curriculum Vitae

[My curriculum vitae does not appear in the electronic version of my dissertation for reasons of data protection.]

[My curriculum vitae does not appear in the electronic version of my dissertation for reasons of data protection.]

# Publications list

Nazari-Shafti TZ*, Neuber S*, **Duran AG*,** Exarchos V, Beez CM, Meyborg H, Krüger K, Wolint P, Buschmann J, Böni R, Seifert M, Falk V, Emmert MY. MiRNA profiles of extracellular vesicles secreted by mesenchymal stromal cells – can they predict potential off-target effects?. Biomolecules. 2020. (* shared first authorship)

Nazari-Shafti TZ, Neuber S, **Duran AG**, Xu Z, Beltsios E, Seifert M, Falk V and Stamm C. Human mesenchymal stromal cells and derived extracellular vesicles: Translational strategies to increase their proangiogenic potential for the treatment of cardiovascular disease. Stem Cells Transl Med. 2020

**Duran AG**, Reidell O, Stachelscheid H, Klose K, Gossen M, Falk V, Röll W, Stamm C. Regenerative Medicine/Cardiac Cell Therapy: Pluripotent Stem Cells. Thorac Cardiovasc Surg. 2018;66(1):53-62.

Torreira E, Louro JA, Pazos I, Gonzalez-Polo N, Gil-Carton D, **Duran AG**, Tosi S, Gallego O, Calvo O, Fernandez-Tornero C. The dynamic assembly of distinct RNA polymerase I complexes modulates rDNA transcription. Elife. 2017;6:1–23.

Putker M, Vos HR, van Dorenmalen K, de Ruiter H, **Duran AG**, Snel B, Burgering BM, Vermeulen M, Dansen TB. Evolutionary acquisition of cysteines determines FOXO paralog-specific redox signaling. Antioxid Redox Signal. 2015 Jan 1;22(1):15-28.

# Acknowledgements

I would like to thank my supervisor Prof. Christof Stamm for opening the doors of his laboratory to me. A special thanks goes to my mentoring committee members Dr. Manfred Gossen, Prof. Andreas Kurtz and Dr. Martina Seifert for their commitment and input during these three years. My deep gratitude goes to Dr. Manfred Gossen and Dr. Timo Nazari-Shafti for their engagement and unconditional support, without their guidance and persistent help this thesis would not have been possible.

Worth to mention are also the Charité- University of Medicine Berlin and the German Heart Center Berlin for funding this project.

My appreciation also extends to the Berlin-Brandenburg School for Regenerative Therapies for giving me the opportunity to do my PhD at the former Berlin-Brandenburg Center for Regenerative Therapies, and nowadays BIH Center for Regenerative Therapies. I would like to thank Dr. Sabine Bartosch for being resourceful and excelling at creating an academic framework where graduate students can learn, get in touch with each other, and most importantly feel supported. I would like to take the opportunity to thank Medicoach at the Charité, an excellent counseling service for students, for helping me identifying and mitigating my fears during the PhD.

At the BCRT, I thank my group members. I would like to thank Elena Putscher, a former master student, who help me doing some of the replicates of the second chapter. Also, to Dr. Janita Maring for granting permission to use a piece of her data as part of this dissertation as well as for her seed ideas and suggestions during our group meetings. Also, to Dr. Sebastian Neuber, for proofreading this thesis and for inspiring me to develop in other fields and regain self-confidence. In addition, I would like to acknowledge the BIH stem cell core facility, particularly Dr. Harald Stachelscheid, Kristin Fischer and Dr. Valeria Fernandez-Vallone for sharing their expertise and providing an excellent service.

I am also very grateful to my colleagues and friends at the BCRT, including Hanieh, Dania, Jörg, Ahmed, George, Lorenz, Melanie, Marcos, Bella, Iris, Laia, Tine, … for the hands-on help and the numerous lunch breaks together, the smiles, chit-chats, and hugs around the BCRT corridors, which sweetened my time here. Special thanks to my dearest friends Krithi and Valeria for teaching me beyond science.

In Berlin, I would like to thank my closest friends, especially Paula, Rella, Gábor, Josh W., Kate, Natalie, Josh F., Anna G., for being supportive, loving, and for shimmering my time in Berlin; without them I would not have managed. Also, to all of those who have made this journey even more special, to Sina, Felipe and all my yoga teachers who have taught me essential values and techniques to stay balanced and focused. All of those proved very effective when writing this whole dissertation during a world pandemic!

I would like to express my deepest appreciation to my PhD-journey and dearest friends: Thijs Wildschut, Marc Abella, Michaela Diakatou, Adrián Álvarez, and Anna Huguet. It was great to support each other during the famous “PhD phases” over phone calls and meetings- it’s flattering to be contemporary to such great scientists!

Also, I can’t begin to express my gratitude to my friends and mentors who have intensively supported and inspired me during trips, visits, and phone calls: Laura C., Laura D., Marieke, José, Alex Marteen, César, Nuño, Oriol, Aitor…This list of acknowledgements would be incomplete without mentioning my life mentor and friend Ana Gasol; thanks for the summer stopovers and all the light and love you brought with you every time you were here.

Millones de gracias a mis padres, Domi y Julián, por simplemente haber hecho todo esto posible: empezando por darme la libertad de elegir, pasando por confiar sin cuestionar mis decisiones, para finalmente darme vuestro apoyo incondicional incluso en momentos cuando mis decisiones parecían no haber sido las más acertadas: ¡os quiero!

A mi hermana Sara por ser mi pequeña-gran fuente de energía. A l’Aida, la meva germana postissa, per ser com una fada madrina en tots els àmbits de la meva vida. A tú, Arnau, per ser el meu amor incondicional. Y al resto de la familia muchas gracias por las visitas a Berlín y la cercanía aún estando lejos de casa.

Finally, I would like to thank the little warrior inside of me for always taking any opportunity, as challenging as it may be, to learn and grow.

# Statistics certificate